

See discussions, stats, and author profiles for this publication at: <https://www.researchgate.net/publication/51391857>

# Micro- and Nanopatterning Techniques for Organic Electronic and Optoelectronic Systems

ARTICLE *in* CHEMICAL REVIEWS · APRIL 2007

Impact Factor: 46.57 · DOI: 10.1021/cr050139y · Source: PubMed

---

CITATIONS

386

READS

65

## 8 AUTHORS, INCLUDING:



Matthew Meitl

Semprius

47 PUBLICATIONS 3,686 CITATIONS

[SEE PROFILE](#)



Yugang Sun

Temple University

153 PUBLICATIONS 21,304 CITATIONS

[SEE PROFILE](#)



Jang-Ung Park

Ulsan National Institute of Science and Tech...

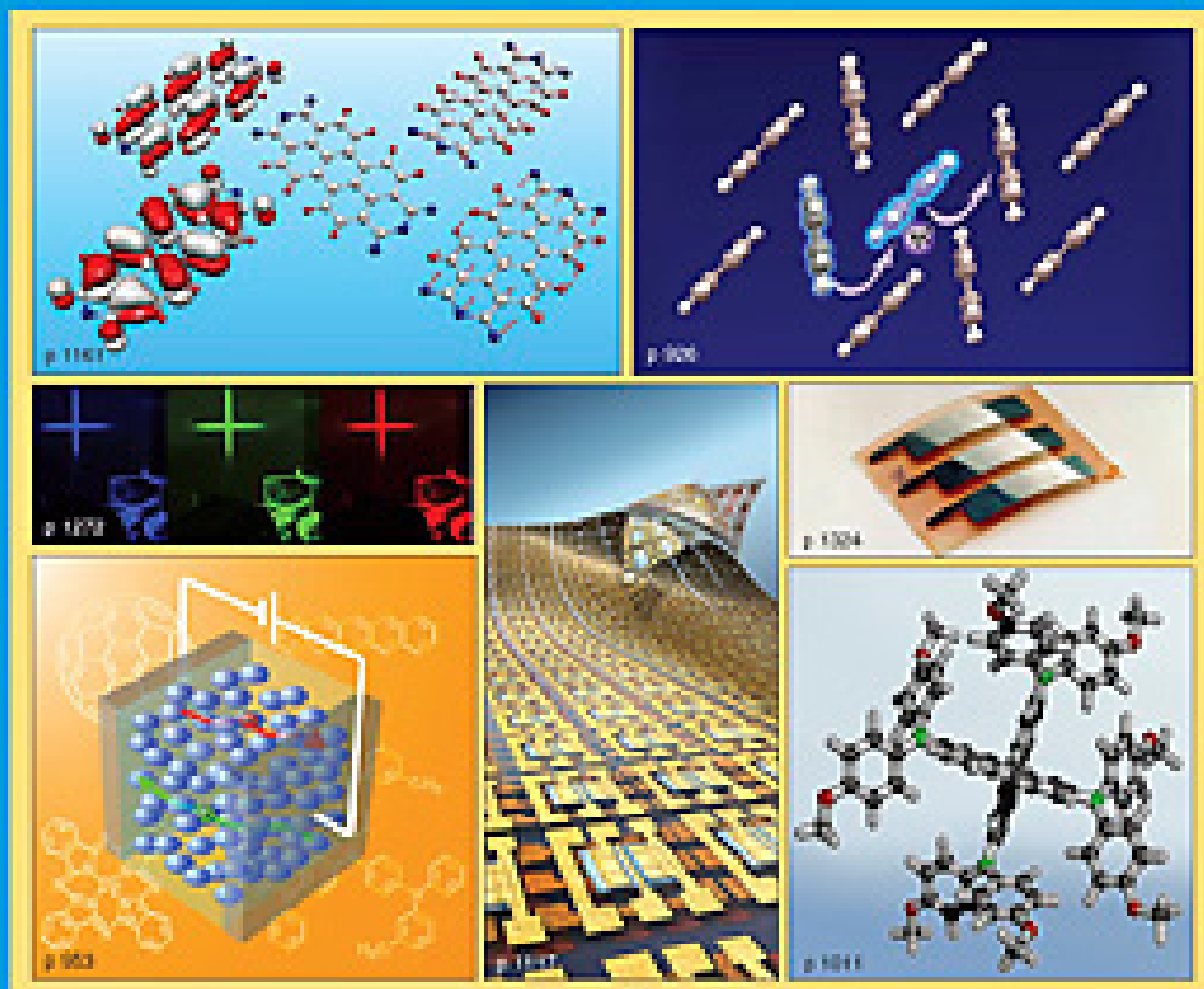
17 PUBLICATIONS 1,546 CITATIONS

[SEE PROFILE](#)

# CHEMICAL REVIEWS

APRIL 2007  
VOLUME 107  
NUMBER 4

## ORGANIC ELECTRONICS AND OPTOELECTRONICS



# Micro- and Nanopatterning Techniques for Organic Electronic and Optoelectronic Systems

Etienne Menard,<sup>†</sup> Matthew A. Meitl,<sup>†</sup> Yugang Sun,<sup>‡</sup> Jang-Ung Park,<sup>†</sup> Daniel Jay-Lee Shir,<sup>†</sup> Yun-Suk Nam,<sup>†</sup> Seokwoo Jeon,<sup>†</sup> and John A. Rogers\*,<sup>†</sup>

*Department of Materials Science and Engineering, Department of Chemistry, Beckman Institute, and F. Seitz Materials Research Laboratory, University of Illinois at Urbana-Champaign, Urbana, Illinois 61801; and Center for Nanoscale Materials, Argonne National Laboratory, 9700 South Cass Avenue, Argonne, Illinois 60439*

Received August 3, 2006

## Contents

1. Introduction	1117
2. Light-Based Patterning Techniques for Organic Electronics	1120
2.1. Photopatternable Organic Electronic Materials	1121
2.1.1. Photopatternable Organic Materials for Semiconductor	1121
2.1.2. Photopatternable Organic Conductive Materials	1121
2.1.3. Photopatternable Organic Light-Emitting Materials	1123
2.2. Optical Soft Lithography	1124
2.3. Focused Laser Beam Scanning	1125
3. Patterning Organic Layers by Embossing, Imprint Lithography, and Capillary Molding	1126
3.1. Fabrication of Molds	1127
3.2. Embossing	1127
3.2.1. Waveguides, Light Couplers, Spectral Filters, Reflectors, and Sensing Devices	1129
3.2.2. Distributed Feedback and Distributed Bragg Reflector Lasers	1130
3.2.3. 2D Photonic Crystals and Lasers	1131
3.2.4. Nonlinear Optical Polymer-Based Electro-optic Devices	1132
3.2.5. Light-Emitting Devices	1132
3.3. Imprint Lithography	1133
3.3.1. Light-Emitting Devices	1134
3.3.2. Thin-Film Transistors	1134
3.4. Capillary Molding	1136
4. Patterning by Printing	1137
4.1. Stamps	1137
4.1.1. Microcontact Printing Chemical Templates	1138
4.1.2. Direct Patterning with a Stamp	1140
4.1.3. Lamination	1144
4.2. Laser Printing and Imaging	1146
4.3. Physical Masks	1148
4.3.1. Screen Printing	1148
4.3.2. Shadow Masks (Stencil Masks)	1148
4.4. Scanned Nozzles	1150
4.4.1. Organic Vapor Jet Printing	1150
4.4.2. Inkjet Printing	1150
5. Conclusion	1155
6. Acknowledgment	1156
7. References	1156

## 1. Introduction

The first organic transistors on plastic substrates were reported in 1990, providing an early hint of the possibilities offered by plastic electronics. These devices used vacuum-evaporated films of  $\alpha$ -sexithiophene for the semiconductor, bendable thin sheets of poly(paranic acid) resin (PPA) for the substrate, solution-cast cyanoethylpullulan (CYEPL) for the gate dielectric, and evaporated layers of gold for the source, drain, and gate electrodes.<sup>1,2</sup> These transistors followed reports of devices achieved on rigid substrates a few years earlier using the polymer polythiophene as a semiconductor.<sup>3</sup> Similar levels of excitement accompanied the first light-emitting diodes based on small molecules<sup>4</sup> and polymers,<sup>5</sup> in 1982 and 1990, respectively. Devices such as these, in which the active and passive elements can be formed by low-cost processing techniques on lightweight, rugged, bendable substrates, have the potential to enable new classes of electronic devices, from flexible, large-area emissive displays to low-cost radiofrequency identification tags to smart labels and sensors. It is interesting to note that the first transistor, invented by Bardeen, Brittain, and Shockley at Bell Laboratories in 1947, also used plastic for a key component, although not the active material. In this device, an insulating plastic triangle pressed a strip of gold against a germanium crystal to form the point contacts.<sup>6</sup> One can speculate that plastic was attractive for this component for reasons—easy processability, low cost, mechanical toughness, and compliance—similar to some of the reasons that drive current interest in organic materials for active and passive elements in electronics and optoelectronics.

The evolution of inorganic technology from its discovery to its current state provides a useful context to evaluate progress with the organics. Ten years passed after the invention of the first transistor before Jack Kilby of Texas Instruments and Robert Noyce of Fairchild Semiconductor co-invented the integrated circuit. Initial demonstration systems involved one transistor, one capacitor, and three resistors integrated on a  $7/16 \times 1/16$  in. single-crystal germanium substrate. Noyce's "planar" layout remains the founda-

\* Address correspondence to this author at the Department of Materials Science and Engineering, University of Illinois at Urbana-Champaign, 1304 W. Green St., Urbana, Illinois 61801 [telephone (217) 244-4979; fax (217) 333-2736; e-mail jrogers@uiuc.edu].

<sup>†</sup> University of Illinois at Urbana-Champaign.

<sup>‡</sup> Argonne National Laboratory.



Etienne Menard was born in 1980 in Limoges, France. He obtained an engineering diploma in electronics from the National Polytechnic Institute of Engineering in Electrotechnology, Electronics, Computer Science and Hydraulics (Toulouse, France) in 2002. From the University "Pierre et Marie Curie" (Paris, France), he received in 2005 a Ph.D. degree in chemistry under the direction of Denis Fichou at the Laboratoire des Semi-Conducteurs Organiques (CEA/SACLAY, France) and Professor John A. Rogers in the Department of Material Science and Engineering at the University of Illinois at Urbana–Champaign. He recently joined Semprius, Inc. (founded by Professors John A. Rogers, Ralph G. Nuzzo, and George M. Whitesides) as co-founding scientist.



Matthew A. Meitl earned a B.S. degree in Materials Science and Engineering from the University of Illinois at Urbana–Champaign in 2002. He is currently a Ph.D. candidate at the same university, with a fellowship from the Fannie and John Hertz Foundation.

tion of today's integrated circuits. The dominant technique for patterning these circuits is photolithography, which represents an adaptation of much older photo-based methods used in the graphic arts as early as the 1800s. Projection mode tools were introduced 15 years after the integrated circuit to improve production throughputs and to avoid contact induced damage of the expensive optical masks. Improvements in the resolution of this process enable smaller devices, higher operating speeds, and lower operating voltages in progressively denser circuits, all with roughly the same chip sizes. This favorable scaling has led to a central role for photolithography in realizing improvements in microelectronics, where levels of integration have doubled every 18 months, a scaling known as Moore's law. The current generation of commercial logic chips for microprocessors, for example, involves critical dimensions of 90 nm, chip sizes of  $\sim$ 100–200 mm<sup>2</sup>, and total numbers of transistors in the range of  $\sim$ 100 million. The cost associated with the fabrication facilities needed to build such systems, however, increases at rates similar to those that govern the



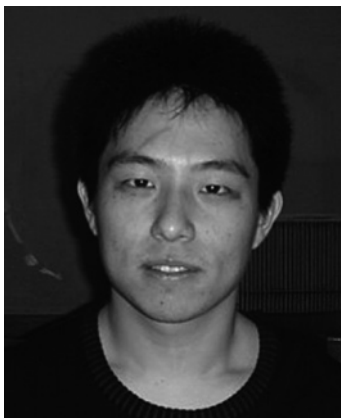
Yugang Sun received B.S. and Ph.D. degrees in chemistry from the University of Science and Technology of China (USTC) in 1996 and 2001, respectively. From March 2001 to July 2006, he worked with Professor Younan Xia at the University of Washington and Professor John A. Rogers at the University of Illinois at Urbana–Champaign as a postdoctoral research associate. He is currently Assistant Chemist—Nanoscientist of the Center for Nanoscale Materials in Argonne National Laboratory. His research interests include synthesis and characterization of nanostructures, micro/nanofabrication, nanobiology and nanomedicine, and devices for optics and electronics.



Jang-Ung Park was born in the Republic of Korea (ROK). He received his master's degree in materials science and engineering from Korea Advanced Institute of Science and Technology (KAIST) in 2003. He is currently a Ph.D. candidate in materials science working under the direction of Professor John A. Rogers at the University of Illinois at Urbana–Champaign. His thesis research focuses on the materials and device designs for printed optoelectronic devices.

levels of integration. This cost scaling, which is sometimes known as Moore's second law, makes the economics difficult to justify for all but the largest companies and consortia. This situation is expected to be particularly acute beyond the 45 nm resolution node, where many expect that the basic paradigm of photolithography as it exists today (soon likely to be carried out at 193 nm in water immersion systems), will be abandoned in favor of other approaches. In any case, one can argue that patterning technologies, at least as much as materials and device designs, have provided, and may continue to provide, a tremendously powerful tool to help enable exponential increases in capabilities and market sizes for traditional microelectronics.

Different kinds of electronic systems, built with thin-film materials over large areas (recently referred to as "macroelectronics") are capturing an increasingly large fraction of worldwide sales in electronics, mainly through their use as backplane circuits for active matrix liquid crystal displays. Here, area coverage is the key metric, rather than operating



Daniel Shir graduated with distinction and obtained a B.S. degree in materials science and engineering from the Pennsylvania State University in 2005. He is currently pursuing a Ph.D. degree in materials science and engineering at the University of Illinois at Urbana–Champaign under Professor John A. Rogers's guidance.



Yun-Suk Nam obtained a Ph.D. degree in chemical engineering from Sogang University, Seoul, South Korea, in 2004. He is currently a postdoctoral researcher in the Department of Materials Science and Engineering at the University of Illinois at Urbana–Champaign.

speeds or integration densities. The size of the substrate defines the technology generation, rather than channel lengths of the transistors. Some of the first commercial flat-panel displays used substrates (glass) with sizes of  $270 \times 200$  mm, known as Gen 0 glass, and were adopted by Sharp in 1987 to manufacture 8.4 in. displays. Currently, Gen 7 glass is in production ( $1870 \times 2200$  mm), and by 2006, systems will be built on Gen 8 glass, which is expected to be  $2200 \times 2500$  mm in size. As with conventional integrated circuits, the manufacturing procedures and the patterning processes are the main drivers of progress. These large-area systems are currently patterned with photolithographic processes, although instead of optics that project a demagnified image of the mask, for the case of integrated circuits, magnifying optics and step-and-repeat stages capable of stitching together multiple images are used. Whereas the integrated circuit industry uses mainly single-crystal silicon in wafer form, the semiconductor of choice for flat-panel displays is sputtered thin-film amorphous silicon (a-Si). Deposition, etching, and patterning of this material, and other vacuum-deposited materials needed for the circuits, become very challenging technically and, as a result, costly at these large size scales. In addition, basic mechanical manipulation of extremely large, thin, and brittle glass substrates is a major concern.

Organic systems are being developed against the backdrop of these conventional and large-area electronics technologies,



Seokwoo Jeon was born in Seoul, Korea, in 1975. He received his B.S. degree in 2000 and his master's degree with Professor Shinhoo Kang from Seoul National University in 2003 after one year as an exchange graduate student with Professor Paul V. Braun at the University of Illinois at Urbana–Champaign (UIUC). He is currently pursuing his Ph.D. degree in materials science and engineering at UIUC under the direction of Professor John A. Rogers. His research interests include soft lithography, 3D nanopatterning, microfluidic systems, and optically functional materials and devices.



John A. Rogers obtained B.A. and B.S. degrees in chemistry and in physics from the University of Texas, Austin, in 1989. From MIT, he received S.M. degrees in physics and in chemistry in 1992 and the Ph.D. degree in physical chemistry in 1995. From 1995 to 1997, Rogers was a Junior Fellow in the Harvard University Society of Fellows. He joined Bell Laboratories as a Member of the Technical Staff in the Condensed Matter Physics Research Department in 1997 and served as director of that department from the end of 2000 to the end of 2002. He is currently Founder Professor of Engineering at the University of Illinois at Urbana–Champaign, with appointments in the Departments of Materials Science and Engineering, Electrical and Computer Engineering, and Mechanical and Industrial Engineering and Chemistry.

where the dominant semiconductor is silicon in single-crystalline, polycrystalline, or amorphous forms. Much of this work seeks to create, at least initially, niche applications where established materials and/or patterning techniques might not provide the necessary low-cost structure (e.g., radiofrequency identification tags for product level implementation), form factor (e.g., mechanically flexible displays), area coverage (e.g., aircraft sensor skins), or performance (e.g., fast, high brightness, and power-efficient light-emitting displays). This last example is emerging as a potential success story, as organic light-emitting diodes can now be found in commercially available small, emissive flat-panel displays. This development comes roughly 10 years after Kodak and Sanyo demonstrated the first prototype of a full-color 5.5 in. diagonal display of this type. More recently, in 2004,

**Table 1.**

	resolution on plastic/glass substrates	materials compatibility	readiness level	ref
large-area photolithography	~3 μm	resists, functional organics	in production (e.g., LCD displays)	7
optical soft lithography embossing	~90 nm ~1 nm	resists, functional organics moldable resists, functional organics	research in production (e.g., DVDs)	8, 9 10–14
hard imprint lithography	<10 nm	moldable resists, functional organics	early production	15–19
soft imprint lithography	<10 nm	moldable resists, functional organics	research	20
capillary molding	~2–5 μm and below	resists, low-viscosity inks, functional organics	research	21–24
soft printing	~0.1–2 μm	SAMs, thin metals, organic and inorganic semiconductors	development	25–29
laser imaging	~5 μm	organic conductors, semiconductors and electroluminescent materials, others	early production (LCD color filters)	30–32
inkjet printing	~10–20 μm without surface treatment	organic conductors, low molecular weight polymers, wax, others	in production (graphic arts)	33–35

Epson produced a 40 in. display with organic light-emitting diodes and silicon backplanes, thereby demonstrating organics as a serious alternative to LCD technology for large-area devices. For the near term, these kinds of displays as well as systems that demand low-cost, bendable, or large-area form factors appear to offer the most promise for potential consumer applications because conventional approaches cannot easily achieve such characteristics. The area of displays has the additional feature that the most widely used semiconductor (*a*-Si) has modest carrier mobilities (typically of only ~1 cm<sup>2</sup>/V·s), comparable to those that can be achieved routinely with the organics. The development of new materials for these circuits and the continued improvement of organic light-emitting diodes represent promising areas for fundamental and applied research, as described in other papers in this issue.

By analogy with integrated circuits and thin-film electronics, where progress has been driven largely by the manufacturing and patterning techniques, we speculate that the promise of organic electronics and optoelectronics will be realized fully when efforts to develop low-cost, large-area printing-like manufacturing techniques are successful. This paper reviews work in this area, with an emphasis on those methods that have been successfully applied to the fabrication of working organic devices. The examples range from sophisticated forms of inkjet printing, laser thermal imaging, and microcontact printing, which have been used to build prototype displays (see Figure 35c), to soft imprinting and capillary molding, which have been used only in research demonstrations of discrete transistors. The goals of these techniques are similar: to pattern active or passive components of optoelectronic systems in ways that enable (i) low-cost manufacturing, (ii) manipulation of unusual, and often chemically and mechanically fragile, organic materials, (iii) patterning capabilities (e.g., straightforward compatibility with continuous reel-to-reel processing or rough/curved substrates) that scale to large areas and high throughput, or (iv) some combination of these attributes. The paper begins with established and unconventional procedures for using light to form devices. An advantage (and disadvantage) of these types of approaches is that they are operationally similar to the well-established photolithographic techniques used for conventional electronics. Next, the paper describes methods that rely on physical molding, where the commercial analogue is embossing for replication of compact discs and digital video discs (Table 1). Printing methods are then discussed, with highlights from techniques that range from inkjet printing to screen printing and rubber stamping. In

these cases, the most similar existing manufacturing techniques are those used in the printed paper industry: flexography, inkjet and laser printing, offset printing, and so on. We conclude with some thoughts on the progress of developments in organic optoelectronics, as benchmarked against the integrated circuit and thin-film electronics areas and liquid crystal devices, the future of this technology, and some emerging trends.

## 2. Light-Based Patterning Techniques for Organic Electronics

Projection mode photolithography represents, by far, the dominant manufacturing approach for inorganic electronics and optoelectronics, due to its high speed, parallel patterning capability, and high resolution. These features also make it attractive for applications for organic devices, although straightforward implementations can be difficult due to (i) the incompatibility of photoresists, solvents, developers, and ultraviolet (UV) exposure light with many organic active materials, (ii) challenges in resolution and registration caused by rough, and often dimensionally unstable, plastic substrates, and (iii) cumbersome implementations needed for large-area patterning. Nevertheless, there are a very large number of cases of organic devices in which certain layers are patterned by photolithographic methods and conventional photoresists. This section does not attempt to summarize these examples or the many cases in which dielectric or waveguide materials are patterned by photolithography. Instead, it reviews materials and processing strategies to form active layers of organic devices by photolithography and some unusual photolithographic techniques that appear to have promise for this area.

In the most general sense, a photopatterning process starts by coating a substrate with a material having properties that can be changed by exposure to light. Patterned exposure is most commonly achieved by passing light through a rigid mask that manipulates the phase and/or amplitude. The mask can be located in direct contact with (contact mode) or in proximity to (proximity mode) the photosensitive material. Alternatively, imaging optics can magnify or demagnify the mask image and project it onto this material (projection mode). Although contact mode offers high resolution, it was abandoned as a technique for patterning inorganic devices due to unavoidable contamination and damage of the masks and/or substrates due to the required physical contact. Difficulties with maintaining small, fixed distances between masks and substrates and poor resolution represent significant drawbacks for proximity mode operation. Projection mode

photolithography avoids these problems, and it does not require contact with the substrate. In addition, its reduction optics enable the use of masks with low-resolution features (i.e., low cost) compared to those needed for the devices. Reviews on photolithography and photoresist materials provide additional details.<sup>36–40</sup> Many examples of organic electronic and optoelectronic devices use photolithography and conventional photoresists to pattern the electrodes, dielectrics, encapsulating layers, and other elements. In these systems, care is taken to develop processing sequences and material choices that yield device properties that are not degraded by the photolithographic process steps. For example, the photolithographic steps often are designed to occur before the deposition of the active organic layers. Alternatively, thin protecting layers of materials, such as parylene, can be deposited on top of these active layers, such as the organic semiconductor pentacene, to protect them from the photoresists, solvents, and developers.<sup>41</sup> The following sections describe methods that use photopatternable active materials for these devices or nonstandard techniques for performing the exposures in ways that are beneficial to organic devices.

## 2.1. Photopatternable Organic Electronic Materials

Careful chemical design enables organic active materials that can be both photodefinable and effective at charge transport or light emission. Efforts over the past few years have yielded several promising examples. This section provides a short overview of some of these materials for the conducting, semiconducting, and electroluminescent layers, with descriptions of their use in transistors, light-emitting diodes, and related devices.

### 2.1.1. Photopatternable Organic Materials for Semiconductor

Several types of organic semiconductors have been designed to enable direct photopatterning. Pentacene is probably the most extensively studied organic semiconductor due mainly to its good field effect mobility as high as  $\sim 1 \text{ cm}^2/\text{V}\cdot\text{s}$ . Figure 1a shows, as an example, a photopatternable pentacene precursor.<sup>42</sup> Exposing a spin-cast layer of this precursor (**1** in Figure 1a) to UV light polymerizes the exposed regions to form the polymer (**2** in Figure 1a), as illustrated in Figure 1a. Washing the sample in methanol removes the unexposed precursor. Heating then converts the polymerized precursor to pentacene and a carbonyl and *N*-sulfinyl group substituted polymer. Figure 1b shows another type of photopatternable pentacene precursor.<sup>43</sup> In the presence of a photoacid generator (PAG), 3 mol % of di-*tert*-butylphenyliodonium perfluorobutanesulfonate in this case, UV irradiation generates protons from the PAG and cleaves the pentacene precursor into *N*-sulfinyl-*tert*-butyl-carbamate and pentacene. Washing the sample in methanol removes the unexposed regions.<sup>43</sup>

The patterning process for these materials is similar to photolithography with a conventional negative-tone photoresist. Figure 1c shows patterns of pentacene formed using the precursors in Figure 1a,b. The mobilities of devices using the precursor in Figure 1a are in the range of  $0.021 \text{ cm}^2/\text{V}\cdot\text{s}$  in the saturation regime,<sup>42</sup> which is somewhat lower than that obtained with evaporated pentacene, possibly due to the presence of the residual polymer from the patterning process. The  $I_{\text{on}}/I_{\text{off}}$  ratios were  $>2 \times 10^5$ . The precursor in Figure 1b yields better performance. The highest measured

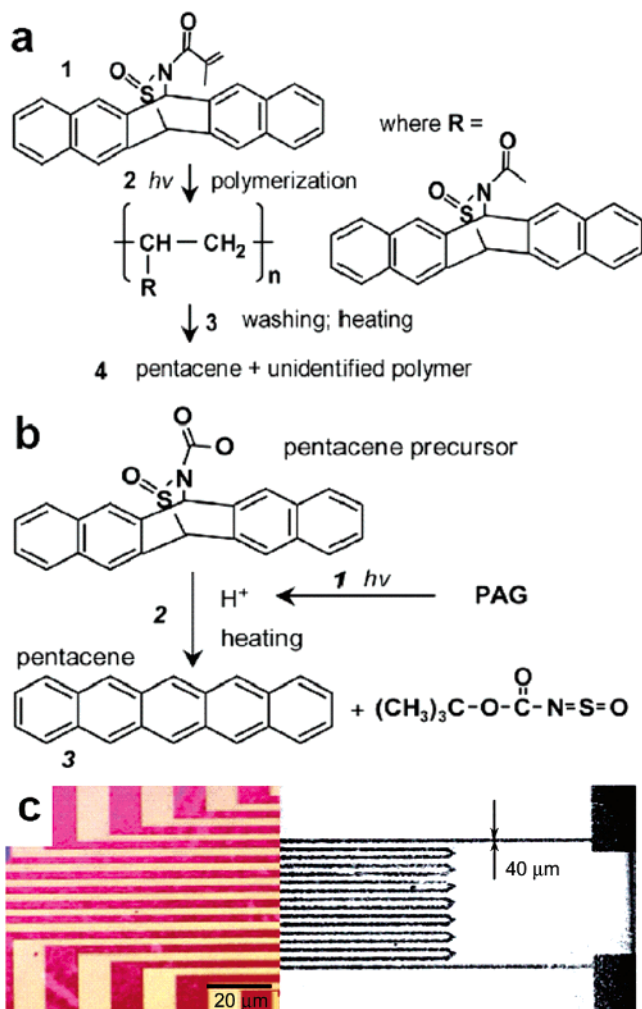


**Figure 1.** (a) Process of photopatterning pentacene by use of a polymer precursor approach. UV exposure polymerizes the pentacene precursor **1**. Washing the sample in methanol removes the unexposed precursor **3**. Heating converts the polymerized precursor to pentacene **4**. (Reprinted with permission from ref 42. Copyright 2003 Wiley-VCH Verlag.) (b) Process of photopatterning pentacene by use of a decomposition approach: 1, UV exposure generates  $\text{H}^+$  from PAG; 2,  $\text{H}^+$  decomposes the pentacene precursor to pentacene; 3, washing with methanol removes the unexposed precursor. (Reprinted with permission from ref 43. Copyright 2004 American Chemical Society.) (c) Optical image of a photopatterned layer of pentacene; patterns on the left and right used chemistries illustrated in (a) and (b), respectively. (Reprinted with permission from refs 42 and 43. Copyright 2003 Wiley-VCH Verlag and 2004 American Chemical Society, respectively.)

mobilities and  $I_{\text{on}}/I_{\text{off}}$  ratios were  $0.25 \text{ cm}^2/\text{V}\cdot\text{s}$  and  $>8 \times 10^4$ , respectively.<sup>43</sup> Background information on organic electronic device fundamentals, architecture, and operation can be found in recently published textbooks.<sup>44,45</sup>

### 2.1.2. Photopatternable Organic Conductive Materials

Photopatternable organic conductors, which can serve as hole-transport layers in organic light-emitting diodes (OLEDs) and interconnects or electrodes in organic thin-film transistors (OTFTs), also exist. Polyaniline (PANI) and polythiophenes represent two examples of organic conductors that are widely studied. The nonconductive and undoped form of PANI is soluble in organic solvents, whereas the doped PANI is typically insoluble. Direct photopatterning of conducting PANI can take advantage of this solubility difference.<sup>46–48</sup> For example, UV or electron-beam (e-beam)

exposure of PANI mixed with onium salts through a rigid mask initiates decomposition of the onium salts and generates acid. The acid converts the exposed PANI into insoluble conductive form, with onium salts as the dopant, whereas the unexposed (undoped and nonconductive) PANI remains soluble and can be removed by washing with 2-methoxyethyl ether/*N*-methylpyrrolidinone (NMP) solution. This material can also be used for electrodes and interconnects in OLEDs and OTFTs. For example, all-polymer integrated circuits (ICs) can be formed using camphorsulfonic acid (CSA) doped PANI (PANI-CSA) for the conductors, polythiophenevinylene (PTV) as the semiconductors, and polyvinylphenol (PVP) as the dielectrics.<sup>49</sup> In this case, PANI-CSA with a photoinitiator, 1-hydroxycyclohexylphenylketone, was spin-coated onto a polyimide foil. UV exposure generates free radicals from the photoinitiator. These radicals cleave the CSA group from the PANI and produce a nonconductive leucoemeraldine base PANI.<sup>50,51</sup> The unexposed regions have sheet resistances of 1 k $\Omega$ /square after removal of the photoinitiator by postbaking. The resistance of the exposed region increases dramatically from 1 k $\Omega$ /square to 10<sup>14</sup>  $\Omega$ /square. Conducting pathways formed in PANI film serve as interconnects and electrodes.<sup>49</sup> Panels a and b of Figure 2 show the current–voltage ( $I$ – $V$ ) characteristics of an individual device and an image of integrated circuit formed in this manner.<sup>49</sup>

Functional group substituted PANI provides another route to photopatternable PANI. For example, a *tert*-butoxycarbonyl (*t*-BOC) substituted PANI, dissolved in THF with PAG such as norborneneimide compounds with different organic counter groups of *N*-(10-camphorsulfonyloxy) norbornene-imide (CSNBI), and *N*-(tosyloxy)norborneneimide (TSNBI), or onium salt triphenylsulfonium triflate (TPSOTf) can be patterned by photolithography.<sup>52</sup> To pattern the *t*-BOC substituted PANI mixed with PAG, a solution is spin-coated onto a substrate and exposed to UV light. UV exposure decomposes the PAG and generates acid. The acid cleaves the *t*-BOC group from PANI and converts the PANI into an conductive and insoluble PANI–emeraldine salt after postbaking at 110 °C. Figure 2c gives the scheme for the chemical process. The unexposed regions can be removed by washing in chloroform (CHCl<sub>3</sub>) to generate negative tone conducting patterns.<sup>52</sup> The electrical conductivity of the patterned PANI film is ~10<sup>-3</sup> S/cm. Further doping by hydrochloric acid (HCl) vapor can improve the conductivity to 3–5 S/cm, which is similar to that achieved with the conventional HCl doping method.<sup>52</sup>

In addition to PANI, polythiophenes can be used as photopatternable organic conductors. One example uses a photocatalytic chemical reaction of poly(3-(2-(tetrahydropyran-2-yloxy)ethyl)thiophene) (PTHPET) with *N*-(trifluoromethylsulfonyloxy)-1,8-naphthalimide as the PAG.<sup>53</sup> Here, UV exposure generates trifluoromethanesulfonic acid (triflic acid; CF<sub>3</sub>SO<sub>3</sub>H) from PAG, as shown in Figure 2d. The triflic acid initiates a catalytic reaction to cleave the tetrahydropyran (THP) from the PTHPET. THP cleavage generates another proton, thereby amplifying the reaction. The resulting polymer has a shorter side chain with a different polarity compared to the original PTHPET and is, therefore, insoluble in most common solvents.<sup>53</sup> This PTHPET can be patterned with feature sizes as small as 15  $\mu$ m and with conductivities of 1–4 S/cm depending on the doping oxidants.<sup>53</sup> Figure 2e shows a PTHPET pattern formed in this manner. Other classes of conductive materials that can be patterned by

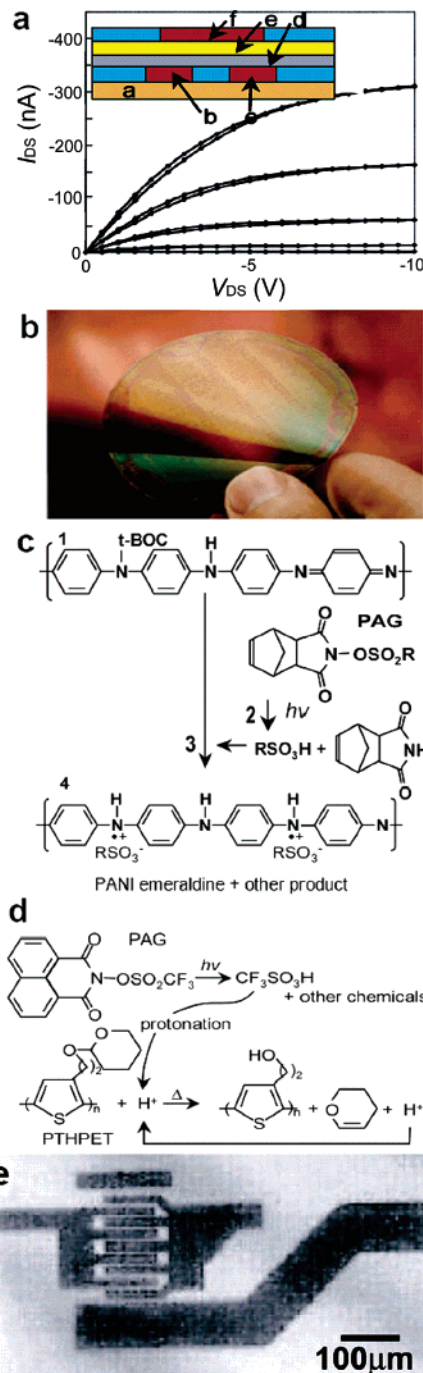
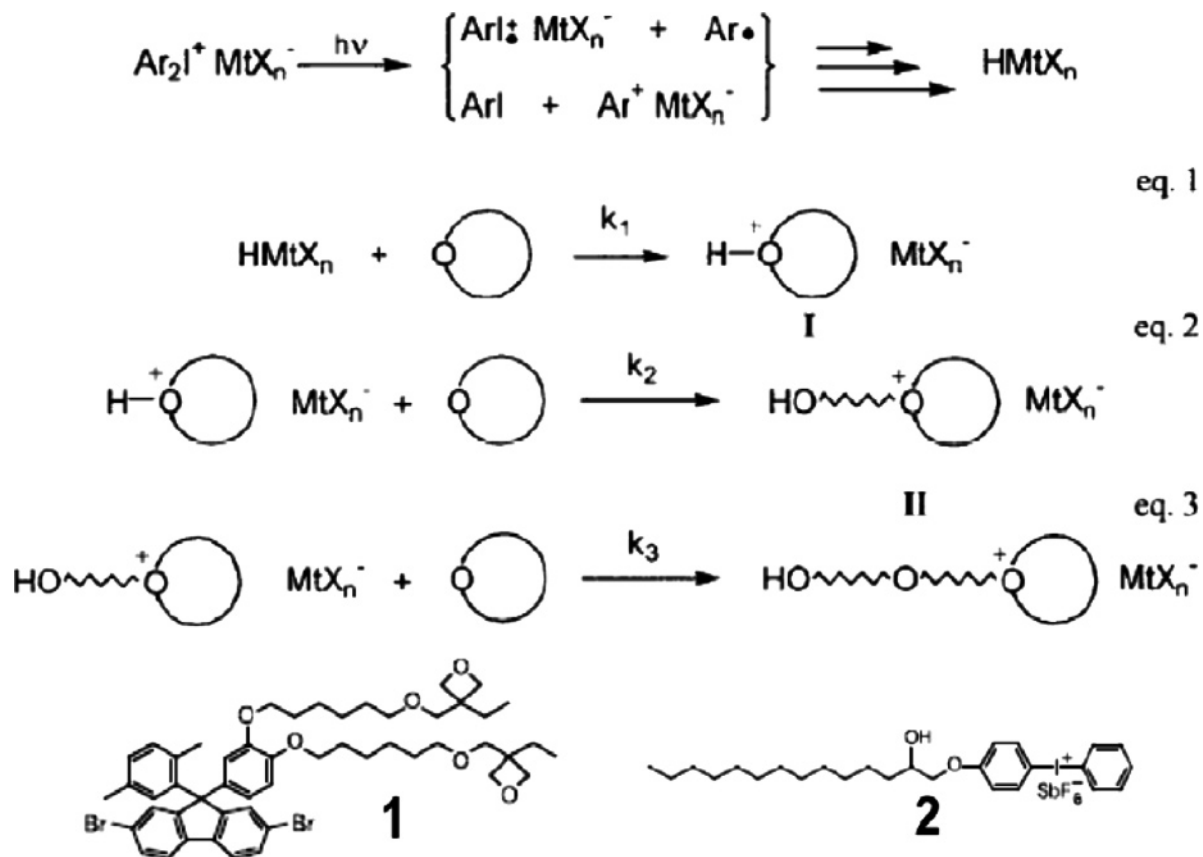


**Figure 2.** (a) Electrical characteristics of an all-polymer transistor. The inset shows the structure, which involves a polyimide substrate (a), source (b), and drain (c) electrodes of photopatterned PANI, a semiconductor layer of PTV (d), a dielectric layer of PVP (e), and a top gate electrode of PANI (f). (Reprinted with permission from ref 49. Copyright 1998 American Institute of Physics.) (b) Image of a 3 in. flexible substrate with a variety of polymer-based electronic devices. (Reprinted with permission from ref 49. Copyright 1998 American Institute of Physics.) (c) Acid-catalyzed reaction of doped PANI induced by exposure to UV light: 2, UV exposure decomposes the PAG and generates protonic acid; 3, this acid donates H<sup>+</sup> and cleaves the *t*-BOC group from doped PANI **1** to convert the *t*-BOC-substituted PANI into a PANI emeraldine salt **4**. (Reprinted with permission from ref 52. Copyright 2004 American Chemical Society.) (d) Chemically amplified reaction of PTHPET initiated by UV exposure. The H<sup>+</sup> generated from PAG cleaves the THP from PTHPET. (Reprinted with permission from ref 53. Copyright 1998 Chemical Communications.) (e) Pattern of PTHPET formed by photolithography. (Reprinted with permission from ref 53. Copyright 1998 Chemical Communications.)

**Scheme 1.** Photoinduced Polymerization and Chemical Structure of an Oxetane-Functionalized Electroluminescent Material **1** and the Cationic PAG **2**<sup>59,60a</sup>



<sup>a</sup> Reprinted with permission from *Nature* (<http://www.nature.com>), ref 59. Copyright 2003 Nature Publishing Group. Reprinted with permission from ref 60. Copyright 2004 Wiley Periodicals, Inc.

photopolymerization include oxetane functionalized triphenyl amine<sup>54</sup> and cross-linkable bis(diarylamino)biphenyl-based copolymers.<sup>55</sup>

Poly(3-hexylthiophene) (P3HT) can also be patterned by cross-linking through a photooxidation process. The photo-oxidation of P3HT begins by chain scission initiated by residual metal salts, ferric salt in this case, from the polymer synthesis. UV or visible light exposure initiates the photoreaction to generate free radicals. The free radicals can remove the hydrogen atoms on the hydrocarbons and form hydroperoxide in the presence of oxygen. Further light exposure cleaves the peroxide and produces radicals bound to the polymer that can form ether linkages.<sup>56</sup> The exposed region of P3HT is insoluble, whereas the unexposed regions remain soluble. Light exposure through a rigid photomask can, therefore, selectively expose P3HT film to form desired patterns. Washing the exposed sample in toluene gives a negative tone pattern. Lines as narrow as 1  $\mu$ m can be patterned by this photopatterning technique.<sup>57</sup> The conductivity can be improved by oxidation. For example, 5 S/cm was obtained by immersing the P3HT film into an anhydrous saturated solution of nitrosonium tetrafluoroborate.<sup>58</sup>

### 2.1.3. Photopatternable Organic Light-Emitting Materials

Photolithography can also be used to define patterns in electroluminescent layers. Three oxetane-functionalized spiro-bifluorene-*co*-fluorene polymers that can emit blue, green, and red light represent important examples. The detailed compositions of each polymer can be obtained elsewhere.<sup>59</sup> Briefly, UV irradiation decomposes a PAG, ({4-[2-

hydroxytetradecyl)oxyl]phenyl})phenyliodonium hexafluorantimonate), to generate an acid that initiates cross-linking through a protonic polymerization of the oxetane functionalized precursors. The protons generated from PAG open the oxetane ring of the oxetane precursor and initiate the chain polymerization.<sup>60</sup> Scheme 1 illustrates the chemistry. The resulting polymers have cations at the chain ends instead of the oxetane groups. To neutralize the polymer, the sample is rinsed in pure THF. These materials enable multicolor OLEDs to be patterned directly using a process similar to conventional photolithography.<sup>59</sup> The resulting devices exhibit slightly improved efficiency compared to the non-cross-linked references (Figure 3b) at high luminance and with slightly reduced turn-on voltages.<sup>59</sup>

Another route to photopattern electroluminescent layers involves selective photobleaching. This technique can be used with a variety of materials such as poly(*p*-phenylenevinylene) (PPV) derivatives including poly(2-methoxy-5-(2-ethylhexyloxy)-1,4-phenylenevinylene) (MEH-PPV),<sup>61</sup> didodecylpoly-dialkylstilbenevinylene (didodecyl-PSV),<sup>62</sup> and poly(2,5-dialkoxy-*p*-phenylene ethynylene) derivatives (EHO-OPPE) blended with polyethylene (PE) and 1,4-bis(5-phenyl-2-oxazolyl)benzene (POPOP) mixed with linear low-density polyethylene (LLDPE).<sup>63</sup> The photobleaching process involves photon-induced chemical damage and covalent modification to the fluorophore, which lead to permanent loss of luminescence. EHO-OPPE/PE, which exhibits green color, and POPOP/LLDPE, which possesses blue color, patterned by photobleaching provide an examples.<sup>63</sup> Panels a and b of Figure 4 show the chemical structures and an image of the

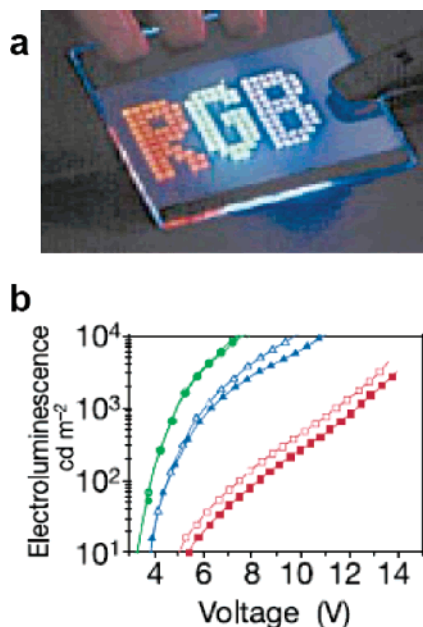


**Figure 3.** (a) Image of a color OLED device formed with photo-patterned layers of these materials. [Reprinted with permission from *Nature* (<http://www.nature.com>), ref 59. Copyright 2003 Nature Publishing Group.] (b) Electroluminescence as a function of applied voltage. [Reprinted with permission from *Nature* (<http://www.nature.com>), ref 59. Copyright 2003 Nature Publishing Group.]

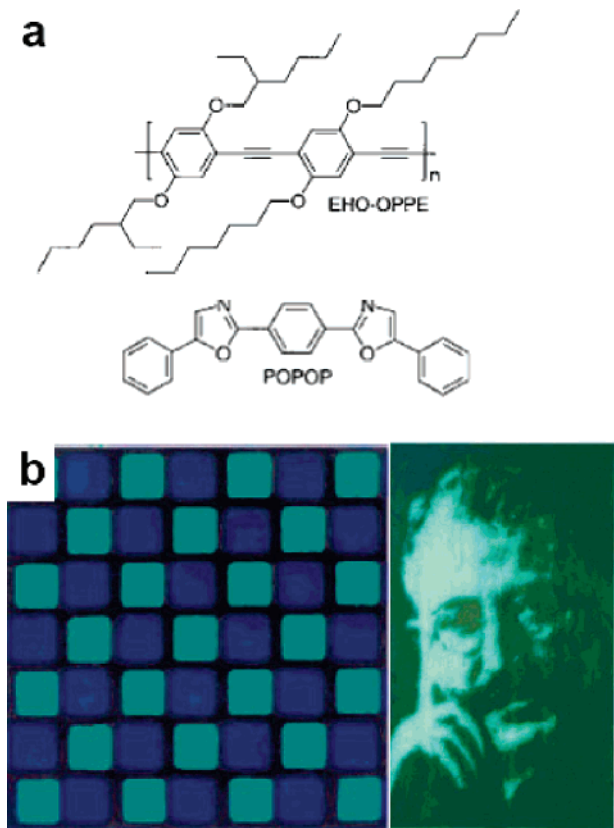


**Figure 4.** (a) Molecular structures of the photoluminescent compounds EHO-OPPE and POPOP. (b) Image of luminescence by photobleaching of an oriented EHO-OPPE film fabricated by 365 nm UV exposure. (Reprinted with permission from ref 63. Copyright 2001 Wiley-VCH Verlag.)

emitting device consisting of an EHO-OPPE/PE and POPOP/LLDPE bilayer oriented in a pattern similar to that of a chessboard.<sup>63</sup> Although photobleaching can pattern the

emission layer effectively and simply, the material in the bleached areas remains on the substrate, which may affect the device layout and/or the architecture of the interconnects to neighboring devices.

## 2.2. Optical Soft Lithography

Soft lithography refers to a collection of techniques that use soft, conformable elements for pattern transfer by various forms of molding and printing, as described in subsequent sections, as well as unusual versions of contact mode photolithography discussed here.<sup>64,65</sup> In this last approach, which we refer to as optical soft lithography, conformable elastomeric elements with relief features on their surfaces serve as photomasks for patterning the exposure of layers of photoresist or other photosensitive materials.<sup>8,9,20,66–73</sup> The nondestructive, reversible, atomic scale contacts that can be established, without applied pressure, through generalized adhesion forces (typically van der Waals) between the mask and the resist layer (typically a solid thin film) are key to this process.<sup>74–76</sup> Figure 5 presents a schematic illustration of a relief structure on a mask, along with computed intensity profiles and corresponding structures produced in photoresist. A casting and curing process with a prepolymer to poly(dimethylsiloxane) (PDMS) forms elastomeric phase masks that are transparent in the UV range (> 300 nm). A following section describes some details of the fabrication procedures, which are the same as those for soft stamps and molds. Placing such a mask against a thin layer of photosensitive material leads to conformal contact, without applied pressure. Shining UV light through the mask, while in this configuration, exposes the thin layer of photoresist to the distribution of intensity that forms as a result of light transmission through mask. The relief structures modulate the phase of the transmitted light by an amount determined by their depth and the index of refraction of the mask material. In the simple case of binary relief with a depth that causes a shift of the phase of  $\Pi$ , nulls in the intensity appear at each step edge of the relief. The widths of these nulls can be ~100 nm when using ~365 nm light from a conventional mercury lamp and standard photoresists.<sup>8,67,68</sup> Exposing a positive resist, removing the mask, and then developing yields ~100 nm wide lines of resist. Depositing a uniform layer of metal and then lifting off the resist with acetone leaves ~100 nm wide gaps in the metal. These types of structures are useful for short-channel organic transistors, in which the slits define the channel lengths and a separate patterning step defines the widths. Figure 6a shows an example of a Au film (~20 nm thick with 1 nm Ti adhesion layer) with a 100 nm channel formed by lift-off of the patterned positive resist. Figure 6b presents the  $I$ - $V$  characteristics of *n*-channel transistors formed with copper hexadecafluorophthalocyanine ( $F_{16}CuPc$ ).<sup>68</sup> These devices use source/drain electrode pairs patterned by phase-shift lithography on a thin dielectric (much thinner than the width of the channel) and back gate electrode, with the organic semiconductor on top. The  $I$ - $V$  characteristics of a typical device show behaviors (i.e., nonlinear response in the regime of small source/drain voltages) that indicate contact limited response.<sup>68</sup> The mobility,  $I_{on}/I_{off}$ , and saturation currents of such device are ~0.001 cm<sup>2</sup>/V·s, >25:1, and ~1–4  $\mu$ A, respectively. Complementary inverter circuits formed using *n*- and *p*-channel devices of this type further demonstrate the utility of this approach, which represents one of the simplest methods to sub-micrometer channel length devices.<sup>68,77</sup>

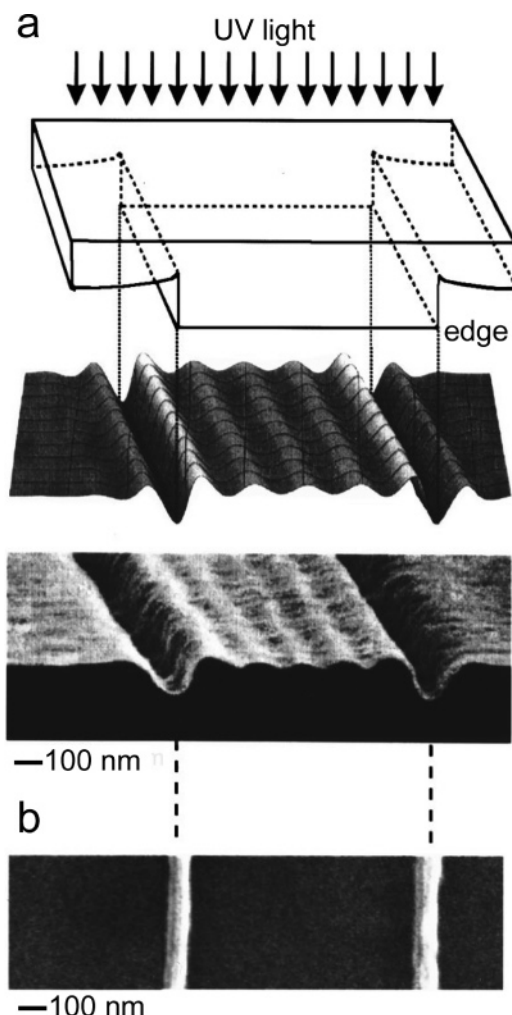


**Figure 5.** Mechanism and experimental results for a form of photolithography that uses a conformable phase mask. (a) Passage of light through a binary elastomeric phase mask (top frame) and distribution of intensity near its surface computed (middle frame) and measured using an image reversal photoresist (bottom frame). The dips in intensity at the step edges have characteristic widths of  $\sim 100$  nm when 365 nm light is used. The small-amplitude oscillations in intensity are associated with diffractive effects due to the step edges in the mask. (b)  $\sim 100$  nm wide lines formed using this process. (Reprinted with permission from ref 68. Copyright 1999 American Institute of Physics.)

These phase effects can also be exploited to generate structures with more complex geometries. In particular, they can be designed to cause shadowing to pattern broad features<sup>71,73</sup> or as subwavelength lenses and light-coupling elements to define features in the geometry of the relief structures.<sup>9,73</sup> They can also create complex two- and three-dimensional patterns.<sup>66,69,72</sup> Figure 7 shows the different line patterns formed using a single phase mask (5.6  $\mu\text{m}$  line width, 4.4  $\mu\text{m}$  spacing, and a relief depth of 1.42  $\mu\text{m}$ ) by using different exposure doses.<sup>73</sup> The two-dimensional patterns can serve as electrodes for light-emitting devices using polymer electroluminescent materials, with interesting spatial emission patterns and performance characteristics.<sup>52,71</sup> Figure 8 illustrates, as an example, patterned devices with sub-micrometer emission widths.<sup>78</sup> The OLED demonstrated in Figure 8 consists of 150 nm Au lines on PDMS patterned by phase shift lithography. The line width of pattern emission ( $\sim 600$  nm) is close to the resolution limit of the optical imaging system (590 nm) with efficiency of 0.23% ph/el.<sup>78</sup>

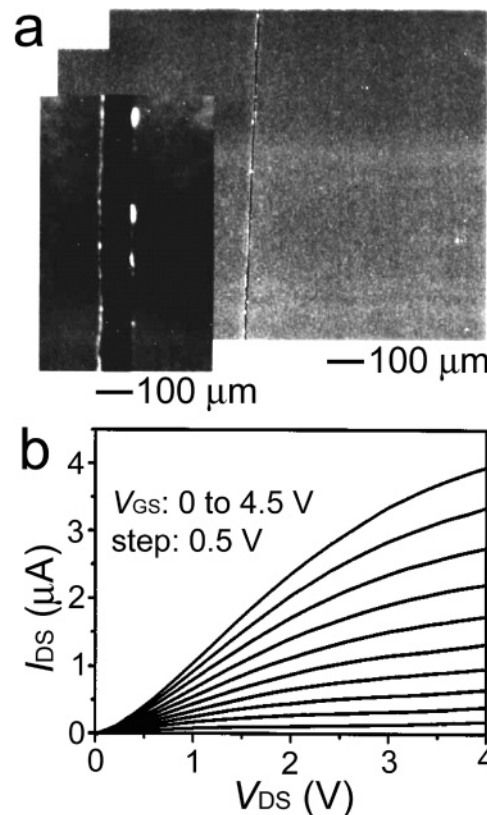


**Figure 6.** Contact mode photolithography with a conformable mask, for organic transistor fabrication: (a)  $\sim 100$  nm wide slit in a film of gold formed by lift-off using a patterned photoresist formed using this process; (b) current–voltage characteristics of an *n*-channel transistor that uses the organic semiconductor  $\text{F}_{10}\text{CuPc}$  and a channel similar to that shown in (a). (Reprinted with permission from ref 68. Copyright 1999 American Institute of Physics.)

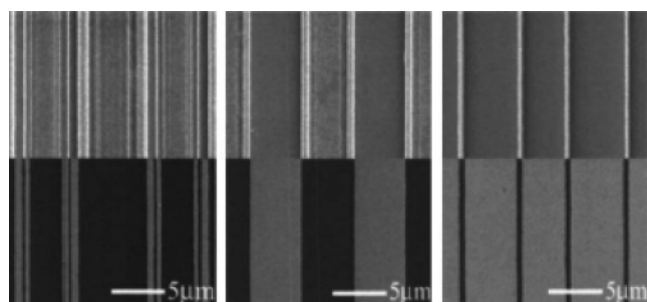


**Figure 7.** Metal structures (bottom of each image) formed by lift-off using patterns of photoresist (top of each image) defined with a conformable phase mask. Controlling the exposure and development conditions enables various patterns to be generated from a single mask. (Reprinted with permission from ref 73. Copyright 2006 American Vacuum Society.)

This type of approach provides extremely high resolution and parallel operation with inherently low-cost, simple experimental setups. It also avoids issues associated with contact between mask and photoresist (PR) in conventional photolithography, as discussed previously.<sup>79</sup> These features, in addition to its possible direct use with photodefinable organic active materials, indicate some promise for certain applications in organic electronics and optoelectronics.

### 2.3. Focused Laser Beam Scanning

Focused laser beam scanning provides another optical approach to pattern organic materials.<sup>57,80–83</sup> Laser ablation

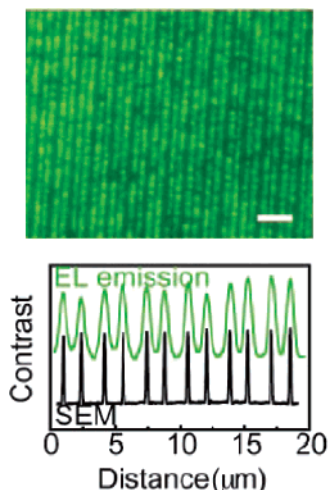


**Figure 8.** Patterned OLEDs with electrodes defined by optical soft lithography: (top) image of emission (scale bar, 5  $\mu\text{m}$ ); (bottom) averaged line scan of this emission (green) and a line scan from a scanning electron micrograph (SEM) of the electrode structure. The electrodes were Au (20 nm) and the electroluminescent (EL) layer was a polyfluorene derivative. (Reprinted with permission from ref 78. Copyright 2004 PNAS.)

and selective laser polymerization represent the two most widely explored methods. Laser ablation simply removes the organic material from selected regions to generate the desired patterns. This procedure must, however, be carefully controlled to avoid damage in other material layers or in the plastic substrates that are often used. Laser exposure can, alternatively, polymerize organic materials, typically with much lower intensities than those used for ablation. The resolution of such techniques is often limited by the laser beam diameter, modulated by the nonlinear processes that result from interaction with the material, and can be controlled by exposure dose.

There are several examples of these methods in the area of organic devices. For example, pentacene thin-film transistors can be patterned by laser ablation, using the 532 nm output of a Nd:YAG laser.<sup>80</sup> Figure 9 gives the schematic of a four-terminal device formed in this way, together with its  $I$ - $V$  characteristics. This four-terminal design yields information on the channel and contact resistances. Related work demonstrates that the same type of process can be applied to organic field effect transistors (OFET) that use poly(3-dodecylthiophene) (P3DDT) as semiconductor, poly(4-vinylphenol) (PVP) as insulator, and poly(3,4-ethylenedioxythiophene) (PEDOT) as electrodes.<sup>81</sup> Laser ablation with a 248 nm excimer laser patterned the PEDOT layer in this case, with a resolution as high as  $\sim 1 \mu\text{m}$ . The threshold voltage,  $I_{\text{on}}/I_{\text{off}}$ , and charge carrier mobility of devices formed in this manner were  $-5 \text{ V}$ ,  $10^2$ , and  $1.5 \times 10^{-3} \text{ cm}^2/\text{V}\cdot\text{s}$ , respectively, which is slightly worse than values obtained in similar devices with gold electrodes:  $0 \text{ V}$ ,  $10^3$ , and  $10^{-2} \text{ cm}^2/\text{V}\cdot\text{s}$ . Details can be obtained elsewhere.<sup>81</sup>

Focused laser beam induced photochemical cross-linking can pattern poly(2-hexylthiophene) (P3HT) thin films as described in section 2.1.1.<sup>57,82,83</sup> For instance, 442 nm light from a helium–cadmium (He–Cd) laser irradiates a P3HT film to create cross-linked, insoluble regions that remain after exposure of the sample to a developer. The cross-linked polymer was reported to have a bulk conductivity of  $\sim 6 \Omega\cdot\text{cm}$ .<sup>82</sup> A related study demonstrated resolution as high as  $1 \mu\text{m}$  when poly(3-methylthiophene) (P3MT) and poly(3-

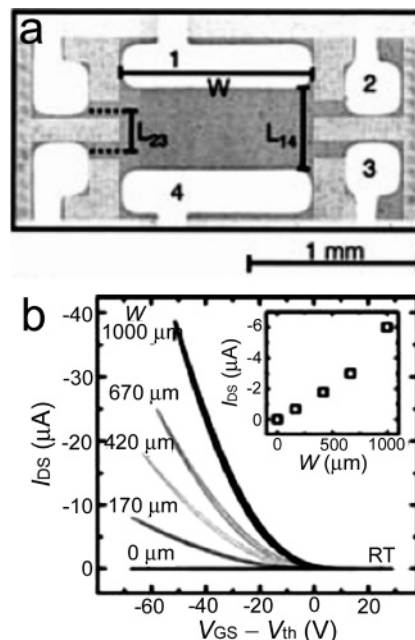


**Figure 9.** (a) Schematic of a four-terminal transistor device that uses a semiconductor layer patterned by a 532 nm Nd:YAG laser utilizing the laser ablation technique. The channel length between electrodes 1 and 4 ( $L_{14}$ ) is 475  $\mu\text{m}$ , and the channel length between electrodes 2 and 3 ( $L_{23}$ ) is 230  $\mu\text{m}$ . The channel width ( $W$ ) is 1100  $\mu\text{m}$ . (Reprinted with permission from ref 80. Copyright 2004 American Institute of Physics.) (b) Channel width dependence of the  $I_{\text{sd}} - V_{\text{g}}$  characteristic of the pentacene TFT; (inset) change of  $I_{\text{sd}}$  at  $(V_{\text{sd}}, V_{\text{g}} - V_{\text{th}}) = (-20 \text{ V}, -20 \text{ V})$  with various channel widths. (Reprinted with permission from ref 80. Copyright 2004 American Institute of Physics.)

butylthiophene) (P3BT) were patterned using a 325 nm He–Cd laser.<sup>57</sup> In addition to generating physical patterns of organic materials, focused laser beam scanning can spatially define the electrical properties of these materials. A 248 nm pulsed excimer–laser was used in this study. The transistors incorporate P3HT as semiconductor, poly(silsesquioxane) (PSQ) as gate insulator, indium tin oxide (ITO) as gate electrode, and Au as source and drain electrodes. With sufficient exposure doses ( $\sim 50 \text{ mJ/cm}^2$ ), the mobility in the P3HT can be reduced by 2 orders of magnitude, namely, from  $(2-4) \times 10^{-3}$  to  $(0.7-3) \times 10^{-4} \text{ cm}^2/\text{V}\cdot\text{s}$ ,<sup>83</sup> due to photoinduced disruption of the  $\pi$ -conjugation. This capability can be useful in device and circuit applications because it can reduce leakage currents and cross-talk.<sup>83</sup>

### 3. Patterning Organic Layers by Embossing, Imprint Lithography, and Capillary Molding

Organic devices can also be patterned using molding elements (i.e., solid objects with structures of relief on their surfaces) to direct the flow of liquids or softened solids into desired shapes.<sup>84–87</sup> In the simplest example, the mold creates a solid relief structure designed for use directly in a device. Most application examples of this form of lithography, which we refer to as embossing (sometimes also referred to as imprinting), are in photonics or optoelectronic systems. Embossing a film and then etching away the thin regions yields isolated polymer structures that can be used either as resists, in a manner similar to photoresist in photolithography, or as functional components of a device. This process is commonly known as imprint lithography. In a third type of process, sealing a mold against a substrate forms capillary

channels that can be filled with liquids. These patterned liquids can be used directly in the devices. Alternatively, solidifying them and removing the mold can form functional components or resists for further processing. This section reviews each of these techniques and their use in patterning elements of organic optoelectronic devices. It begins with procedures for fabricating the molds and for chemically functionalizing their surfaces. The methods for using these molds are then described, with an emphasis on patterning capabilities, the range of materials that can be patterned, and examples in organic-based lasers, photonic crystals, electro-optical devices, light-emission diodes (LEDs), and thin-film transistors (TFTs).

### 3.1. Fabrication of Molds

The simplest and most commonly used method for fabricating molds begins with traditional photolithography or related techniques, such as optical soft lithography as discussed in the previous section,<sup>68</sup> laser interference lithography,<sup>88,89</sup> surface plasmon interference nanolithography, and<sup>90</sup> X-ray lithography,<sup>91</sup> to define patterns of resists (Figure 10a). These processes can generate features with sizes down to  $\sim 15$  nm (e.g., extreme UV interference lithography) and over areas up to several square meters (e.g., Gen 8 display glass). Molds can be formed by using the resist as an etch mask to produce relief structures in the substrate material with depths defined by the etching time and etching conditions. Removing the resist completes the fabrication. These molds are typically generated from high-modulus inorganic wafers (e.g., silicon, GaAs, quartz, diamond, glass), making them suitable for embossing or imprinting processes that manipulate soft organic matrixes. For this reason, they are often referred to as *hard molds*. The patterns of resist, or the hard molds, can be used as “masters” to form *soft molds* made of polymers by an embossing or a casting process schematically illustrated in Figure 10b. Although various materials, including polycarbonate resins,<sup>92</sup> cross-linked novolak-based epoxy resins,<sup>93</sup> fluoropolymer materials (such as Dupont Teflon As 2400: a copolymer of 2,2-bistrifluoromethyl-4,5-difluoro-1,3-dioxole (PDD) and tetrafluoroethylene (TFE),  $\alpha$ - $\omega$ -methacryloxy functionalized perfluoropolyether),<sup>20,94</sup> etc., have been used, PDMS represents the most popular choice. PDMS molds have low surface energy and low modulus, both of which are beneficial for easy, nondestructive removal from molded structures, especially of organic materials. Additionally, the low modulus enables spontaneous conformal contact with substrate surfaces, through generalized adhesion forces, with modest or no applied pressure.<sup>74–76</sup> Such soft molds are often used to manipulate liquid precursors or solutions that are solidified or dried as part of the lithography process. Both hard and soft molds with feature sizes substantially below the limits of optical or related processes can be formed by use of electron or focused ion beam lithography, as examples. The former technique has been used to generate hard and soft molds with feature sizes down to a few nanometers.<sup>14,95–97</sup> The ultimate limit in resolution and the influence of the mold materials on this resolution represent topics of both fundamental and applied interest. To investigate these limits, etched superlattices of  $\text{GaAs}/\text{Al}_x\text{Ga}_{(1-x)}$  grown by molecular beam epitaxy (MBE) and high-resolution electron beam lithography were used to create hard molds for imprint lithography at resolutions down to 5 nm (top frame of Figure 10c), thereby establishing an upper bound on the smallest

sizes of features that are possible in hard systems.<sup>96,97</sup> Substantially smaller length scales have been explored in the case of soft molds. For example, casting and curing PDMS against step edges in fractured crystalline substrates and latent images in electron beam exposed films of polymethylmethacrylate (PMMA) yield soft molds with relief features that have heights from 2 nm down to  $< 1$  nm.<sup>14</sup> Individual single-walled carbon nanotubes (SWNTs) with diameters as small as  $\sim 0.7$  nm have been used as masters to produce PDMS molds that have relief features with heights and widths approaching 1 nm (Figure 10d).<sup>95,98</sup> Data from those experiments suggest that the density of cross-links in the PDMS is an important parameter that influences resolution at these molecular scales.

The interaction between the molds and the organic layers that are manipulated by them plays a critical role in embossing, imprinting, and molding processes. In general, the surfaces of the molds should exhibit some level of lipophilicity to provide wettability toward most organic films. This property facilitates the flow of softened or liquid organic materials into the recessed structures (in particular, for deep wells with high aspect ratios) of the molds or through the capillary channels formed by their contact with substrates. In addition, the surfaces of the molds should prevent the formation of chemical bonds or strong adhesion with the organic films during the process. Low surface energy is also valuable in this context. One strategy involves modifying the surfaces with monolayers of molecules that strongly bond to the molds and have inert, hydrophobic termination groups. For example, halogenated silane molecules, such as (tridecafluoro-1,1,2,2-tetrahydrooctyl)-1-trichlorosilane and 1H,1H,2H,2H-perfluorodecyl trichlorosilane, represent a common choice for hard molds that have surface hydroxyl groups (e.g., molds of Si and  $\text{SiO}_2$ ). The silanes spontaneously react with these groups to form chemical bonds through condensation reactions. The fluoro-terminated alkyl chains prevent the molds from sticking to the imprinted organic films. Similar treatments are necessary for preparing soft molds by casting and curing against masters. Here, the monolayers prevent adhesion of the mold material to the master. Similarly, soft molds can also be treated with surfactant molecules of fluoropolymers to form antisticking layers on their surfaces. Because these layers have nanometer thicknesses, they do not significantly affect, in either the hard or soft mold cases, the feature sizes or resolution for typical organic optoelectronic device applications. These monolayers can, however, be avoided entirely by the use of materials, such as perfluoro polyethers (PFPEs) for soft molds, that are intrinsically hydrophobic, have low surface energies, and are chemically inert.<sup>94</sup> The low surface energy combined with the low modulus and high elongation at break for elastomers such as PDMS allows them to detach nondestructively even from very fragile molded organic layers. Detailed comparisons of PDMS and PFPE molds for embossing, imprinting, and soft lithographic processes suggest that PFPE can yield similar or moderately better resolution and replication fidelity than PDMS.<sup>94,99</sup>

### 3.2. Embossing

A typical embossing process (Figure 11a) begins with casting of a solution or liquid precursor of a uniform thin film of an organic material(s) on a solid substrate. The casting procedures (e.g., rod casting, spin casting, or drop casting) define the thickness and thickness uniformity of the film.

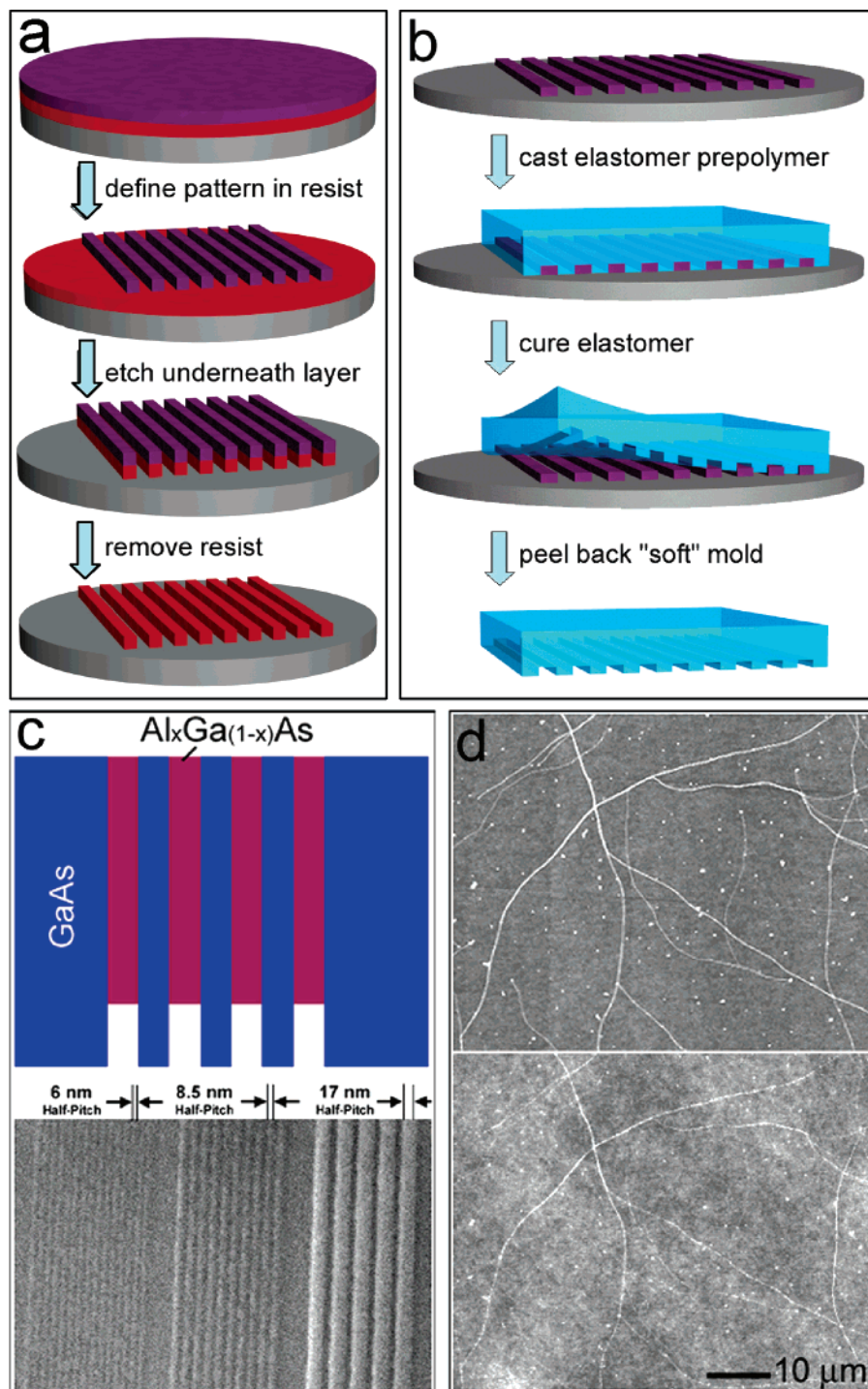


**Figure 10.** (a) Pattern of resist (red) is first defined on a layer of material (purple; “hard” layer for mold) on a supporting substrate (gray; “hard” substrate). Using this resist layer to remove selectively parts of the hard layer, followed by removal of the resist, yields a substrate with a patterned hard layer. The element serves as the hard mold. (b) Pattern of resist (purple) on a substrate serves as a template for casting and curing a prepolymer to a soft material such as an elastomer. Peeling away the cured material forms a soft mold. (c) Mold generated through selective etching of the Al<sub>x</sub>Ga<sub>(1-x)</sub>As epilayers from a superlattice of GaAs/Al<sub>x</sub>Ga<sub>(1-x)</sub>As (top frame); (bottom frame) SEM image of polymer patterns with gratings of 6, 8.5, and 17 nm half-pitches embossed with a mold like that shown in the top frame. (Reprinted with permission from ref 97. Copyright 2005 IOP Publishing Ltd.) (d) AFM images of SWNTs grown on a SiO<sub>2</sub>/Si wafer (top frame), which serve as master for generating a PDMS mold, and embossed relief in a polyurethane film (bottom frame) formed with the PDMS mold. (Adapted from ref 95.)

Contacting a hard or soft mold fabricated using procedures outlined in Figure 10a,b to the surface of the organic film leads, initially, to contact between the raised portions of the mold and the film. For solid films and hard molds (or soft molds made of rigid polymers), some degree of applied pressure is typically needed to achieve uniform contact. In contrast, elastomeric molds, such as the soft photomasks

described in the previous section, can spontaneously establish conformal contact, due to the action of generalized adhesion forces.<sup>74–76</sup> This difference between hard and soft molds is important for applications in organic optoelectronics, where the substrates and the layers of active materials often cannot be exposed to significant pressures without deforming them in undesired ways. With the configuration shown in the top

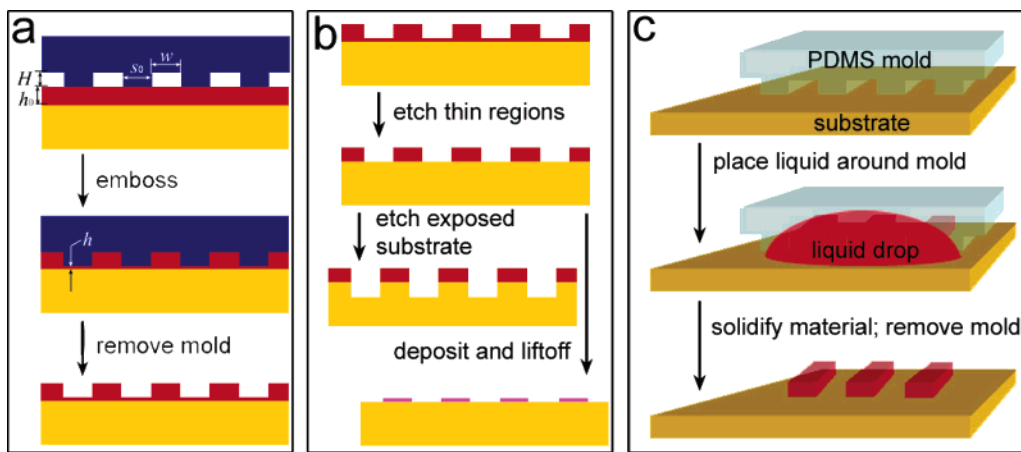


**Figure 11.** Schematic illustration of (a) embossing a thin film and (b) processing the embossed pattern including etching away the thin regions to yield isolated features that can act as resists, etching the exposed substrate material, or depositing other materials and then removing the resist. The combination of (a) and (b) is referred to as imprint lithography. (c) Schematic illustration of a capillary molding process to pattern liquid materials in microchannels formed by contact of a mold with a substrate.

frame of Figure 11a, the raised regions of the molds tend to embed into the film when the film material has low viscosity and/or when pressure is applied. In this process, the organic material flows up into the spaces formed between the recessed portions of the mold and the organic film, due to either externally applied pressure, adhesion forces, or capillarity. The result, in an optimized process, is the formation of structures of relief on the surface of the organic film in the geometry (lateral widths and relief heights) of the mold. In practice, the organic material flows and fills the cavities formed between the molds and the organic films according to two different ways, that is, lateral filling and bottom-up filling, depending on the dimensions of the mold relief and the thickness of the organic films. For a mold with a simple geometry of periodic grooves as shown in Figure 11a, that is, protrusions with a width of  $s_0$  and a height of  $H$ , and grooves with a width of  $w$ , the molded material fills into the cavities via lateral flow when the thickness ( $h_0$ ) of the organic film is less than  $s_0$ ; bottom-up filling occurs when  $h_0$  is larger than  $s_0$ . The height ( $h$ ) of the organic film underneath the raised portions of the mold after embossing depends on the viscosity ( $\eta$ ) of the molded material, the pressure ( $p$ ) applied to the mold, embossing time ( $t$ ), and the wetting properties of the mold surface. For example, as for the case of  $h_0 > s_0$ ,  $h$  is determined by  $t = (\eta s_0^2/2p) (1/h^2 - 1/h_0^2)$  until the cavities are filled.<sup>100</sup> The ratio of  $h$  to  $H$  can play an important role in certain applications.

Embossing can create relief on the surfaces of organic films composed of most materials, ranging from inert polymers for waveguide claddings, to active polymers and small organic molecules for functional devices, to liquid precursors, if their viscosities are sufficiently low. In fact, this method already has widespread commercial use for the fabrication of compact discs (CDs) and digital video discs (DVDs). These discs, which are made of polycarbonate, are patterned via hot embossing and injection molding and then coated with thin layers of aluminum as reflective layers. The dimensions of the pits are usually on the scale of hundreds of nanometers. For example, pits on CDs are approximately 100 nm deep by 500 nm wide and vary in length from 850 nm to 3.5  $\mu\text{m}$  long. The spacing between the tracks, that is, the pitch, is 1.6  $\mu\text{m}$ . In organic optoelectronics, the embossed films consist of materials that either play an active role in a device (e.g., electroluminescent layer) or serve as structures onto which active materials are deposited. A broad range of

devices can be achieved, including light couplers and wavelength filters for waveguides, distributed feedback (DFB) and distributed Bragg reflector (DBR) lasers, two-dimensional (2D) photonic crystals and lasers, and other systems.

### 3.2.1. Waveguides, Light Couplers, Spectral Filters, Reflectors, and Sensing Devices

Polymeric waveguides have the potential to be important in photonics and optoelectronics due to their ease of fabrication, chemical flexibility of polymer compositions, and low cost. Embossed waveguides are typically fabricated with passive polymers, such as PMMA, amorphous polycarbonate (APC), and polystyrene (PS) as the core and/or cladding materials. Figure 12a shows an example of waveguides that use a polyurethane core, embossed with a PDMS stamp.<sup>101</sup> Grating structures can also be embossed on the surfaces of polymer waveguides to form other functional devices, such as couplers and reflectors. For example, waveguides in polyimide and PMMA can be formed with embossed gratings with a 500 nm pitch as input couplers, with efficiencies of  $\sim 25\%$ .<sup>102</sup> Such gratings can also act as output couplers and as wavelength filters. Grating periodicities of  $\Lambda$  reflect wavelengths corresponding to  $\lambda_B = 2n_{\text{eff}}\Lambda$  (where  $n_{\text{eff}}$  is the effective refractive index of the waveguide mode) back to the input ports of the devices.<sup>103</sup> This kind of wavelength filter, known as a Bragg reflector, can be integrated with a heater to modulate  $n_{\text{eff}}$  through the thermo-optic effect, thereby producing a tunable filter. The large thermo-optic effects in polymers enable power efficient operation in devices of this type, compared to similar systems in inorganic materials such as SiO<sub>2</sub>.<sup>104</sup> Furthermore, the surfaces of the gratings can be modified with chemical or biological molecules that recognize a desired species and trap them through specific interactions. The attachment of these species changes the effective refractive index around the waveguide device, thus shifting the wavelength of the reflected light. This system provides the basis for chemical and biological sensors.<sup>105</sup> Conceptually similar devices that rely on different physics can be achieved by coating an embossed structure with a thin film of metal (e.g., silver or gold) that supports surface plasmons. In this case, surface binding changes the positions and amplitude of the plasmon resonances, which can be probed optically.<sup>106</sup> Figure 12b presents the structure of a plasmonic crystal formed by depositing a thin gold layer

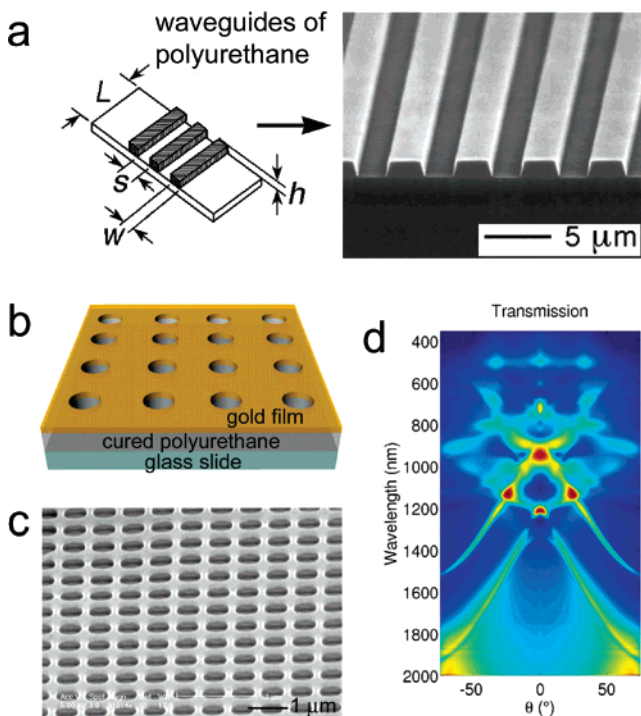


**Figure 12.** (a) Waveguide structure fabricated in a polyurethane film with a PDMS mold. (Reprinted with permission from ref 101. Copyright 1997 American Institute of Physics.) (b) Schematic illustration of a plasmonic crystal generated by depositing a thin gold film onto a 2D grating formed by embossing a thin film of polyurethane on a glass side with a PDMS mold. (c) SEM image of an as-fabricated plasmonic crystal with periodic depressions with diameter, depth, and periodicity of 545, 300, and 700 nm, respectively. (d) Sensitivity map of the surface sensitivity of the plasmonic crystal. Sensitivity scale increases from blue to red.<sup>106</sup> (Adapted from ref 106.)

onto a 2D grating with depressed holes embossed in a layer of polyurethane with a PDMS mold. Figure 12c shows an SEM image of a typical as-fabricated plasmonic crystal that consists of Au/Ti (50 nm/5 nm) on a 2D grating of depressed holes with a diameter and depth of 545 and 300 nm, respectively, and with a periodicity of 700 nm. This structure offers the ability to probe bonding events on the gold surface. For example, Figure 12d gives a sensitivity map of a crystal modified with a self-assembled monolayer (SAM) of hexadecanethiol, where sensitivity is defined as the difference between the transmissions before and after binding. Although polymers are the most widely used materials for embossed gratings and waveguides, sol–gel precursors to hybrid organic–inorganic materials (e.g., organo-alkoxy silane) can also be used.<sup>107–109</sup>

### 3.2.2. Distributed Feedback and Distributed Bragg Reflector Lasers

Light-emitting organic materials can be combined with embossed grating structures such as those described in the previous section, or they can be directly embossed themselves to produce DFB and DBR lasers. DFB resonators involve uniform or phase-shifted gratings, whereas DBR resonators use aligned grating structures separated by some distance. Such resonators can be achieved by embossing into non-emissive polymer (or sol–gel) materials, or films of emissive organics, as shown in Figure 13a. Photoluminescence from films of fluorescent organic molecules often exhibits spectral line narrowing under high optical excitation intensities, which

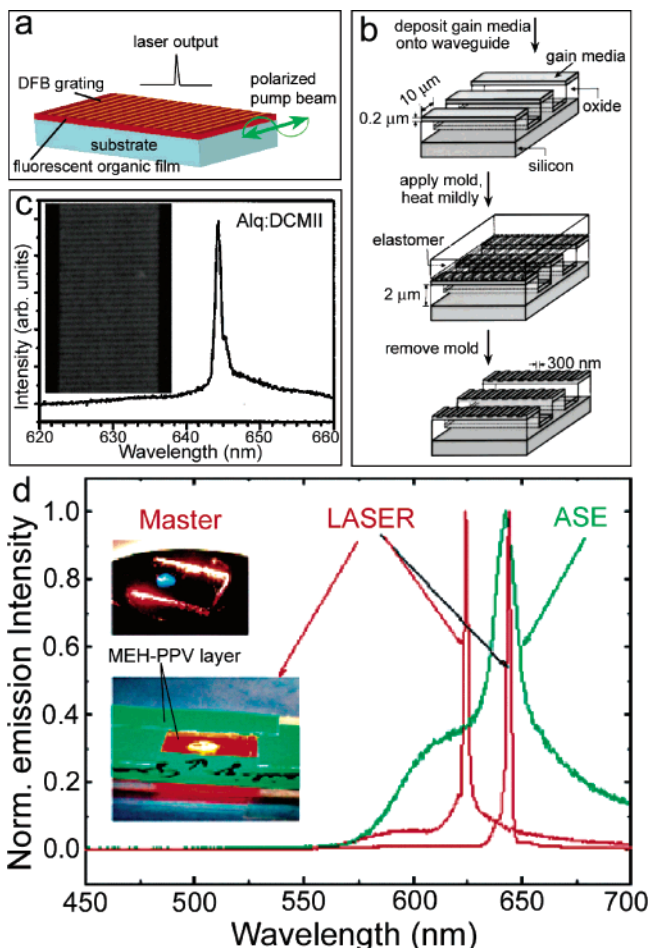


**Figure 13.** Organic laser devices with DFB grating resonators. (a) Schematic illustration of laser action in a film of organic gain medium on a surface with a DFB grating. (b, c) Fabrication procedures and emission spectrum of a DFB laser with Alq<sub>3</sub>:DCMII as the gain material. (Reprinted with permission from ref 10. Copyright 1999 American Institute of Physics.) (d) Emission spectrum from MEH-PPV in the presence of ASE (green) and laser action (red) from two different DFB grating periodicities. The insets show the master and DFB laser samples. (Reprinted with permission from ref 112. Copyright 2003 Wiley-VCH.)

can be caused by amplified spontaneous emission (ASE).<sup>110</sup> Some of the photons associated with ASE in a thin film on a transparent material with a lower index of refraction can be trapped in waveguide modes of the film. If this transparent material also supports an embossed DFB or DBR structure, or when the film itself is embossed, then the trapped photons can be reflected back and forth, creating the feedback necessary for lasing, when the optical gain exceeds the loss (Figure 13a). Laser emission of this type occurs near the Bragg wavelength  $\lambda_B$ , which is determined by  $m\lambda_B = 2n_{\text{eff}}\Lambda$ , where  $m$  is the order of diffraction of the grating and  $n_{\text{eff}}$  is the effective refractive index for the waveguide. Demonstrations include DFB lasers formed by directly embossing a ~200 nm thick gain medium film of tris(8-hydroxyquinoline) aluminum (Alq<sub>3</sub>) doped with 0.5–5.0 wt % of the laser dye 4-dicyanomethylene-2-methyl-6-(*p*-dimethylaminostyryl)-4*H*-pyram II (DCMII), deposited on a SiO<sub>2</sub>/Si wafer with patterned rib waveguides, by using a PDMS mold (see the schematic illustration of Figure 13b).<sup>10</sup> In the fabrication, a pulsed nitrogen laser (337 nm, ~2 ns, ~10 kW/cm<sup>2</sup>) softens the gain material to enable it to be embossed without applied pressure. The inset of Figure 13c shows an SEM image of the DFB structure, which involves lines and spaces with

widths of 300 nm. The plot in Figure 13c gives the laser emission from a waveguide DFB laser formed in this manner. The resonant reflections that yield the feedback are due to third-order interactions with the gratings; the diffraction that provides output coupling is first order. The presence of a single peak located at  $\sim 645$  nm is consistent with this third-order interaction. Similar lasers, with both DFB and DBR layouts, can also be produced by casting or evaporating organic gain films onto pre-embossed substrates.<sup>111</sup>

Gain materials can also be softened with solvents to facilitate the embossing process. For example, a solution of the conjugated polymer MEH-PPV (in chloroform) drop-cast onto a glass slide was embossed with a PDMS grating mold, resulting in the formation of DFB lasers.<sup>112</sup> The insets of Figure 13d show the master used for creating the PDMS mold and the DFB structure. Illuminating the sample with the focused output of a frequency-doubled Nd:YAG laser (532 nm, pulse duration of 4 ns) generates emission perpendicular to the film surface in the regions of the DFB and ASE in the unstructured regions at sufficient excitation intensities. The emission shows a single narrow line, consistent with laser action. As shown in Figure 13d, the laser line has a line width of 2 nm, compared to 11 nm for the ASE. The spectral position of the lasing can be adjusted by changing the periodicity ( $\Lambda$ ) of the DFB grating. For example, the laser line shifts from 625 to 645 nm when  $\Lambda$  increases from 370 to 405 nm. In a different but related fabrication approach, PDMS molds serve as reservoirs to deliver, upon contact, solvents to selected locations on organic films. For example, films of the conjugated polymer poly[2-methoxy-5-(3,7-dimethyloctyloxy)-*p*-phenylenevinylene] (OC<sub>10</sub>-PPV) can be embossed with a PDMS mold “inked” by chlorobenzene to form DFB gratings.<sup>113</sup> Solid-state DFB lasers from other gain materials, such as thiophene-based oligomer 3,3',4''3'''-tetracyclohexyl-3'',4''-dihexyl-2,2':5',2'':5'',2''':5''',2''':quinquethiophene-1'',1''-dioxide (T5oCx) can be achieved by embossing with Si molds by applied pressure without heating or solvents.<sup>114–117</sup>

### 3.2.3. 2D Photonic Crystals and Lasers

A wide range of embossed structures that are more complex than gratings can also be formed and used in active organic optoelectronic devices. 2D photonic crystal structures, similar to the plasmonic crystals described previously, represent one example. Figure 14a shows, as an example, a pattern of cylindrical wells (or posts) with diameters of 0.4  $\mu\text{m}$  and center-to-center separations of 0.6  $\mu\text{m}$ , in a triangular lattice geometry. Figure 14b shows patterned wells in the geometry of Figure 14a, prepared by embossing with a PDMS stamp with raised posts (heights of 50 nm) into a liquid sol–gel precursor of an organic–inorganic hybrid glass, that is, organically modified silicate (ORMOSIL).<sup>11</sup> Baking this material at 60 °C while in contact with the PDMS forms the ORMOSIL; removing the mold completes the fabrication. 2D grating structures of this type can serve as photonic crystals that can, for example, slow or prevent the propagation of certain wavelengths of light propagating in the plane of the crystal.<sup>118</sup> In a manner conceptually similar to the DFB and DBR lasers, these 2D crystals can form resonators, as shown in Figure 14b. For example, deposition of the host Alq<sub>3</sub> and the laser dye DCMII (concentration of 0.5–2 wt %) on the surface of the embossed structure forms a 2D photonic crystal-based organic waveguide laser. The film acts as a planar waveguide with Alq<sub>3</sub>:DCMII (core) and

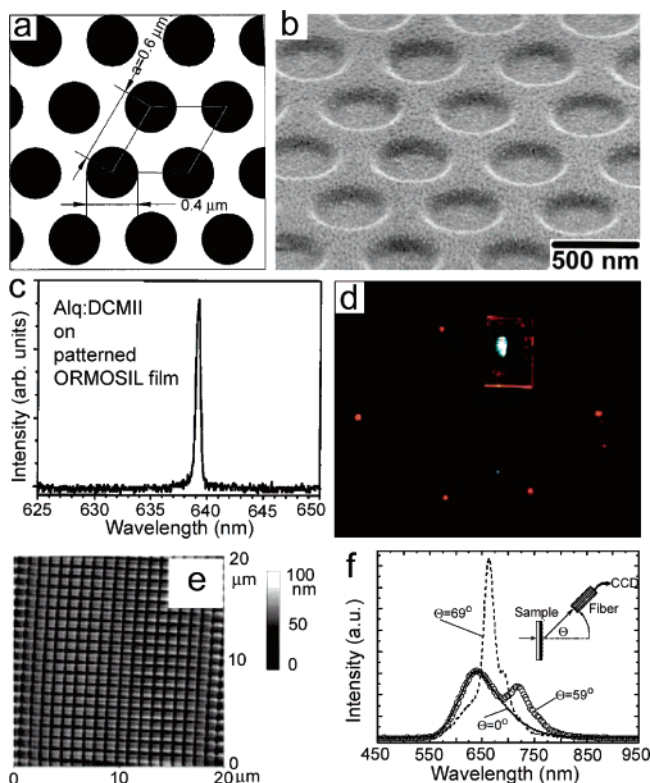


**Figure 14.** 2D photonic crystals for laser devices. (a) Lattice pattern of a photonic crystal with triangular symmetry. (b) SEM image of a 2D crystal structure embossed in a thin (2  $\mu\text{m}$ ) film of ORMOSIL with cylindrical wells (50 nm in depth) and lattice parameters same as shown in (a). (c) Emission spectrum from a photopumped laser that incorporates the structure shown in (b) covered with a layer of Alq<sub>3</sub>:DCMII. (Reprinted with permission from ref 11. Copyright 1999 Optical Society of America.) (d) Photograph of the far-field emission pattern from a 2D photonic crystal laser constructed with a film of Alq<sub>3</sub>:DCMII on a layer of polyurethane film embossed with a 2D structure similar to that shown in (b). The diameter of the holes is 0.52  $\mu\text{m}$ , and lattice constant  $a = 0.72 \mu\text{m}$ . (Reprinted with permission from ref 12. Copyright 1999 American Institute of Physics.) (e) AFM image of 2D grating pattern in a conjugated polymer embossed twice with a 1D grating mold and the fluorescent spectra (f) collected from a sample using a red-emitting polymer. (Reprinted with permission from ref 119. Copyright 2005 American Chemical Society.)

the air and ORMOSIL (cladding) layers. Pumping the device with the output of a pulsed nitrogen laser ( $\sim 2$  ns, 337 nm) induces lasing output (Figure 14c) due to Bragg reflections caused by the photonic lattice embossed in the ORMOSIL.<sup>11</sup> Embossed 2D structures in other dielectric materials, such as polyurethane, can play a similar role in laser devices formed by deposition of uniform coatings of organic gain materials.<sup>12</sup> Figure 14d displays the far-field image of a laser consisting of a Alq<sub>3</sub>:DCMII layer on a polyurethane crystal similar to that of Figure 14b. For a triangular lattice, laser output emerges along six corresponding directions in the plane of the waveguide, consistent with the observation shown in Figure 14d. The absence of significant amounts of scattered light in this emission pattern provides evidence of the very high quality of the resonator structures that can be formed by embossing.

2D gratings formed in the gain media through multiple, repeated embossing processes can also be used, in principle, to create laser devices as shown above. For example, 2D photonic crystal-like patterns can be created in films of conjugated compounds, such as a red-, a green-, and a blue-

emitting polymer.<sup>119</sup> Figure 14e gives an AFM image of a 2D grating of square posts with edge lengths of 500 nm and heights of 28.7 nm patterned in the polymer film. Experimental results indicate that the structuring of active materials by embossing can be achieved without degrading their luminescent properties. Although laser action was not reported, the dependence of the fluorescent spectra of the red-emitting polymer (i.e., poly[{2-methoxy-5-(2-ethylhexyloxy)}-1,4-(1-cyanovinylenephylene)-co-{2,5-bis(*N,N'*-diphenylamino)-1,4-phenylene}]) on the collection angle related to the sample surface shows interesting effects (Figure 14f). For example, the emission peak of the embossed DFB microcavities shifts from 736 nm (at 55°) to 649 nm (at 73°), with a strongly enhanced and narrowed peak at 663 nm (at 69°). The dependence of the diffraction peak on the collection angle is attributed to the wavelength dependence of the effective refractive index,  $n_{\text{eff}}$ , inside the organic slab. The increase of the quantum yield emitted at a particular angle (i.e., 69°) for the patterned film and the enhancement of the output light is due, at least in part, to the matching of the Bragg periodicity of the embossed grating to the emission wavelength of the polymer.

### 3.2.4. Nonlinear Optical Polymer-Based Electro-optic Devices

Nonlinear optical (NLO) materials that use organic small molecules and/or polymers have potential applications in a range of optoelectronic devices, such as frequency converters, high-speed electro-optical modulators, and switches, because of their high NLO susceptibility, fast response time, low dielectric constant, small dispersion in the index of refraction from DC to optical frequencies, possibilities for structure modification, and ease of processability. The versatility of the embossing technique for patterning organic/polymeric materials enables electro-optical devices to be fabricated with NLO polymers with easy processing steps and experimental setups. For example, polymeric Mach–Zehnder interferometer-based modulators can be fabricated by patterning the core material of a second-order NLO polymer composed of CLD-1 (a highly nonlinear optical chromophore) and APC (1:4 ratio in weight) using a PDMS mold.<sup>120</sup> Panels a and b of Figure 15 illustrate top and side views of the modulator. UV-cured epoxy UV15 and low-refractive-index epoxy Epo-Tek OG-125 served as the lower cladding and upper cladding of the integrated device, respectively. In the geometry shown in Figure 15, input light splits into two beams propagating in separate arms of the modulator. The multilayered structure (Figure 15b) in one or both of the arms controls, using an applied voltage, the relative phase of light emerging from each arm. The induced phase change is given by  $\Delta\phi = (\pi r n^3 L E / \lambda)$ , where  $n$  is the refractive index of the NLO polymer film,  $r$  is its electro-optical coefficient,  $L$  is the propagation length (i.e., waveguide length),  $\lambda$  is the operation wavelength, and  $E$  is the applied electric field. The phase mismatch between the two beams leads to a variation of the amplitude of the combined output, controlled by the applied voltage to the electrodes. Figure 15c shows voltage-intensity characteristics of the interferometer with CLD-1/APC, clearly showing good modulation. The minimum voltage necessary to create a phase mismatch of  $\pi$  is called the half-wave voltage,  $V_\pi$ , and is given by  $V_\pi = (d\lambda / rn^3 L \Gamma)$ , where  $d$  is the waveguide thickness and  $\Gamma$  is a correction factor close to 1. The value of  $V_\pi$  of the modulator shown in Figure 15 is  $\sim 80$  V. Modulators with operating speeds up to 200 GHz have been demonstrated.<sup>121</sup> In addition to electro-optical devices,

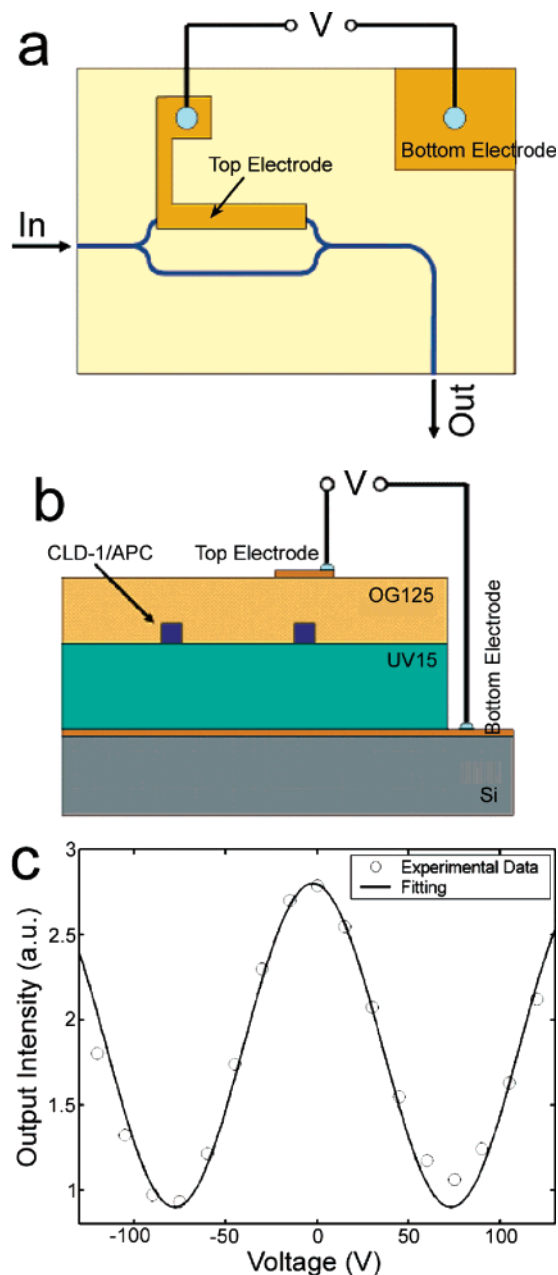


**Figure 15.** (a) Top view and (b) side view of a polymeric Mach–Zehnder interferometer-based modulator. (c) Dependence of output intensity on the applied electrode voltage of a modulator device with a core NLO polymer of CLD-1/APC. (Reprinted with permission from ref 120. Copyright 2004 American Chemical Society.)

waveguides consisting of core NLO polymer (such as Disperse Red 1 doped PMMA) films embossed with gratings can serve as optical switching devices on the basis of the intensity-dependent refractive index associated with the NOL polymer.<sup>122</sup> For additional information, we refer interested readers to other reviews that have been written on these topics.<sup>123–127</sup>

### 3.2.5. Light-Emitting Devices

Unlike organic lasers and modulators, OLEDs form the basis of existing and expanding commercial product lines, in the form of emissive display systems. Embossing techniques can be applied to build patterned OLEDs.<sup>13</sup> In one example, fabrication begins by spin-casting a 50–150 nm thick layer of *p*-xylenebis(tetrahydrothiophenium chloride)

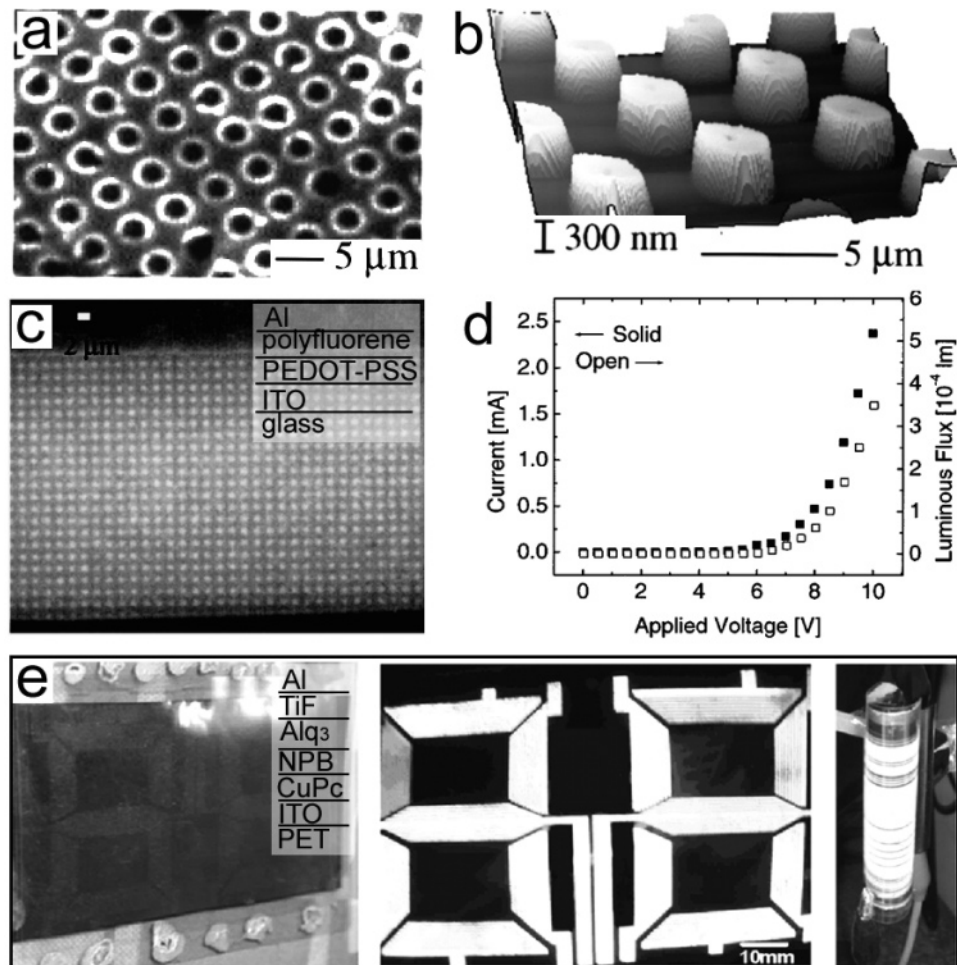


**Figure 16.** OLEDs fabricated by embossing and imprint lithography. (a) Optical image of emission from OLEDs that incorporate embossed films of PPV and (b) AFM image of the surface of the PPV structure. The intensity of the emitted light correlates with the thickness measured. (Reprinted with permission from ref 13. Copyright 1998 American Institute of Physics.) (c) Optical micrograph of light emission from a pixel array of OLEDs (with glass/ITO/PEDOT-PSS/polyfluorene/Al geometry) fabricated by patterning electrodes with imprint lithography and (d) current and luminous flux versus applied voltage. (Reprinted with permission from ref 16. Copyright 2002 American Vacuum Society.) (e) Optical images of LEDs with structure of ITO/CuPc/NPB/Alq<sub>3</sub>/LiF/Al on plastic PET substrates. The image shown in the right picture indicates the mechanical flexibility of the devices. (Reprinted with permission from ref 18. Copyright 2005 IEEE.)

(a precursor to the electroluminescent polymer poly(*p*-phenylenevinylene) (PPV)), onto a glass substrate coated with a uniform layer of indium tin oxide (ITO, serving as electrode of LED). Laminating a PDMS mold wetted with a thin layer of methanol onto the surface of precursor film causes the partially dissolved precursor to wick into the cavities in the mold. Evaporation of methanol through the gas-permeable PDMS, followed by removal of the stamp, leaves a film of the precursor with surface relief complementary to that of the mold. Baking the precursor at 260 °C in a vacuum ( $\sim 10^{-6}$  Torr) for 10 h converts the material to PPV, without substantial loss of the embossed relief features. Evaporation of Ca ( $\sim 40$  nm) and Al ( $\sim 200$  nm) (electrode of LED) onto the PPV completes the fabrication of an LED. The LED emits light in a geometry defined by the PDMS mold due to the much higher turn-on voltages of the thick regions of the PPV than in the thin regions. Panels a and b of Figure 16 show the emission image and surface relief profile (as measured by AFM) of such a device, respectively. At moderate applied voltages, emission is highest at edges of posts, due to a combination of enhanced output coupling, high electric fields, and locally thin areas in these regions. The broader features of the emission patterns correlate well with the variations in thickness. The widths of the light-

emitting areas in these devices can be small; in the sample shown in Figure 16a they are  $< 800$  nm.

Embossed grating or scattering structures in the active or passive components of OLEDs can increase their external quantum efficiency by causing photons that would otherwise be trapped in waveguide modes associated with the device structure to be deflected out of the device. In one example, an aqueous solution of poly(3,4-ethylenedioxythiophene)-polystyrene sulfonate (PEDOT-PSS) was drop-cast onto ITO-coated glass and then embossed with a Bragg grating using a PDMS mold. Spin-casting a film of OC<sub>1</sub>C<sub>10</sub>-PPV in a 1,2-dichlorobenzene solution on the embossed film of PEDOT-PSS followed by thermal evaporation of Ca and Ag completes the device. The results show that one-dimensional (1D) gratings increase the efficiency by  $> 15\%$  with respect to similar devices without gratings. Devices modified with 2D gratings further increased the efficiency by 25%. In this example, the introduction of the gratings did not change other properties of the devices, such as turn-on voltage.<sup>128</sup>

### 3.3. Imprint Lithography

Embossing produces relief structures in films or on substrate surfaces. Many applications such as transistors, diodes, and other components benefit from isolated features.

Imprint lithography combines embossing of films with a subsequent etching step that removes the thin regions to produce these types of isolated features (Figure 11b).<sup>86</sup> Typically, the etching step should be highly anisotropic, with much higher etch rates out of the plane than in the plane. However, the etching rates of polymeric resists are the same in the thick and thin regions. As a result, the ratio of the height ( $H$ ) of the embossed relief to the thickness ( $h$ ) of the thin regions and the spatial uniformity of this ratio across the patterned sample are important parameters. Careful control of process parameters can achieve favorable results, routinely. Commercial imprint lithography tools are now available from several vendors and are common in academic and industrial research cleanroom facilities.

Some of the earliest imprint methods used thermally softened materials of polymers such as PMMA and high pressures for the embossing.<sup>15–19</sup> Although this approach can work well, challenges associated with achieving good overlay registration in a high-temperature and high-pressure process and the slow flow rates associated with most of the polymers that have been explored led several groups to develop means for room temperature and low-pressure approaches.<sup>20</sup> One such method, known as “step and flash imprint lithography” (SFIL),<sup>15,19,129</sup> uses a low-viscosity UV-curable material on top of a traditional resist. The top fluid layer can quickly fill the relief features on the molds (even with relatively high aspect-ratio relief) at room temperature and with low pressure. Irradiation of the precursor with UV light, often transmitted through the mold itself, induces a polymerization reaction that solidifies the molded top layer in the geometry of the mold. Acrylate-based materials are often used because they provide high etch contrast with respect to the bottom resist layer films in O<sub>2</sub> reactive ion etching (RIE). The resulting isolated features in the top layer can be transferred directly to the bottom organic layer by using the top layer as an etch mask. Furthermore, the bottom thermoplastic/thermoset polymer layer with transferred patterns can serve as a mask for etching underlying materials or for patterning other materials by lift-off processes. This type of approach has the potential for large-area, low-cost fabrication on both flat and nonflat substrates with low pressure and at room temperature.<sup>17</sup> Although most efforts in imprint lithography focus on electronic and photonic devices made with traditional materials, opportunities and some examples exist in the area of organic devices. Active organics can, in principle, be patterned directly in this way. Most demonstrations, however, use imprint to define inorganic components of devices that use active organic layers, with several representative cases in LEDs and TFTs, as described in the following.

### 3.3.1. Light-Emitting Devices

Unlike the directly embossed layers in the OLEDs of Figure 16a,b, imprint lithography typically forms resist masks for patterning isolated electrodes for these devices, rather than the active organic layers. For example, a glass slide with a uniform ITO layer can be coated with a layer of PMMA resist, imprinted with a rigid Si mold and then used as a template to build LEDs with patterned emission. In one example, a hole-transporting layer, that is, PEDOT-PSS, and a red-emissive polyfluorene derivative polymer layer consecutively spin-cast form the transport and emission layers.<sup>16</sup> Al evaporated on top forms the cathode, with the ITO as

the anode. Here, the PMMA layer with imprinted holes serves as a template to isolate the LED pixels; that is, light does not emit from the PMMA-coated regions due to the inability of charge to be injected from the anode. Figure 16c displays a gray-scale optical micrograph of emission from an array of red LEDs with pixel sizes as small as  $2 \times 2 \mu\text{m}^2$ . Figure 16d shows the characteristics of these LEDs. The data indicate that the turn-on voltage and the corresponding current are  $\sim 5.5 \text{ V}$  and  $\sim 30 \mu\text{A}$ , respectively, with a luminous flux of up to  $\sim 10^{-3} \text{ lm}$ .

Similar processing of ITO-coated plastic substrates, such as polyethylene terephthalate (PET), produces mechanical flexible OLEDs.<sup>18</sup> Here, imprinting of PMMA and etching of the ITO itself forms isolated anodes where the PMMA acts only as a sacrificial resist. Sequential deposition of a hole-injection layer of copper phthalocyanine (CuPc), a hole-transport layer of *N,N'*-di(naphthalen-1-yl)-*N,N'*-diphenylbenzidine (NPB), an electron transport and emission layer of Alq<sub>3</sub>, and a cathode layer of lithium fluoride (LiF)/Al onto the PET substrate with patterned ITO anodes generates arrayed pixels of OLEDs. Figure 16e shows a series of optical images for a two seven-segment light-emitting patterns on a PET film for a numerical display. The right frame shows a similar display bent to a radius of curvature of 1 cm. The characteristics of these devices are comparable to those fabricated using standard means. The turn-on voltage was 7.5 V for achieving both current and light emission. The luminous efficiency reached 1.13 lm/W (3.04 cd/A) at a luminance of 3.8 cd/m<sup>2</sup>, and luminance increased to a maximum of 244 cd/m<sup>2</sup> at a drive voltage of 30 V. Luminous efficiencies as high as 25 lm/W can be achieved in state of the art white OLEDs.<sup>130,131</sup>

Although patterning electrodes by imprint lithography is useful, most realistic display systems also benefit from patterning of the emissive layers. We are unaware of any published reports of imprint lithography for this process, in working OLEDs. On the other hand, the influence of the imprinting process on the luminescent properties of various organic materials has been investigated.<sup>132–136</sup> Additional work will be needed to optimize material choices and process parameters to eliminate the adverse effect of imprinting on OLED device performance.

### 3.3.2. Thin-Film Transistors

In addition to OLEDs, imprint lithography has potential applications in OTFTs, particularly for defining the channel lengths, where the extremely high-resolution capabilities and low-cost operation of imprint are most valuable. In this mode of use, imprint lithography defines the electrodes of the devices. In one example, such procedures defined source and drain electrodes of polymer TFTs with channel length as small as 70 nm.<sup>137</sup> In the fabrication sequence, an imprinted polymeric resist layer on a heavily doped *n*-type silicon substrate (serving as a gate electrode for OTFTs) with a thermally grown oxide layer of 5 nm in thickness (serving as a dielectric layer for OTFTs) serves as a mask for deposition of Au to form patterned source and drain electrodes on the substrate by lift-off. Spin-coating or -casting *p*-type semiconducting polymer of P3HT completes the OTFTs. The SEM images shown in Figure 17a illustrate high-quality electrodes and channels with uniform dimensions of 70 nm and sharp edges. The results demonstrate that OTFTs with channel lengths varying from 1  $\mu\text{m}$  to 70 nm can be fabricated by imprint lithography. Figure 17a gives

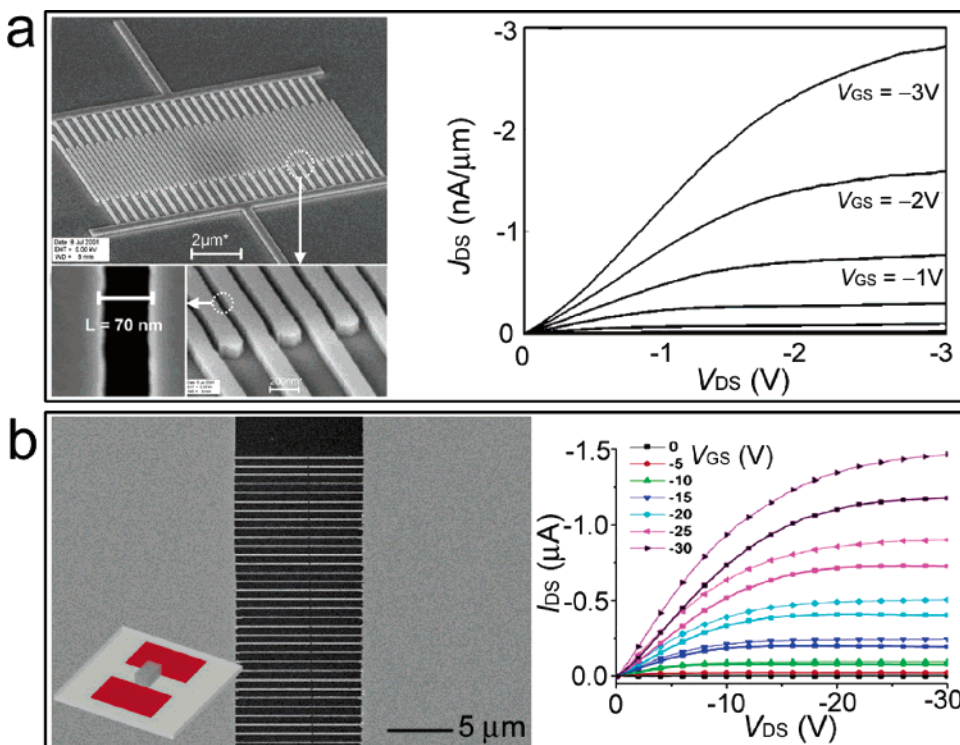


**Figure 17.** OTFTs fabricated by imprint lithography. (a) SEM images of an interdigitated finger-type OTFT with channel length of 70 nm and channel width of 4  $\mu\text{m}$  (left frame); typical electrical characteristics (right frame) of an OTFT with geometry similar to that shown in the left frame, with a channel length of 1  $\mu\text{m}$ . (Reprinted with permission from ref 137. Copyright 2002 American Institute of Physics.) (b) SEM image of an OTFT device constructed with finger-shaped nanoelectrodes and large probing pads (left frame) and electrical characteristics (right frame) of the device shown in the left frame with pentacene as semiconductor. (Reprinted with permission from ref 139. Copyright 2006 IOP Publishing Ltd.)

The  $I-V$  curves of the transistors with channel lengths of 1  $\mu\text{m}$ , showing good overall performance. Although the current densities significantly increase by  $\sim 10$  times when the channel length decreases from 1  $\mu\text{m}$  to 70 nm, effects of contact-limited performance become apparent. Also, the saturation mobilities are fairly low, that is,  $8 \times 10^{-4} \text{ cm}^2/\text{V}\cdot\text{s}$ . This behavior, which is similar to that in previously described devices formed by optical soft lithography with channel lengths in this same range, is important because it illustrates that high-resolution patterning techniques are not sufficient to realize fully the performance improvements that can, in principle, be obtained from reducing the length of the channel. Other materials and technologies, such as contact doping in this case, are required.

Integrating or probing short-channel OTFTs such as those shown in Figure 17a often requires larger scale electrode pads and interconnect lines. In practice, it can be difficult with imprint lithography to form features with a wide range of sizes, due to challenges associated with filling completely the raised regions of the molds and yielding thin layers with uniform thicknesses.<sup>138</sup> A class of hybrid molds that include both narrow relief structures suitable for imprinting and wide mask patterns for photolithographic processes overcome some of these challenges.<sup>139</sup> The inset of the left frame of Figure 17b shows an imprint mold integrated with large-area photomask pads (in red). The substrate of this hybrid mold-mask (HMM) is transparent to UV light. The fabrication process begins with a triple-layered structure formed by spin-casting a PMMA layer, thermally evaporating a Ge layer, and spin-coating a layer of resin resist (i.e., SU-8) on a highly doped *n*-type silicon wafer (serving as bottom gate electrode) covered with a 200 nm thick thermal oxide layer (serving as gate dielectric). The SU-8 layer is imprinted by

mechanical impression and cross-linked via UV irradiation. Pressing the HMM into the SU-8 layer, exposing the system to UV irradiation, developing the unexposed resist, removing the thin residual layer with O<sub>2</sub> RIE, etching away the Ge layer, overetching the exposed PMMA layer, depositing metal (e.g., Au) film, and lifting off the resist layer leave metal patterns containing finger electrodes separated by a nanoscale gap ( $\sim 50$  nm) for source and drain connection and large metal pads ( $\sim 150 \mu\text{m}$ ) for probing. The left frame of Figure 17b presents an SEM image of OTFTs fabricated in this manner, where pentacene is the semiconductor. The right frame of Figure 17b shows the electrical characteristics, clearly illustrating good modulation. The saturation mobility was  $\sim 1 \times 10^{-2} \text{ cm}^2/\text{V}\cdot\text{s}$ , in the range of similar devices fabricated with conventional means.

OTFTs formed by imprint lithography typically use a bottom common gate configuration,<sup>137,139,140</sup> which can be difficult to integrate into advanced circuits. Multiple-step imprint processes with registration and alignment can solve this problem and, at the same time, enable top gate device configurations. Work in the area of imprint for silicon microelectronic applications demonstrates that accurate registration is possible, but typically on small chip scale areas.<sup>141</sup> Registration over the large areas that represent the target of many organic optoelectronic applications, especially in systems where the dimensional stability of the plastic substrates is often low, requires additional work. In addition, as with OLEDs, there is reason to explore the potential to use imprint for patterning the organic active material (i.e., the semiconductor). Indirect implementations of imprint will likely be necessary because the etching process as applied directly to the semiconductor can cause catastrophic degradation of electrical properties.

### 3.4. Capillary Molding

Laminating a mold against a flat substrate forms microfluidic channels, into which liquid materials (e.g., solutions, liquid metals, liquid prepolymers) can be filled, either by capillary force (often referred to as micromolding in capillaries, MIMIC) or external pressure (Figure 11c). After the liquid is solidified through solvent evaporation or curing, or after solid objects carried by the liquid are delivered to the substrate surface, the mold is removed to complete the fabrication. This technique is usually performed with elastomeric molds, such as those made of PDMS, because they can form reversible, liquid-tight seals against flat surfaces. This kind of process offers the ability to pattern organic films as well as other conductive films with geometries complementary to the mold relief, to yield active devices of various types.

As an example, source and drain electrodes for OTFTs can be patterned using the MIMIC method. Figure 18a

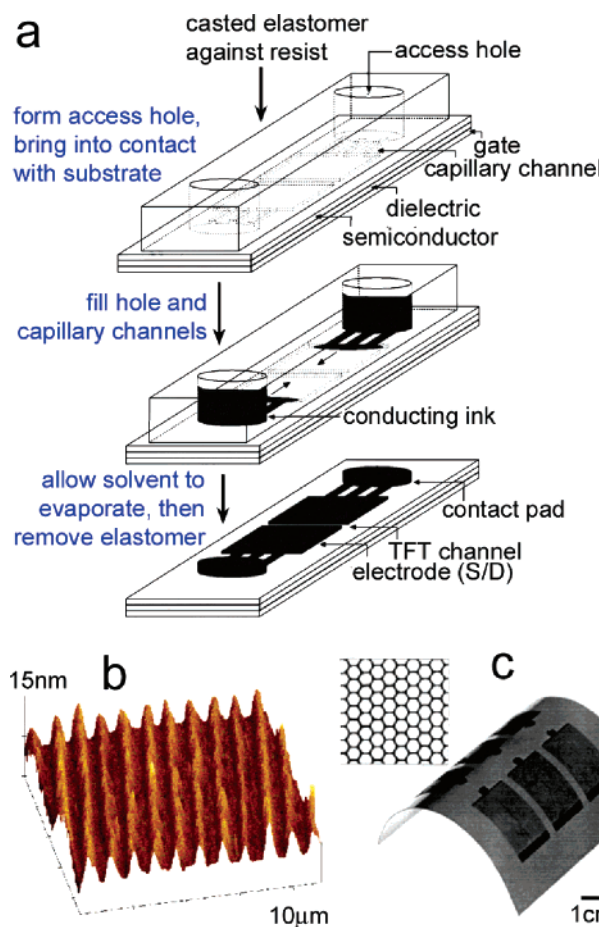


**Figure 18.** (a) Schematic illustration of steps for using micro-molding in capillaries (MIMIC) to pattern organic electrodes for OTFTs. (Reprinted with permission from ref 23. Copyright 1998 American Institute of Physics.) (b) AFM image of semiconducting luminescent polymer POWT nanowires with widths of 833 nm fabricated through this MIMIC method. (Reprinted with permission from ref 21. Copyright 2002 American Chemical Society.) (c) Photograph of patterned polypyrrole on a flexible polyimide substrate by vacuum-assisted MIMIC. The inset is a high-resolution picture showing the quality of the pattern. (Reprinted with permission from ref 142. Copyright 1999 Wiley-VCH Verlag.)

illustrates the procedures.<sup>23</sup> Conducting carbon in ethanol (with a concentration of ~2 wt % of solid carbon) or *m*-cresol solutions of PANI fill capillary channels created by contact

of a suitably designed PDMS mold against a substrate. Evaporation of the solvent through the PDMS, followed by removal of the PDMS mold, yields solid electrodes of carbon or PANI to form source/drain of transistors with channel lengths as small as 2  $\mu\text{m}$ . In this case, the molding was performed on top of a layer of P3HT that served as the semiconductor. Wires with widths on the sub-micrometer scale composed of conducting polymer (e.g., PEDOT-PSS), semiconducting polymer (e.g., poly(3-(2'-methoxy-5'-octyphenyl) thiophene, POMeOPT), and semiconducting luminescent polymer (e.g., poly(3-[*S*]-5-amino-5-carboxyl-3-oxapentyl]-2,5-thiophenylene hydrochloride, POWT) have also been molded in this way.<sup>21</sup> Figure 18b shows an AFM image of POWT wires. Although this technique provides high printing resolution, formation of densely integrated or isolated features can be challenging because each structure must be connected to an inlet access hole. In addition, with high-viscosity inks or narrow fluidic channels, the capillary filling rates can be slow. The filling rate can be dramatically enhanced by applying a vacuum to an end of the channel<sup>142</sup> or by heating the liquid to decrease its viscosity.<sup>22</sup> Figure 18c shows a pattern of polypyrrole on a flexible polyimide substrate molded with the assistance of vacuum.<sup>142</sup>

Not only do these microfluidic channels provide means to pattern solid structures of active materials, but they also create opportunities for the use of liquid active materials in devices that, for example, can be tuned by pumping. Organic transistors with tunable electrical outputs can be achieved, for example, by controlling the position of mercury source/drain electrodes,<sup>143</sup> as shown in Figure 19a. This device uses a thin film of pentacene as the semiconductor. Microfluidic channels formed on top of this layer by conformal contact of a PDMS mold define, after filling, mercury-based fluid source/drain electrodes in a top contact geometry. Fluidic motion alters the channel width of this transistor to tune the source-drain current in this type of microfluidic organic transistor.

An extension of this capillary molding approach uses different fluids that flow inside a single microfluidic channel to define patterns. In microfluidic systems at moderate flow rates, the flow is laminar when the Reynolds numbers are below 2000. As a result, separate fluid streams can flow next to one another in a single channel, where mixing occurs only by interfacial diffusion transverse to the flowing direction.<sup>144,145</sup> This technique was recently applied to the area of organic electronics by using it to pattern aligned films of SWNTs with controlled density and alignment.<sup>146</sup> In this case, solvent (for example, methanol) and an aqueous solution of SWNTs dispersed using a surfactant flow in a channel of a microfluidic system. SWNTs precipitate at the interfacial diffusion zone, due to local reduction in the concentration of the surfactant in this region, as shown in Figure 19b. The precipitated tubes align parallel to flow direction. The flow duration and rate determine the coverage and width, respectively, of the deposited SWNT stripes. Multiphase laminar flow streams generate multiple high-coverage SWNT stripes for arrays of source/drain electrodes in organic transistors that use pentacene as the semiconductor (Figure 19c). Such transistors show mobilities and on/off current ratios of 0.01  $\text{cm}^2/\text{V}\cdot\text{s}$  and 1000, respectively, similar to the values of control devices that use Au source/drain electrodes. SWNTs deposited in this way or by use of other techniques have the potential to be useful for various components of organic electronic and optoelectronic devices. This technique can also

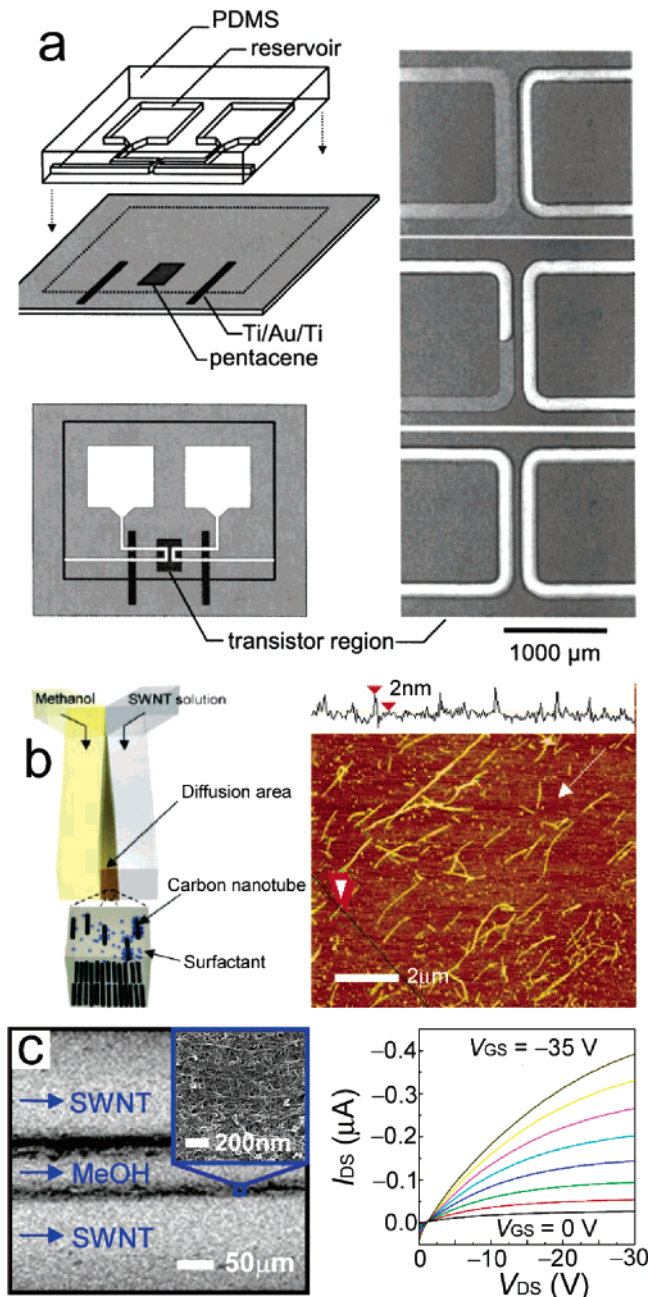


**Figure 19.** Fluidic-based approaches to organic transistors. (a) Schematic angled view of a PDMS mold with relief on its surface and a substrate that supports the semiconductor, gate dielectric, metal contact lines, and gate electrode for TFT (left top). Image in left bottom shows a schematic illustration of the assembled device as viewed from the top through the transparent PDMS. The right frame presents optical micrographs of the transistor region with mercury (white) pumped into the channel on the left-hand side to various degrees. The extent to which the mercury fills the channels defines the effective transistor channel width. (Reprinted with permission from ref 143. Copyright 2003 American Institute of Physics.) (b) Diagram of *in situ* deposition and patterning of SWNTs by laminar flow and controlled flocculation (left). AFM image of the deposited SWNT array (right). Here, SWNTs align parallel to the flow direction (white arrow) due to shear flow. (c) SEM image of two SWNT stripes patterned in a microfluidic channel using three-phase laminar flows (left). These two stripes served as source/drain electrodes of an OTFT.  $I_{DS}$ – $V_{DS}$  characteristics of the as-fabricated transistor with pentacene semiconductor (right). (Reprinted with permission from ref 146. Copyright 2006 Wiley-VCH Verlag.)

define source/drain patterns with tunable channel lengths for similar devices by flowing water, gold etchant, and water through the same channel formed between PDMS stamps.<sup>147</sup> The resulting electrode patterns can be integrated into transistors that use networks of SWNTs as channel material and a wafer substrate covered with a uniform thin Au layer.<sup>147</sup> Evaporating or casting organic semiconductor films onto such electrode patterns can generate OTFTs.

#### 4. Patterning by Printing

“Printing”, as we broadly define it here, refers to methods in which patterns of materials are supplied to (and sometimes removed from) a substrate simply by physical contact or exposure through the mediating use of stamps, nozzles (e.g., inkjet printheads), or masks (e.g., silk screens). Printing methods can be used for each material layer in an organic optoelectronic device, from the metal contacts to the insulating elements to the active transport or emissive layers, whether these materials are supplied in vapor, liquid, or solid form. Printing methods may be either parallel or serial in their operation, depending upon how the pattern is defined. Pattern definition may come, for example, from relief features on a stamp, from masks that protect regions on a substrate from exposure to a printed material, or by focused jets that trace a path across the substrate. Many of these strategies show promise for large-area, low-cost implementation mostly due to the simplicity inherent to printing processes (e.g., minimization or absence of resists, solvents, and tooling), but their success depends critically on the ability to engineer the chemical and materials properties of the printable components. The following sections review several classes of printing techniques that have been used to pattern organic optoelectronic systems, either in research laboratories or in manufacturing/prototyping facilities. The descriptions include characteristics of the techniques, with an emphasis on their capabilities for forming devices that rely critically on organic materials for the device layers or their supporting substrate. Numerous stamp-based approaches in which materials are supplied by physical contact between two bodies are discussed in section 4.1. Section 4.2 describes methods that use scanned laser beams to deposit materials in a serial fashion. Section 4.3 reviews the use of physical masks and stencils to pattern materials from solution (i.e., screen printing) or from vapors (i.e., shadow mask patterning). Finally, section 4.4 outlines recent progress in fluid printing through small nozzles.

#### 4.1. Stamps

Micro- and nanopatterning techniques that use stamps have been successfully applied to many areas of organic electronics and optoelectronics. Their ability to pattern large areas in a single process step (i.e., their parallel operation) and their high resolution represent key features of these approaches. Generally, a stamp supplies a chemical or material (“ink”) to a substrate by physical contact. This transferred material acts as either a functional layer of a device, a resist for etching underlying materials, or a catalyst for directing the deposition or growth of other materials. The “stamps” used for this process come in widely different forms and can be made of materials ranging from rigid solids such as glass or silicon to flexible plastic sheets to soft, viscoelastic elastomers, most notably polydimethylsiloxane (PDMS) like those of the soft molds and photomasks described in the

previous sections. Resolution limits are often very good, limited by the resolution of the stamps themselves or the materials characteristics of the inks. In many instances, stamping methods reduce the number of process steps by minimizing the use of sacrificial layers or even eliminating them by employing purely additive approaches. In addition, many of the methods are noninvasive, thermally and chemically, leading to simplicity in process engineering and sometimes to increased performance in devices.

#### 4.1.1. Microcontact Printing Chemical Templates

One of the earliest demonstrated strategies for stamp-based micro-/nanofabrication is known as microcontact printing ( $\mu$ CP).<sup>148</sup> This section will use the term  $\mu$ CP to refer to stamping methods in which the ink serves as a chemical template for the patterning of functional device components as either an etch mask, a (de)wetting site, an electrochemical insulator, or a catalyst. Stamping methods that involve the direct patterning or transfer of solid inks or functional components of devices are often referred to as variations of  $\mu$ CP (e.g., nanotransfer printing, nTP); those methods are discussed in section 4.1.2. Many inks commonly employed by  $\mu$ CP are chosen to form self-assembled monolayers (SAMs) after or during the printing. Some of these include alkanethiols for SAMs on noble and coinage metals,<sup>148–151</sup> alkanephosphonic acids on aluminum,<sup>152,153</sup> and organosilanes for SAMs on silica.<sup>154</sup>

“Print and etch” approaches use these layers as ultrathin masks for subsequent wet etching to form metal electrodes for organic thin-film transistors (OTFTs). Figure 20a shows a schematic illustration of the process. This type of approach requires (i) a stamp that can make direct molecular contact with the metal and (ii) an ink that can bind sufficiently strongly to the metal and serve as a protective mask against a wet etchant for the metal. Stamps for microcontact printing stamps are elastomers and are similar to the molds and photomasks described previously. Contact is driven by generalized adhesion forces<sup>74–76</sup> and typically does not require externally applied force. The stamps are composed of PDMS, with only a few exceptions.<sup>155</sup> PDMS absorbs a significant amount of ink when brought into contact with a solution of small, hydrophobic molecules such as alkanethiols that can diffuse through the stamp.<sup>156</sup> A variety of methods exist for inking a PDMS stamp with thiols, ranging from applying the ink solution to the surface of the stamp, and then blowing it dry, to using another PDMS stamp as an “ink pad”.<sup>157</sup> Because the SAM layers often present non-wetting surfaces to the inks (i.e., the systems are autophobic)<sup>158,159</sup> and the formation of the SAM is self-limiting, the uniformity of the ink applied to the stamp usually does not affect the quality of the printed monolayers, provided that sufficient ink is present at all locations. Inking stamps with hydrophilic inks requires additional treatments to ensure good loading onto the (usually hydrophobic) PDMS by rendering its surface hydrophilic. This condition can be achieved by oxidation<sup>153</sup> and, optionally, functionalizing the surface of the stamp.<sup>160</sup>

Remarkably, molecularly thin organic films can serve as reliable masks against wet etchants.<sup>161</sup> The most commonly printed etch masks for microcontact printing are hydrophobic SAMs of alkanethiols printed onto Au,<sup>150,162</sup> Ag,<sup>151,163</sup> Cu<sup>149,152,162,164</sup> (after oxide removal), and Pd<sup>152,165–167</sup>. The SAMs formed from hexadecane thiol (HDT) on gold serve as effective etch masks for ferricyanides and Fe<sup>3+</sup>/thiourea.<sup>152</sup>

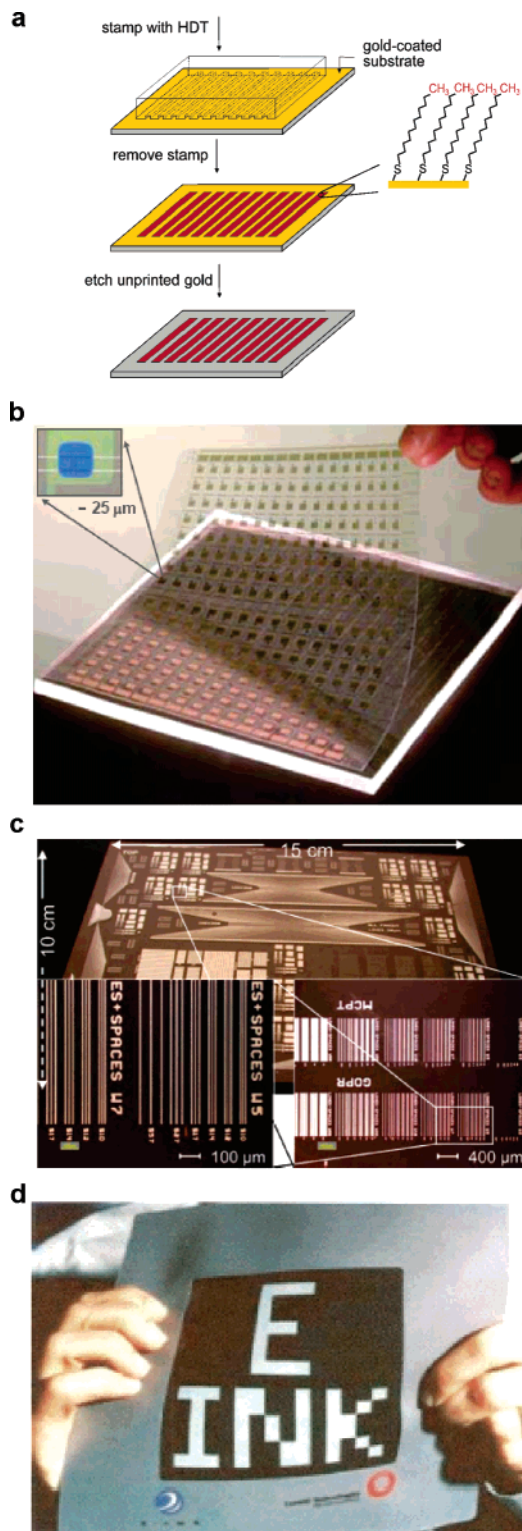


**Figure 20.** Metal patterning by  $\mu$ CP and etching. (a) Schematic for  $\mu$ CP and etching. A self-assembled monolayer of hexadecane thiol (HDT) is printed onto gold from the relief features on a PDMS stamp. Removal of the stamp and wet etching yields micro-/nanoscale patterns in the gold. (Adapted from “Crawford” and “Woodhead” chapters.) (b) Active matrix backplane (12 × 12 cm) of pentacene OTFTs with bottom contacts patterned by  $\mu$ CP and etching. (Reprinted from ref 173. Copyright 2001 PNAS.) (c) 15 cm substrate with patterns of Ag/Mo defined by  $\mu$ CP and etching using a wave-printer. (Reprinted with permission from ref 169. Copyright 2005 American Chemical Society.) (d) Electronic paper-like display that uses electrophoretic ink and an active matrix backplane with electrodes fabricated by  $\mu$ CP and etching, as in (b). (Reprinted with permission from ref 173. Copyright 2001 PNAS.)

Other alkanethiol SAMs form etch masks, but HDT is the most effective.<sup>168</sup> Printed, annealed SAMs of hexadecane-phosphonic acid can protect aluminum from NBSA/PEI, as well as other etchants.<sup>152,153</sup> Other metals may be patterned by  $\mu$ CP and etching using one of the above listed metals as a second etch mask.<sup>169,170</sup>

When applied to organic transistors,  $\mu$ CP and etching usually defines the source and drain electrodes, normally for bottom contact geometries. The distance between source and drain electrodes defines the channel length in OTFTs, which is generally the most demanding feature of the device pattern in terms of resolution.  $\mu$ CP and etching can easily achieve submicrometer resolution, limited by (besides the stamp feature size) the spreading and vapor-phase transport of the printed ink into noncontacting regions during and after printing,<sup>171</sup> by edge disorder that occurs in the patterned SAMs, and by the wet etching step. As a result, inks composed of heavier molecules with relatively low diffusivity and short contact times can improve resolution.<sup>171</sup> In the case of  $\mu$ CP and etching using alkanethiols, the practical limits of resolution are about 100 nm. Channel lengths comparable to this value have been achieved in bottom-gate OTFTs of  $\alpha\alpha$ -diethyl quaterthiophene (DH4T).<sup>172</sup> The performance of organic devices fabricated using  $\mu$ CP and etching is generally comparable to that of devices produced using more conventional approaches (e.g., evaporation through a shadow mask)<sup>173</sup> for both polymer (e.g., P3HT<sup>174,175</sup>) and small molecule (e.g., pentacene,<sup>173,176</sup> F<sub>16</sub>CuPc,<sup>151</sup> CuPc,<sup>176</sup> diethyl quinquethiophene<sup>151,176</sup>) semiconductors, and OTFTs fabricated using  $\mu$ CP and etching have been used to build sexithiophene/F<sub>16</sub>CuPc complimentary inverter circuits<sup>174</sup> and polymer-dispersed liquid crystal (PDLC)<sup>177</sup> and electrophoretic paperlike displays driven by bottom-contact pentacene OTFTs.<sup>173</sup>

Significant research has been directed toward engineering development of  $\mu$ CP and etch approaches. Simple reel-to-reel implementations have been demonstrated for the fabrication of polymer thin-film transistors made using the semiconductor P3HT.<sup>175</sup> The most advanced demonstrations of large-area  $\mu$ CP and etching for organic electronics have planar configurations, with applications in flexible displays.<sup>173</sup> Other related work illustrates the use of  $\mu$ CP for electrode lines in conventional backplane circuits.<sup>178</sup> Figure 20 illustrates some examples of large-area substrates patterned by  $\mu$ CP and etching in planar configurations. Figure 20b displays an array of 256 pentacene transistors on a flexible plastic substrate patterned by  $\mu$ CP and etching of gold electrodes,<sup>173</sup> and Figure 20c displays patterns of  $\mu$ CP and etched Ag/Mo.<sup>169</sup> The prototype black and white display in Figure 20d uses the array in Figure 20b to drive an electrophoretic ink.<sup>173</sup>

Some of the most significant challenges associated with scalability of  $\mu$ CP are the difficulties related to achieving accurate multilevel registration in the presence of mechanical and thermal distortions that can appear during the use of the stamps. In the simplest approach to this problem, these distortions can be reduced by minimizing the extent of stamp handling in a printing process. Distortions of <50–100  $\mu$ m can be achieved across 12 cm flexible plastic substrates by carefully laminating the substrate by hand against a stabilized PDMS stamp<sup>173</sup> (Figure 20b). Distortions can also be minimized by stamp constructions that use high-modulus mechanical backings.<sup>26,28,179</sup> For large-area application, these rigidly backed stamps should be thin to enable bending that

can facilitate their removal from both a master after molding and from rigid, nonflexible device substrates, such as thick glass or semiconductor wafers. Even with such stabilized stamps, registration can be challenging because alignment must be performed before contact. An inventive solution, known as wave printing,<sup>29,169,180</sup> (Figure 20c), accomplishes registration better than 2  $\mu$ m across 15 cm substrates by suspending a thin, glass-backed stamp a small distance ( $\sim$ 100  $\mu$ m) away from the device substrate during alignment and using an array of pneumatic valves to drive contact and separation. Arrays of pentacene OTFTs fabricated by wave printing and etching exhibit high yields (>90%) for micrometer-scale channel lengths.<sup>180</sup>

In addition to etch masks, microcontact printed chemicals can serve as templates for patterning functional organic optoelectronic materials by serving as (de)wetting patterns, catalysts, or as electrochemical insulators. Figure 21 illu-

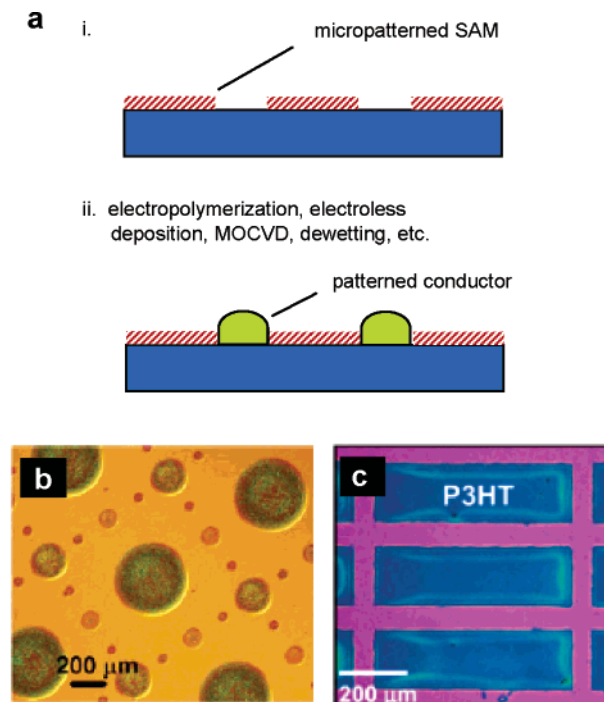


**Figure 21.** Patterning functional materials by selective deposition on microcontact printed chemical templates. (a) Illustration of selective deposition of functional materials, here shown using a stamp-printed SAM as a template. (b) Patterns of PANI (dark) wetting a hydrophilic substrate. PANI dewets from patterns (light) rendered hydrophobic by  $\mu$ CP of OTS.<sup>181</sup> (Reprinted with permission from ref 181. Copyright 2005 American Institute of Physics.) (c) P3HT on SiO<sub>2</sub> patterned by dewetting from printed siloxane oligomers. (Reprinted with permission from ref 182. Copyright 2006 American Chemical Society.)

strates the general principle of depositing functional materials in patterns predefined by printed chemical templates (Figure 21a) with examples of patterned organic conductors (PANI, Figure 21b)<sup>181</sup> and semiconductors (P3HT, Figure 21c).<sup>182</sup> These  $\mu$ CP methods are additive and can be less chemically invasive than print and etch approaches. Typical inks include all of those discussed in section 4.1.1 for printing onto metals, as well as a variety of others that are suitable for printing onto nonmetals, including organosilanes that form SAMs on silica and some other oxides, as well as non-SAM-forming inks. In contrast to inks for etch resists, inks for additive  $\mu$ CP processes can often function well even with high levels of defects. Consequently, a wide variety of printable materials

are employed for these approaches. For example, hydrophobic siloxane oligomers present in common PDMS elastomer transfer onto contacted substrates.<sup>182,183</sup> Those oligomer films can function as dewetting templates for patterning organic semiconductors (P3HT, 5-chlorotetracene) and conductors (PEDOT) with resolutions as good as 1  $\mu\text{m}$ .<sup>182</sup> The solutions of organic semiconductors wet the unstamped, hydrophilic surfaces upon removal from solution but leave the printed, hydrophobic surfaces dry. This method is thus “inkless” in that the stamp is loaded with usefully printable material (siloxane oligomers) even without an intentional inking step, and it can be used to make OTFTs on flexible plastic substrates.  $\mu\text{CP}$  and dewetting methods can also employ OTS SAMs on oxidized silicon wafers to pattern polyaniline in a “stamp-and-spin-cast” method<sup>181</sup> to produce bottom contacts for pentacene transistors that perform as well as transistors that use evaporated gold electrodes. OTS on SiO<sub>2</sub> and hexadecylhydroxamic acid on ZrO<sub>2</sub>, along with other hydrophobic printed templates, can serve as dewetting patterns for hybrid organic/inorganic semiconductors ((C<sub>6</sub>H<sub>5</sub>C<sub>2</sub>H<sub>4</sub>-NH<sub>3</sub>)<sub>2</sub>SnI<sub>4</sub>) in TFT geometries that yield mobilities as high as achievable by other methods for this material, about 0.5 cm<sup>2</sup>/V·s.<sup>154</sup> In another example, regions on a gold film between printed patterns of alkanethiols are filled with another SAM molecule (terphenylthiol) that serves as a template for the growth of large ( $\sim$ 100  $\mu\text{m}$ ) oligoacene single crystals from solution.<sup>184</sup> In all of these methods, the functional (semi)conducting materials remain on the unstamped, hydrophilic regions of the substrate and dewet from or otherwise avoid the hydrophobic, stamped template regions during a spinning/drying step. Organic semiconductors patterned by deposition mediated by patterned surface templates can also produce good performance in OTFTs. For example, large ( $\sim$ 3  $\mu\text{m}$ ) crystal pentacene films deposited by organic physical vapor deposition methods selectively onto a transistor structure exhibit high (1.2 cm<sup>2</sup>/V·s) mobility.<sup>185</sup> In this example, the templating of the surface was implemented without a stamp, but the same treatment can in principle be accomplished by  $\mu\text{CP}$ . In addition, stamped dewetting patterns of hydrophobic silanes on glass<sup>186</sup> and polyethylene naphthalate (PEN) treated with tetramethylammonium hydroxide (TMAH)<sup>187</sup> can also inhibit metallization in those regions by metal–organic chemical vapor deposition or by electroless deposition for the fabrication of gate electrodes in OTFTs.

Microcontact printed templates can also be used as wetting patterns in which materials are deposited on the printed regions and not on the bare regions, in contrast to the aforementioned methods. Examples include deposition solution polymerization of organic conductors, polypyrrole (PPy) and polyaniline (PANI) on OTS SAMs,<sup>188</sup> and electroless metal deposition selectively onto microcontact printed catalytic templates of Pd-containing colloids and organic complexes.<sup>189–191</sup> Printed inks can also template organic optoelectronic elements electrochemically. Microcontact printed thiol SAMs on gold can serve as insulators for patterned electropolymerization of PPy and polyethylene-dioxythiophene (PEDOT) if the SAM is sufficiently thick.<sup>192,193</sup> Thin SAMs of trifluoroethanethiol are not thick enough to impede electropolymerization but can be used as antiadhesion coatings for subsequent removal of electropolymerized PPy films. OTS SAMs on ITO can serve as partially effective barriers for PPy electropolymerization, but OTS-coated regions on Si wafers actually facilitate electropolymerization

of PPy.<sup>194</sup> In a related method, printed SAMs on ITO at elevated temperatures serve as hole-blocking templates for patterning TPD/Alq<sub>3</sub> OLED electroluminescence.<sup>195</sup>

#### 4.1.2. Direct Patterning with a Stamp

In a set of methods that we refer to as “transfer printing,” the materials printed from a stamp are the actual functional materials for organic optoelectronics or other applications. Advantages of this approach include, in many cases, the ability to pattern several types of material on a single device substrate without exposing it to solvents or other invasive processing and levels of resolution that exceed those possible with traditional  $\mu\text{CP}$ . The requirements for these methods are similar to those for  $\mu\text{CP}$ : (i) a stamp that can support a functional ink and can be contacted to a target substrate and (ii) some mechanism for the transfer of this ink from the stamp to the substrate. These substrates can use special surface chemistries, conformable adhesive layers, or other means to guide preferential adhesion. Vacuum, solution, or solid transfer strategies provide means for preparing a printable material on the stamp (“inking the stamp”). Stamps suitable for transfer printing often comprise soft elastomers, such as PDMS, and also hard backings, especially when pressure is applied to guide the transfer and/or when the target/receiving substrate has a soft, conformable surface to facilitate contact. The features of relief on the stamps usually define the patterns in the transfer printed materials. Materials that are transfer-printed can form many of the layers of an organic optoelectronic system, from conductors to semiconductors to dielectrics. The following subsections summarize recent developments in transfer printing materials relevant to organic optoelectronics and some complimentary technologies, namely, metals and their precursors, conducting polymers, carbon nanotubes, and organic semiconductors, as well as ultrathin crystalline inorganic materials that are suitable for use in areas of application commonly explored for organics, for example, large-area, flexible electronics.

**4.1.2.1. Metals and Other Conductors.** Transfer printing of metals, often referred to as nanotransfer printing (nTP), offers levels of resolution that exceed those of  $\mu\text{CP}$  and can be employed, for example, to form the source and drain electrodes in OTFTs<sup>196–203</sup> or the electrodes in OLEDs<sup>204–206</sup> and organic photovoltaics.<sup>199</sup> The printing in this case begins usually with evaporation of metal onto a stamp, as illustrated in Figure 22, optionally with an adhesion-reducing, nonstick layer to aid release of the metal ink. The inked stamp contacts a substrate, and the ink binds to the substrate by chemical bonds, by preferential physisorption, or by means of an adhesive layer. Figure 22b displays the device characteristics of a P3HT OTFT that uses electrodes printed in this manner.<sup>197</sup> When the ink is a solid, vapor-phase transport and other ink-spreading mechanisms inherent to  $\mu\text{CP}$  and etching do not limit the resolution of printed metal features. Instead, the metallic grain structure limits the resolution (edge roughness down to  $\sim$ 10 nm),<sup>199,201</sup> allowing high-resolution ( $\sim$ 100 nm) metal patterning.<sup>199,201,207,208</sup> In the context of organic optoelectronics fabrication, Al patterns with features as small as 80 nm<sup>209</sup> and pentacene OTFTs with 1  $\mu\text{m}$  channels<sup>199</sup> have been demonstrated. Additionally, the additive printing, in which metals are transferred directly onto an organic substrate, avoids the penetration of metal into the organic that occurs during evaporation<sup>210,211</sup> and the loss of resolution that occurs during the etching step of “print and etch”  $\mu\text{CP}$  methods. The performance of the devices

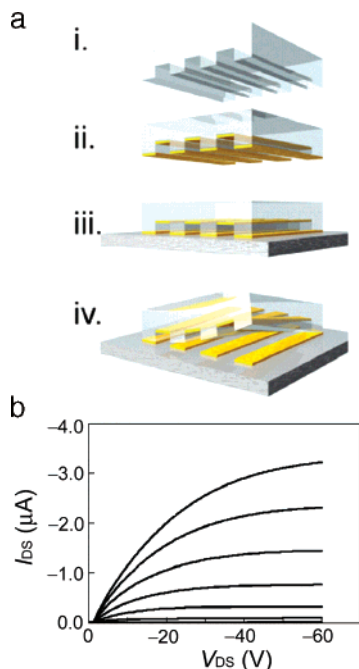


**Figure 22.** Patterning by direct transfer printing of metals. (a) Schematic of nanotransfer printing (nTP) using a PDMS stamp (i). Electron beam evaporation deposits metal on the stamp (ii), which is then brought into contact (iii) with a target substrate. Covalent bonds, metallic bonds, or non-covalent surface forces pull the metal from the stamp when it is separated from the substrate (iv). (b)  $I$ - $V$  characteristics of a P3HT top contact TFT with source-drain electrodes transferred directly onto the semiconductor from a PDMS stamp. (Reprinted with permission from ref 197. Copyright 2004 American Institute of Physics.)

fabricated by printing metals directly from a stamp usually reaches levels comparable or nearly identical to those obtained by more conventional approaches (typically as compared to shadow-mask evaporation), with some variations. Indeed, CuPc devices made with transfer printed gold electrodes show performance virtually identical to that of control devices.<sup>199</sup> In certain cases, the improved pattern definition inherent to the transfer printed metal methods can show improved performance relative to devices with shadow-mask evaporated electrodes.<sup>197</sup> Although these transfer printing approaches offer attractive features in terms of manufacturing simplicity and very good resolution, they are relatively new, and the extent to which these methods have been applied to organic optoelectronics is thus far limited to single devices (e.g., cathodes for OLEDs; source-drain electrodes for OTFTs), small passive matrix OLED displays,<sup>204,205</sup> and simple circuits (e.g., pentacene/ $F_{16}CuPc$  complementary inverters<sup>201</sup>).

Chemistries for good surface binding include surface condensation reactions between ( $-OH$ ) groups,<sup>201,208</sup> thiol–metal reactions,<sup>207,210,211</sup> and cold welding.<sup>199,204,208,212</sup> Cold welding occurs when two clean gold or silver surfaces meet and they are allowed to conform to each other. Such conformability can be supplied by applied pressure,<sup>199,204</sup> or it can be supplied by a soft supporting layer behind one or both of the metal layers.<sup>208,212</sup> A metal layer on the target substrate, the so-called “strike” layer, deposited to bond to the printed metal by cold welding, may be removed after printing to form functional devices.<sup>199,212</sup> In most implementations, regardless of the binding chemistry, at least one highly conformable (e.g., PDMS) or moderately conformable (e.g., heated PMMA) layer is used. Metal thicknesses are

usually small (about  $<50$  nm), because thick ( $>100$  nm) metal layers can impede conformability.<sup>213</sup> Antiadhesion layers useful for metal ink release from a stamp include perfluorinated SAMs,<sup>205,214</sup> fluorinated ethylene propylene,<sup>209</sup> and Alq<sub>3</sub>.<sup>199</sup> PDMS stamps often do not require an additional antiadhesion layer for ink release, especially for gold.<sup>207,208</sup> Alternatively, stamps with sticky or adhesion-promoting layers strongly bound to the stamps’ surfaces may be used to remove metals from surfaces in subtractive patterning approaches to produce organic optoelectronic devices.<sup>202–204</sup>

Non-covalent transfer printing of metals is possible when there is a physical interfacial energy mismatch between the ink–stamp and the ink–substrate interfaces, allowing transfer without extra surface functionalization or activation steps.<sup>197,215</sup> The method is thus an additive process that requires no additional chemicals or materials. As the ink is less strongly bound to the target substrate surface than it is in covalent transfer printing methods, low roughness on the surfaces is important for good transfer.<sup>197</sup> When printing gold from PDMS, mild heating and extended contact time can enhance efficiency, possibly by strengthening the ink–target substrate interface and/or by allowing siloxane oligomers to segregate to the ink–stamp interface to facilitate release.<sup>197</sup> Siloxane oligomers can severely degrade the conductivity of copper films prepared on a PDMS stamp but not that of gold films prepared in the same way.<sup>216</sup> Printing gold electrodes in this manner directly onto P3HT and other semiconductors provides a method for practically noninvasive fabrication of top-contact OTFTs, with characteristics equal or superior to those of similar OTFTs prepared by shadow-mask evaporation.<sup>197</sup> The on/off ratios of these P3HT devices produced by non-covalent transfer-printed electrodes are significantly higher than those for devices prepared using shadow-mask evaporation techniques, possibly due to improved channel definition.<sup>197</sup>

Printing metals onto a conformable adhesive layer provides a means to achieve reliable transfer of metal from a stamp by ensuring full contact between the ink and the receiving substrate,<sup>217</sup> especially when the stamp or ink is rigid. Conformability of the substrate surface is an additional constraint on the system, but it can be supplied by materials with broad compatibility, for example, by heated PMMA,<sup>215</sup> which can serve further as a gate dielectric, or by semiconductors, such as P3Ht,<sup>202,203</sup> to form OTFTs and Alq<sub>3</sub><sup>205</sup> or 4,4'-bis[N-(1-naphthyl)-N-phenylamino] biphenyl ( $\alpha$ -NPD) (the authors of the original work refer to this material as NPB)<sup>209</sup> for the production of OLEDs. The conformable layer may be supplied on the target substrate or on the inked stamp.<sup>209,218</sup> Conformability may also be enhanced by printing nanocrystalline<sup>219</sup> or even liquid precursors to metals.<sup>220</sup> Thermal treatment converts these precursors to solid, conductive electrodes. Chemical functionality may be incorporated into the precursors before stamping to reduce contact resistance in resulting OTFTs. For example, poly(3,3''-didodecylquarterthiophene) devices (PQT-12) fabricated using electrodes derived from printed oleic acid stabilized silver nanoparticle films exhibit mobilities ( $0.12\text{ cm}^2/\text{V}\cdot\text{s}$ ) more than twice as high as those of similar devices prepared from vacuum-deposited silver electrodes.<sup>219</sup> Conformability to the substrate may also be supplied by printing soft organic conductors, such as PEDOT, with or without adhesive additives for OLEDs<sup>206</sup> and for high-performance top-gate pentacene TFTs ( $\mu = 0.71\text{ cm}^2/\text{V}\cdot\text{s}$ ; on/off  $\sim 10^6$ ).<sup>200</sup> The increased performance of these pentacene devices relative

to control devices made using shadow-mask evaporation is attributed to the improved carrier injection in the PEDOT/pentacene system relative to Au/pentacene.<sup>200</sup> Printing PEDOT electrodes in this manner also enables the fabrication of all-organic TFTs that use pentacene as a semiconductor and very thin (<2  $\mu\text{m}$ ) mylar substrates as the gate dielectric.<sup>196</sup>

**4.1.2.2. Organic Semiconductors.** Most conventional organic semiconductors, polymers or small molecules, may be printed using stamps. Figure 23 illustrates the principle with several examples in which  $\alpha$ -NPD (Figure 23a),<sup>221</sup> P3HT (Figure 23b),<sup>222</sup> and pentacene (Figure 23c)<sup>215</sup> are deposited from a stamp to form functional devices. Other examples in this figure (Figure 23d–f) illustrate devices and patterns in organic semiconductors formed by removing regions in them using subtractive stamping methods (see below). Although the resolution capabilities are very good (80 nm patterns achieved<sup>209</sup>), the greatest advantage of direct stamp-based transfer/patterning organic semiconductors is that the materials may be patterned and deposited without the use of solvents, sacrificial masks, etc., that can interfere with the delicate chemistry and physical structure of the device components, for example, by unwanted interaction of solution processable gate dielectrics and P3HT during OTFT solution processing.<sup>223</sup> By printing P3HT onto smooth polyimide surfaces prepared by spin-coating, OTFTs ( $\sim 0.02 \text{ cm}^2/\text{V}\cdot\text{s}$ ; on/off =  $10^3$  or  $10^4$ ) can be produced.<sup>222</sup> These printing approaches begin with vacuum evaporation<sup>221,224</sup> or solution deposition<sup>222,223,225</sup> that form layers of active organic materials on stamps. Transfer is driven by non-covalent binding and, as with other non-covalent transfer methods, extended contact times (several minutes to a few hours) at slightly elevated temperatures improve transferability. Additionally, swelling the inks and receiving surfaces with solvent can strengthen the bond by allowing polymer chain interpenetration for the transfer of, for example, organic light emitting films (8-hydroxyquinoline/poly (9-vinylcarbazole) (Alq<sub>3</sub>/PVK) and (C<sub>6</sub>H<sub>5</sub>C<sub>2</sub>H<sub>4</sub>NH<sub>3</sub>)PdI<sub>4</sub> (PhE-PdI<sub>4</sub>/PS)).<sup>226,227</sup> In one method, PDMS stamps are cured with an imbedded ink that serves as a green-emitting dye (3-(2'-benzimidazolyl)-7-(diphenylamino)-2H-1-benzopyran-2-one), which diffuses into the target during printing at slightly elevated temperatures for blue to green conversion of electroluminescent materials in OLEDs.<sup>228</sup> Substrates onto which the organic semiconductors are printed are typically rendered hydrophobic to more efficiently receive the ink. In some instances, an adhesion-promoting “strike layer” may be used in a manner analogous to the transfer printing of metals by cold welding (see section 4.1.2.1). For example, bonding between two  $\alpha$ -NPD layers may drive the transfer of ink off of a PDMS stamp treated with a well-adhered thin gold film as an antiadhesion layer for the fabrication of OLEDs.<sup>221</sup> The preparation of Al cathodes and active organic layers terminating with  $\alpha$ -NPD (the authors of the original work refer to this material as NPB) on a polyurethaneacrylate (PUA) mold and subsequent printing onto ITO enables RGB OLED pixel fabrication with nanoscale resolution.<sup>209</sup> OLEDs fabricated in this manner show slightly less current than devices made by conventional means due to trapped air and imperfect interfaces produced during printing, but slight heating (60 °C) during printing can improve both the transfer fidelity and the electrical quality of the interface.<sup>221</sup> Application of pressure and/or temperature can help transfer when the receiving interface is near or above its  $T_g$ , especially when the stamp is rigid.<sup>215</sup>

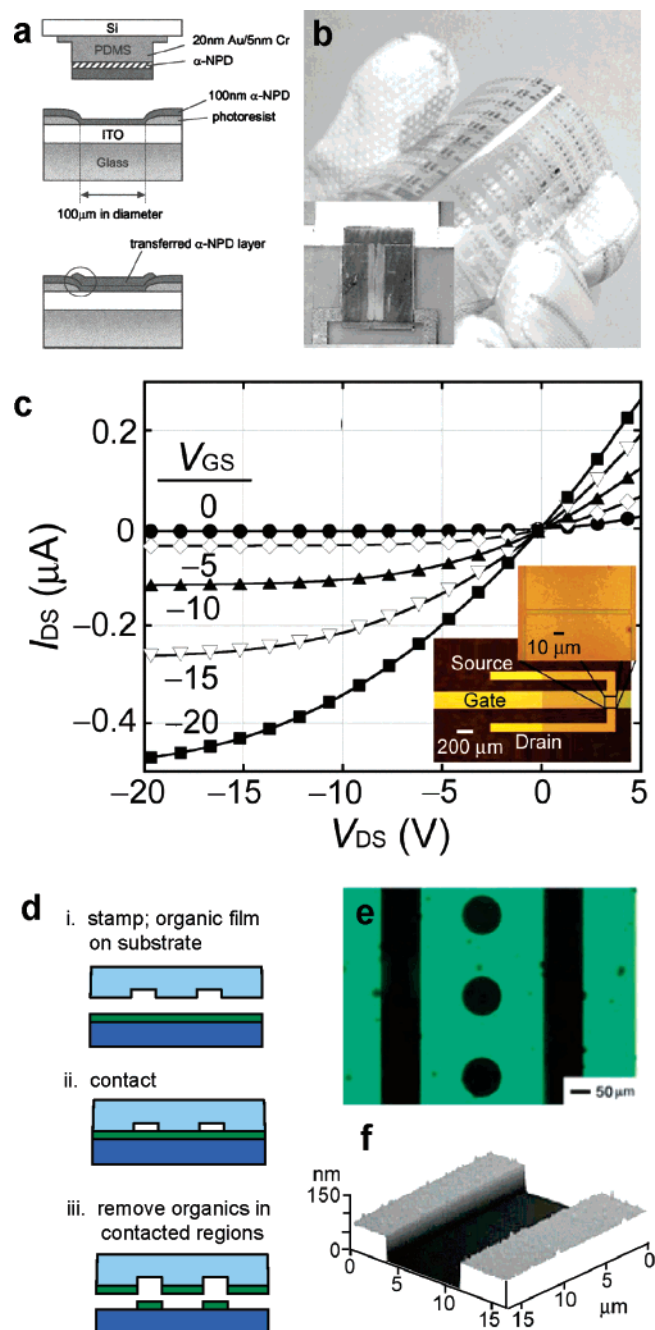


**Figure 23.** Direct stamp-based patterning of organic semiconductors. (a) Schematic illustrating the transfer of an emissive layer ( $\alpha$ -NPD) from a stamp onto a glass substrate using an adhesion-promoting organic “strike layer.” (Reprinted with permission from ref 221. Copyright 2005 American Institute of Physics.) (b) Bottom-contact OTFTs on plastic fabricated using P3HT printed directly from a PDMS stamp. (Reprinted with permission from ref 222. Copyright 2002 IEEE.) (c) Device characteristics and inset optical micrograph of an all-components-printed pentacene transistor on PET transferred using applied heat and pressure from a rigid stamp. (Reprinted with permission from ref 215. Copyright 2005 American Institute of Physics.) (d) Schematic illustrating subtractive stamping patterning approaches. (e) OLED made from  $\alpha$ -NPD (the authors refer to this material as NPB) patterned by subtractive stamping using PDMS. (Reprinted with permission from ref 229. Copyright 2005 Wiley-VCH.) (f) AFM of CuPc patterned by subtractive methods using an epoxy stamp. (Reprinted with permission from ref 230. Copyright 2003 American Chemical Society.)

A number of subtractive stamping methods have been developed for patterning organic semiconductors after deposition onto a device substrate. These methods use a structured

stamp to bind to regions on an organic semiconductor film that are removed from the substrate after it is separated from the stamp (Figure 23d). Panels e and f of Figure 23 display patterns in  $\alpha$ -NPD<sup>229</sup> and CuPc<sup>230</sup> patterned in this way. Subtractive methods in principle do not alter the interface between the substrate and the active material from its original, as-deposited state. By contrast, additive transfer printing approaches often invert the active material, leaving it “upside-down” on the device substrate and in some cases leading to reduced performance. In one demonstration, inversion of pentacene films led to an order of magnitude decrease in mobility.<sup>224</sup> Accordingly, the results of subtractive organic semiconductor stamping methods are OTFTs and OLEDs with operating characteristics that can be essentially identical to those of more conventionally fabricated devices.

Partially cured epoxy stamps are useful for the binding and removal of organics, including CuPc, metal-free phthalocyanine ( $H_2Pc$ ), NPB, and Alq<sub>3</sub> from Si and ITO surfaces, yielding devices with characteristics comparable to conventionally fabricated structures.<sup>230</sup> PDMS is also capable of removing many active materials from ITO, leaving micrometer resolution features of small molecule organic semiconductors including  $\alpha$ -NPD (the authors of the original work refer to this material as NPB), Alq<sub>3</sub>, rubrene, and others, by a simple method in which the PDMS is contacted to a film and then heated to 90 °C for on the order of 1 h before removal.<sup>229</sup> This effect seems to be governed by the hydrophobic character of the PDMS, because stamps with oxidized surfaces are not effective for this subtractive approach. Polymer semiconductors, on the other hand, are not as easily removed using this approach, presumably due to the much higher fracture toughness of the films.<sup>229</sup> In these subtractive methods as well as in others in which the films must be fractured during patterning, it is possible to engineer the organic semiconductors to have low-energy end-groups, for example, isopropyl groups, which can lead to well-defined fracture regions.<sup>224</sup> Low cohesive strength in the organic material is important for achieving high-resolution patterning. For example, contacting a polyurethaneacrylate mold to  $\alpha$ -NPD (the authors of the original work refer to this material as NPB) films for 20 min at 90 °C can produce patterns with features as small as 50 nm.<sup>231</sup> Alternatively, the blanket film for subtractive stamp-based patterning may be liquid. In one method, a benzyl-trichlorosilane-treated PDMS stamp contacted to a thin film of poly[(9,9'-dioctyl fluorine)-co-bithiophene] (F8T2) or poly[5,5'-bis(3-alkyl-2-thienyl)-2,2'-bithiophene] polymer solution absorbs excess solvent (chlorobenzene) and pulls the polymer out of noncontacted regions by capillary action, leaving the dry polymer film only in the regions contacted by PDMS.<sup>232</sup>

**4.1.2.3. Thin Films of Carbon Nanotubes.** Random networks or aligned arrays of single-walled carbon nanotubes (SWNTs) form effective thin films for flexible electronics. They can serve as either conductors or semiconductors in these systems. Such films exhibit several attractive properties, including extreme levels of mechanical bendability,<sup>233</sup> excellent optical transparency,<sup>234</sup> high carrier mobilities,<sup>235–237</sup> the ability to establish good interfaces with other organic electronic materials,<sup>32,234</sup> and compatibility with direct printing from a stamp.<sup>233,234,238–240</sup> Stamps may comprise the SWNT growth substrate itself<sup>215,241</sup> or some other substrate inked by solution<sup>238</sup> or by contact to loosely bound SWNTs on an “ink-pad” or “donor substrate.”<sup>233,234,239,240,242</sup> A

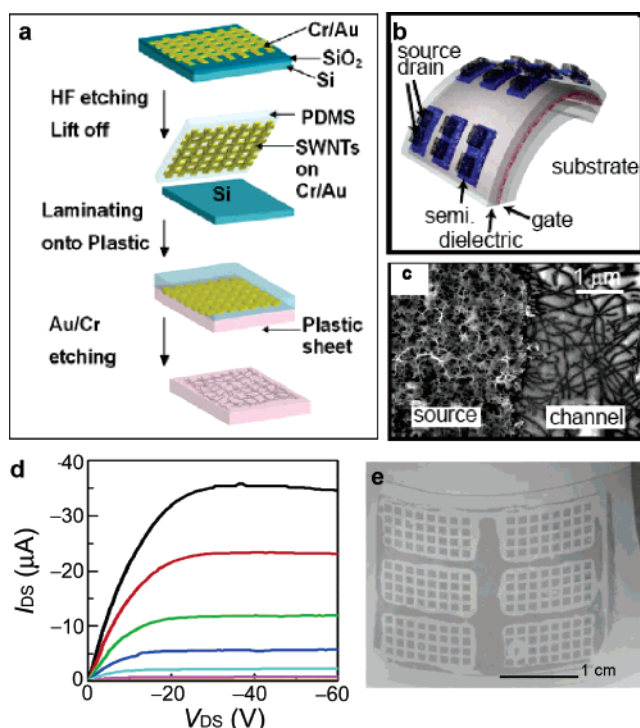


**Figure 24.** Printing carbon nanotubes. (a) Schematic illustration of the transfer printing method using a metal carrier mesh and a PDMS stamp. (b) Illustration of a mechanically flexible TFT array that uses semiconductors and electrodes comprising SWNT networks. (c) SEM image of the contacts and channel region of the SWNT TFTs illustrated in (b). (d)  $I$ – $V$  characteristics of the TFTs in (b) and (c) with a channel 225  $\mu$ m long and 750  $\mu$ m wide.<sup>233,234</sup> (e) Film of SWNT transferred from an alumina filter to a flexible PET sheet. (Reprinted with permission from ref 242. Copyright 2006 American Institute of Physics.)

recently described method (Figure 24a) for retrieving SWNT films prepared by chemical vapor deposition (CVD) on a growth substrate with a stamp is important because the pristine tubes grown by CVD typically show much greater electrical properties than those deposited from solution.<sup>233,234,239,240</sup> In this method, a metal mesh acts as a carrier for the SWNTs after an undercutting etch releases them from the growth substrate. The mesh along with the SWNT film may be retrieved using a stamp after the undercut. Removal of the mesh occurs on the target substrate after printing to yield bare SWNTs. Panels b–d of Figure 24 illustrate the utility of these materials for flexible and/or transparent organic optoelectronic devices that consist of transfer-printed SWNT films as electrodes and semiconductors.<sup>239</sup> Stamp-based printing of SWNT films has been demonstrated using conformable stamps, conformable layers on target substrates, or both. Applied pressure<sup>215,241</sup> facilitates complete contact when the stamp and substrate are both of at least moderate rigidity, thereby allowing transfer of the SWNT films. The SWNTs bind to the target substrate by non-covalent van der Waals forces, and as with non-covalent transfer of metals, mild heating, extended contact times, and low roughness on the target substrate can strongly increase the efficiency of transfer.<sup>238</sup> SWNT films prepared by filtration onto alumina filters (rough) are bound loosely enough to be retrieved using PDMS stamps and subsequently printed onto smoother target substrates (Figure 24e).<sup>242</sup> As conductors, the carbon nanotubes can form good contacts to organic semiconductors such as pentacene, due partly to the similar conjugated molecular structures of the two materials,<sup>234</sup> which may enable high

carrier mobilities even for short-channel devices and high-frequency OTFT operation. As either semiconductors or conductors, the films offer excellent mechanical strength (i.e., the films can survive strains at least as high as 20%<sup>233</sup>) and good optical transparency,<sup>234,238,239</sup> suggesting that these materials might provide promising alternatives to ITO (fracture strain  $\sim 1\%$ )<sup>239</sup> and other brittle materials (e.g., other semiconducting oxides) for application in transparent, flexible electronics. As semiconductors, SWNT films can exhibit high device-level carrier mobilities in TFTs, owing to the very high intrinsic mobilities of the SWNTs themselves, limited by the density and degree of alignment in the film and the resistances associated with tube–tube contacts. The presence of metallic tubes can present problems, due to their contributions to current in the off state of the transistors. Approaches exist, however, for eliminating the effects of these tubes by chemical<sup>243,244</sup> and/or electrical means.<sup>197,245</sup> Transfer printed SWNT network films used as semiconductors routinely exhibit carrier mobilities of  $\sim 15$ – $30 \text{ cm}^2/\text{V}\cdot\text{s}$ ,<sup>233,239,245</sup> and in some cases can approach values of  $\sim 100 \text{ cm}^2/\text{V}\cdot\text{s}$  and greater.<sup>235,246</sup> More recent research indicates that devices based on highly aligned arrays of nanotubes can reach as high as  $100$ – $1000 \text{ cm}^2/\text{V}\cdot\text{s}$ .<sup>236,237,247,248</sup>

**4.1.2.5. Inorganic Semiconductors.** Some attractive features of organic optoelectronics (low cost, large area, mechanical flexibility, etc.) can be achieved with devices made using inorganic materials with special form factors. In particular, micro-/nanowires and ribbons generated by top-down approaches on semiconductor wafers<sup>249</sup>–<sup>265</sup> may be printed using stamps onto flexible or glass substrates for technologies that complement and offer improvements over organic electronics in terms of lifetime, reliability, and performance. Methods for transfer printing these inorganic semiconductor micro-/nanostructures involve (i) the fabrication of the structures on a donor wafer, including optional high-temperature steps, for example, doping,<sup>251</sup> usually followed by an undercutting wet etch to render them at least partially freestanding (Figure 25a–d); (ii) the application of an elastomeric stamp to the surface of the donor wafer and retrieval of the structures (Figure 25e); and (iii) transfer printing the structures onto a target substrate (Figure 25f–h). The methods can thus transfer the micro-/nanostructures to a target substrate (flexible plastic or glass, etc.) in their original patterns/orientations, as defined during the fabrication process. Retrieval of the structures from the donor may be facilitated by chemical treatment<sup>254</sup> or by kinetic amplification of van der Waals bonding between the ink structures and the elastomeric stamp.<sup>256</sup> Transfer of the structures onto the target substrate is mediated usually by a curable glue layer or by conformal contact and non-covalent surface forces. These methods provide flexible forms of silicon and other semiconductors for electronics on plastic that exhibit mobilities as high as  $600 \text{ cm}^2/\text{V}\cdot\text{s}$ ,<sup>260</sup> logic circuits<sup>261</sup> and ring-oscillators operating in the MHz regimes, and single GaAs devices with GHz operation.<sup>253</sup> Furthermore, the additive nature of these stamp-based printing methods enables the generation of heterogeneously integrated circuits<sup>262</sup> (Figure 26a,b) on plastic substrates, with active regions on multiple layers comprising any combination of silicon, GaN, GaAs, SWNTs and other semiconductor microstructures, and other interesting systems, such as stretchable semiconductor forms (Figure 26c).<sup>255,263,264</sup> The stretchability of the devices shown in Figure 26c derives from strain-induced buckling in the thin inorganic semiconductors.

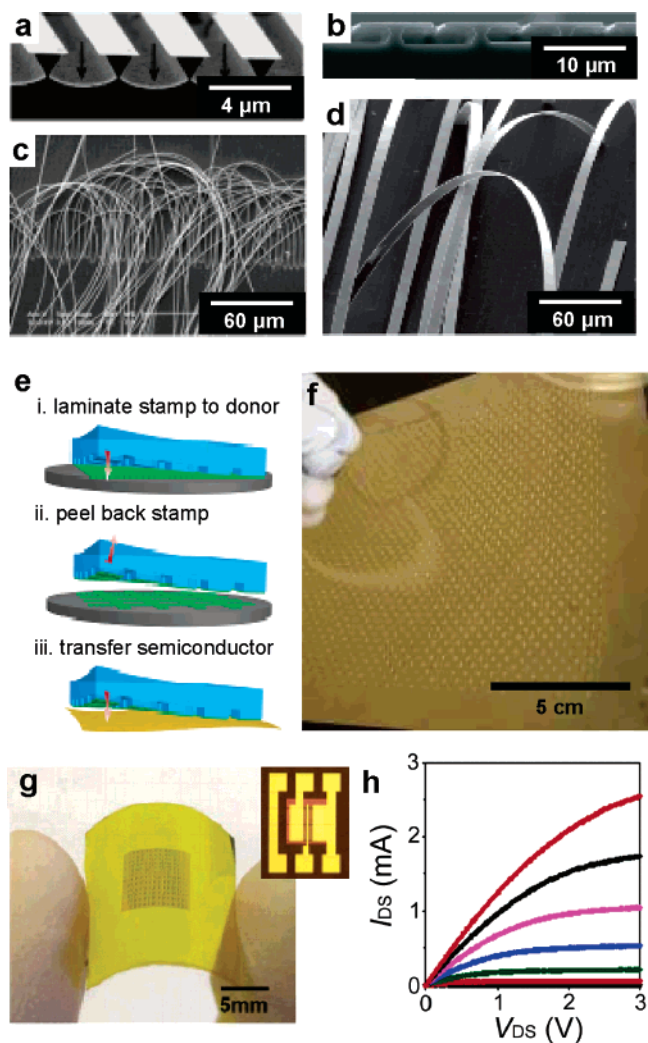


**Figure 25.** Printable single-crystal organic semiconductor forms. (a) Generation of micro/nano wires of InP and (b) ribbons of silicon by anisotropic wet etching. (c) Released, flexible GaAs micro/nanowires and (d) Si ribbons. (Reprinted with permission from ref 252. Copyright 2005 Wiley-VCH Verlag. Reprinted with permission from ref 257. Copyright 2006 American Institute of Physics.) (e) Method for selective retrieval and transfer of semiconductor structures from a donor substrate to a target substrate using a patterned PDMS stamp. (f) Silicon structures distributed across a large PET substrate using the method described in (e). (Reprinted with permission from ref 265. Copyright 2005 Wiley-VCH Verlag.) (g) Thin kapton substrate housing transfer printed silicon top-gate transistors. (h)  $I$ – $V$  characteristics of a top-gate silicon transistor printed onto kapton with a channel  $9 \mu\text{m}$  long and  $200 \mu\text{m}$  wide. (Reprinted with permission from ref 260. Copyright 2006 IEEE.)

The printable semiconductors in these cases can come from relatively inexpensive bulk semiconductor wafers<sup>252,257</sup> and can be dispersed across larger substrates through an area multiplication, repetitive stamping scheme.<sup>263,265</sup> Direct stamp-based transfer thus supplies a method to join two distinct and dissimilar classes of materials together, namely, single-crystal organic semiconductors and plastic substrates, to form patterned systems with unique properties to compliment the capabilities of organic optoelectronics.

#### 4.1.3. Lamination

Often in organic optoelectronics, two or more device components must be prepared using incompatible processes. Fabrication of a device in two separate parts that can be joined together offers process flexibility. This strategy is the

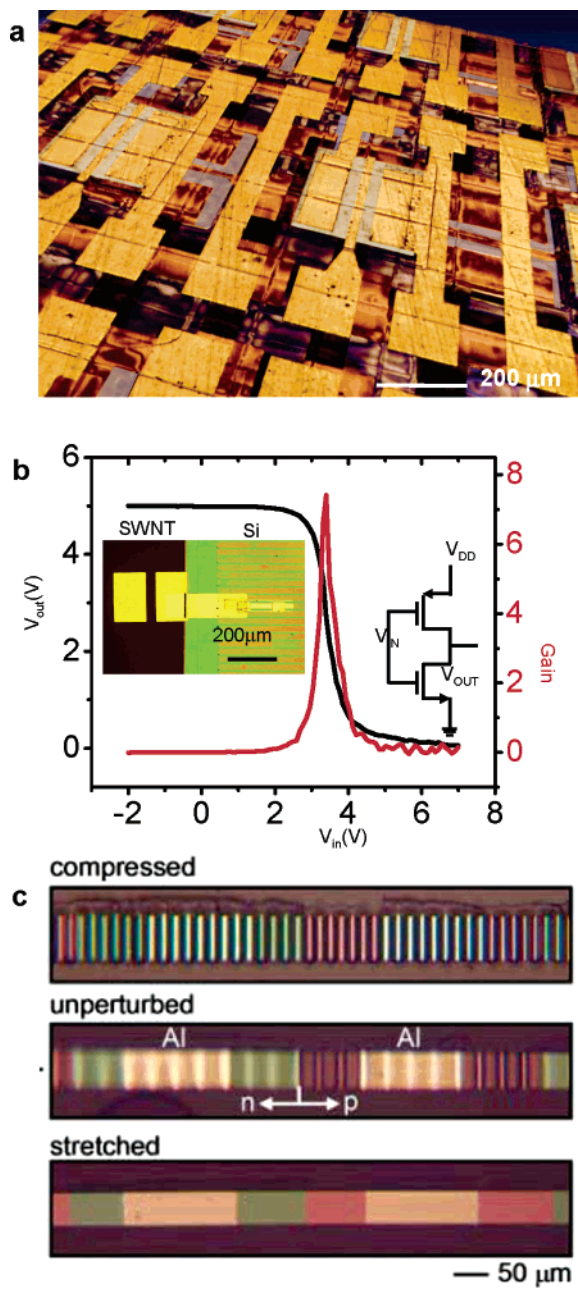


**Figure 26.** Unusual capabilities of transfer-printed semiconductor systems. (a) Confocal microscopy image (false color) of multiple-active layer single-crystal silicon TFT array. The transistors in this array exhibit mobilities of  $>450 \text{ cm}^2/\text{Vs}$ .<sup>262</sup> (b) Heterogeneous integration of SWNT network (p-type) and single-crystal silicon (n-type) transistors that comprise a complimentary inverter.<sup>262</sup> [Reprinted with permission from *Science* (<http://www.aas.org>), ref 262. Copyright 2006 American Association for the Advancement of Science.] (c) Wavy, stretchable silicon photodiodes prepared by transfer from a silicon-on-insulator substrate to pretrained PDMS.<sup>255</sup> [Reprinted with permission from *Science* (<http://www.aas.org>), ref 255. Copyright 2006 American Association for the Advancement of Science.]

principle of lamination. Lamination is similar to stamp-based printing approaches in the sense that two bodies are joined for the fabrication and patterning of the materials, but in the case of lamination, the devices are formed by the union of the two bodies and no materials are transferred.

Lamination methods offer, for example, powerful opportunities for studying single-crystal organic materials, which cannot be processed in the same ways as uniform thin

films. The study of OFETs made from high-quality organic molecular crystals (OMCs) offers insight into the intrinsic electronic properties of organic semiconductors.<sup>266,267</sup> Fabrication of these devices requires unconventional methods that can accommodate the fragile OMCs, which are incompatible with conventional processing. To avoid damage of the active channels in single-crystal OFETs by vacuum deposition of field-effect components (e.g., sputter deposition of gate dielectrics), researchers often form OFETs on OMCs by laminating them against a substrate that supports FET structures or other electrical probes. Examples of such devices are displayed in Figure 27. This substrate may

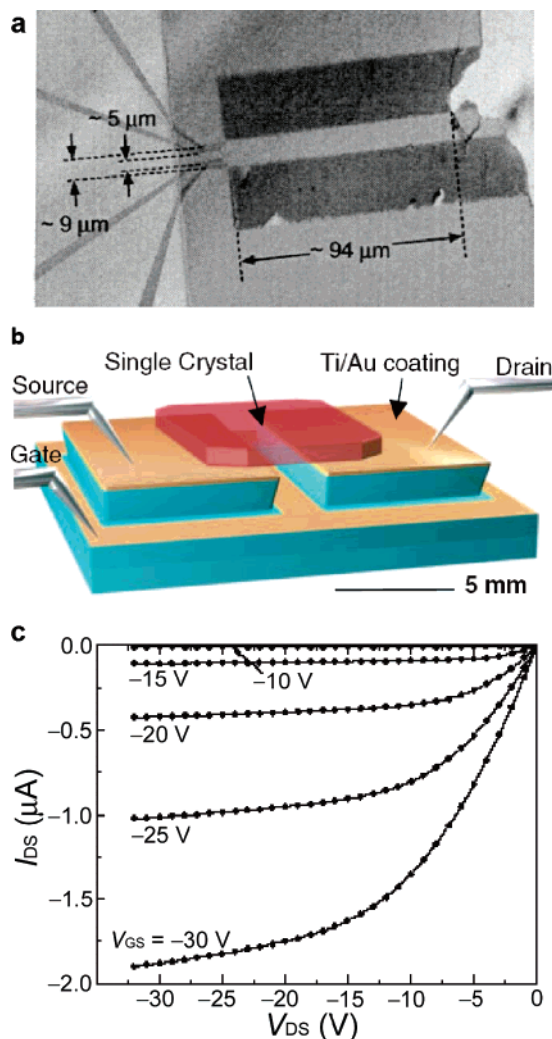


**Figure 27.** Laminated single-crystal OFETs. (a) OFET built by laminating a thin ( $\sim 1 \mu\text{m}$ ) pentacene single crystal against an oxidized silicon wafer with integrated electrodes. (Reprinted with permission from ref 271. Copyright 2003 American Institute of Physics.) (b) OFET with a free-space dielectric built by contacting a rubrene crystal against a metallized PDMS “transistor stamp.” (c)  $I-V$  characteristics of a device of the kind illustrated in (b). (Reprinted with permission from ref 268. Copyright 2004 Wiley-VCH Verlag.)

comprise a rigid Si wafer (Figure 27a) with integrated dielectrics and electrodes (usually gold), or it may comprise a soft elastomeric stamp with analogous features (Figure 27b). Rubrene devices such as those illustrated in Figure 27b exhibit the highest device-level mobilities to date of transistors that use small-molecule organic semiconductors.<sup>268</sup> The use of a rigid substrate requires a thin crystal ( $<1-5 \mu\text{m}$ ) or applied pressure for good lamination<sup>266</sup> (countersunk

electrodes may also help by minimizing step edges on the substrate's contact surface<sup>269</sup>, but soft stamps can laminate to any thin or thick crystal that has at least one smooth surface. The contacting surface of the laminated substrate may be chemically modified to improve the performance of the devices, for example, by treating electrodes with SAMs (e.g., trifluoromethylbenzenethiol) to reduce contact resistance or by treating the dielectric surface with SAMs (e.g., OTS) to reduce interfacial trapping sites (such as surface deep level states; for more detail, see refs 270 and 271) or by depositing PMMA to enable ambipolar behavior.<sup>272</sup> Additionally, patterned stamps may serve to form single-crystal OFETs using free-space dielectrics to minimize or eliminate effects of the semiconductor–dielectric interface, thus enabling the fabrication of rubrene FET having normalized subthreshold swings as low as 0.38 V·nF·decade<sup>-1</sup>cm<sup>-2</sup>.<sup>268</sup> OFETs fabricated in this manner can be very sensitive to active species in the environment.<sup>273</sup> The substrate and the OMC join in a reversible lamination process by which the interface is bound by van der Waals forces. The OMC can be separated and relaminated on the stamp for probing of the crystals along different crystallographic orientations.<sup>274</sup> The resulting devices can exhibit interesting properties, including p-mobilities in the range of 10–20 cm<sup>2</sup>/V·s<sup>268</sup> (in rubrene single crystals, slightly better than values obtained with similar devices fabricated in other ways<sup>275,288</sup>), and n-mobilities greater than 1 cm<sup>2</sup>/V·s (for tetracyanoquinodimethane).<sup>268</sup>

Lamination methods also provide interesting capabilities for the fabrication of amorphous and polycrystalline organic devices. The principle is to separate a device into two halves to avoid damage to each half caused by processing of the components in the other half, as illustrated in Figure 28a, for both high-performance OTFTs (Figure 28b) and OLEDs (Figure 28c). The lamination can be designed to be a permanent mechanical support and encapsulation strategy with robustness introduced by covalent bonds,<sup>276</sup> or it can be reversible, held by van der Waals adhesion between the two halves.<sup>79</sup> Reversibility provides unique opportunities to study changes in interface properties due to operation of the devices. For the fabrication of polymer EL and photovoltaic devices, lamination methods can prepare homo- (MEH-PPV) and heterojunction ( $\alpha$ -NPD/poly(9,9-bis(octyl)-fluorene-2,7-diyl) (BOc-PF)) devices with high-performance and well-defined interfaces that result from solvent-free methods.<sup>277</sup> Bonding between organic layers may be facilitated by heating and mild pressure and/or by inducing roughness in one of the layers.<sup>277</sup> Depositing a layer of MEH-PPV or BOc-PF and cathode materials onto a rough ITO substrate and subsequently removing those layers from the ITO using an adhesive tape transfers the roughness into the newly exposed polymer surface. This enhanced roughness can improve the bonding and device operation after lamination to a hole-transport material.<sup>277</sup> Improved electroluminescence<sup>79,278</sup> and lifetime<sup>278</sup> can be accomplished in organic electroluminescent devices by separating the metal evaporation step from the active layers. Lamination of a substrate that supports electrodes and interconnects to a substrate that supports organic materials prevents in-diffusion of metal and the introduction of quenching centers into the active layer that can occur during evaporation.<sup>79,278</sup> In OTFT fabrication, the same laminated electrodes can exhibit lower contact resistance than evaporated source and drain contacts.<sup>279</sup> Transistors fabricated in this manner represent a type of metal

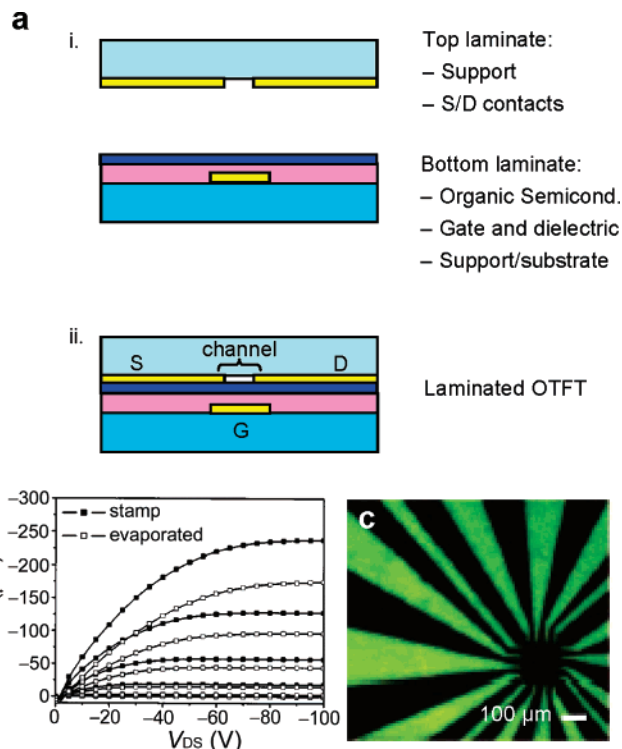


**Figure 28.** Laminated thin-film organic optoelectronics. (a) Schematic illustrating a process for the fabrication of an OTFT by joining a “top part” housing source and drain electrodes and a “bottom part” containing the remaining components. (b)  $I$ – $V$  characteristics of a pentacene TFT with a channel 250  $\mu\text{m}$  long and 5 mm wide fabricated by soft-contact lamination (ScL) of electrodes on a PDMS stamp and by a control device with electrodes evaporated directly onto the pentacene. The laminated devices exhibit higher current levels owing to high-quality contacts. (Reprinted with permission from ref 77. Copyright 2002 American Institute of Physics.) (c) Electroluminescence from a polyfluorene derivative with a laminated electrode on PDMS patterned by a printed SAM. (Reprinted with permission from ref 79. Copyright 2003 PNAS.)

contact, bottom<sup>280</sup> or top-contact device that is robust against harsh treatment,<sup>276</sup> compatible with both p- (pentacene) and n-type ( $\text{F}_{16}\text{CuPc}$ ) organic semiconductors for complimentary inverters,<sup>201,276</sup> and can have channel lengths smaller than 200 nm.<sup>77</sup> Lamination of a stamp prepared with an integrated gate metal and elastomeric gate against a fully fabricated pentacene top-contact device produces a double-gate structure for simultaneous study of transport properties through field-effect measurements on both the bottom and top interfaces of the organic semiconductor.<sup>281</sup> Both interfaces on these double-gated devices showed similar performance, although the top interface showed a slightly reduced mobility (0.1–0.2 cm<sup>2</sup>/V·s) and degraded in ambient conditions much more quickly than the bottom.<sup>281</sup>

## 4.2. Laser Printing and Imaging

Laser printing and imaging refers to methods that use a laser to direct the deposition of templates or functional materials onto a device substrate. Like common office laser printers, these methods can rapidly pattern large areas, even though the operation is serial in nature. In fact, office laser printers may be used to generate functional devices. Toner deposited from a laser printer may be used as a polymer dielectric<sup>282</sup> or as a sacrificial lift-off template for patterning solution-processed SWNT films.<sup>283,284</sup> Organic conductors

and sensors may be patterned in this way. More sophisticated methods may be used to print many kinds of functional organic materials in techniques referred to as thermal transfer and laser-induced thermal imaging (LITI). Figure 29a depicts

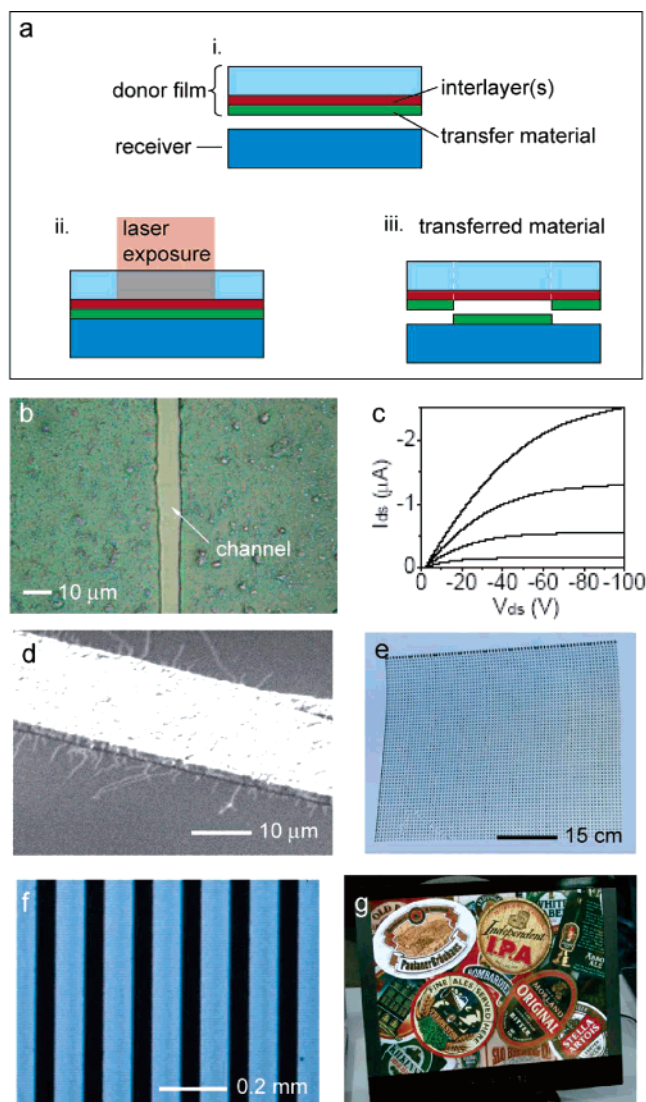


**Figure 29.** Thermal transfer and laser-induced thermal imaging (LITI). (a) Schematic illustration of thermal transfer and LITI. A donor film laminated against a target/device substrate is exposed to laser irradiation. Local heating induces exchange of the transfer material to the target. (b)  $<10\text{ }\mu\text{m}$  channel separating DNNSA-PANI/SWNT composite electrodes patterned by thermal transfer. (Adapted from “Woodhead” and “Crawford” chapters.) (c)  $I-V$  characteristics of a pentacene transistor with electrodes like those in (b). (Reprinted with permission from ref 176. Copyright 2003 Society for Imaging Science and Technology.) (d) SEM electrodes like those in (b) revealing SWNT ropes extending beyond the PANI matrix. (Reprinted with permission from ref 288. Copyright 2003 Wiley-VCH Verlag.) (e) Array of organic electrodes for several thousand OTFTs patterned by thermal transfer. (f) Lines of Covion blue light emitting polymer blended with poly(acenaphthylene) patterned by LITI. (Reprinted with permission from ref 289. Copyright 2004 Wiley-VCH Verlag.) (g) 17 in. AMOLED display with OLEDs fabricated by LITI. (Reprinted with permission from ref 286. Copyright 2004 SPIE).

the general process flow. In these methods, donor and target/device substrates (usually PET films or glass) are registered to each other and brought into contact. A laser illuminates and locally heats the donor substrate and thus induces transfer of a functional ink, or transfer material, onto the target

substrate in the exposed regions. A layer that efficiently absorbs light for conversion to heat, either carbon black<sup>285</sup> or thin metal,<sup>30,31</sup> is usually present, along with other interlayers for the protection of the transfer material<sup>286</sup> or for other purposes. These methods allow good resolution (better than  $10\text{ }\mu\text{m}$ ) and large-area patterning of functional organic materials in which the target substrate is not exposed to solvents or etchants. Several mechanisms for transfer are possible, including the vaporization/ablation of an organic interlayer that propels the transfer materials to the target substrate<sup>30,31,176,287,288</sup> or simply heating the transfer material above  $T_g$  to bond it to the substrate.<sup>285,286,289</sup> Types of materials patterned by these methods include high-conductivity organic conductors and electroluminescent materials, both small molecules and polymers. One particularly interesting high-conductivity organic conductor that can be patterned by this process is a composite composed of PANI doped with dinonylnaphthalene sulfonic acid (DNNSA) and SWNT (Figure 29b–e).<sup>30,31,176,287,288</sup> Other conductive polymers such as PEDOT or otherwise doped PANI degrade due to the high temperatures involved in the transfer process. DNNSA/PANI, however, can withstand the transfer without significant degradation, and loading the material with 3 wt % SWNT can improve the conductivity of the resulting composite by 4 orders of magnitude.<sup>288</sup> This composite material can be patterned to form electrodes defining channels as small as  $7\text{ }\mu\text{m}$ <sup>30</sup> (Figure 29b) and forms very low resistance contacts to semiconductors such as pentacene, sexithiophene, and quaterthiophene,<sup>31,176,288</sup> even with bottom-contact geometries, and the resulting devices can outperform those with top-gate electrodes made of gold ( $0.3\text{ cm}^2/\text{V}\cdot\text{s}$  for pentacene versus  $0.15$  for Au<sup>31</sup>). Pentacene deposited over these printed PANI electrodes assumes large crystallite morphologies at the boundaries of the channel;<sup>32</sup>  $50 \times 80\text{ cm}$  backplanes consisting of 5000 such pentacene/printed PANI electrode OTFTs have been generated, as shown in Figure 29e.<sup>31</sup>

Electroluminescent organics printed by LITI (Figure 29f,g) have been integrated onto the active matrix backplane of a 17 in. OLED display.<sup>286</sup> Detailed modeling<sup>285</sup> of the thermal profiles in the donor substrate show that the temperatures during laser exposure can reach  $350\text{ }^\circ\text{C}$ , but the time that the materials are heated to above  $100\text{ }^\circ\text{C}$  is less than a couple of milliseconds. In the case of printing emissive layers it was found that high- $T_g$  materials ( $200\text{ }^\circ\text{C}$ ) were better suited to LITI processing than low- $T_g$  materials ( $\sim 90\text{ }^\circ\text{C}$ ), which showed significant degradation of performance when patterned by LITI relative to control samples patterned by evaporation directly onto a target substrate.<sup>285</sup> LITI patterns also showed better morphology when high- $T_g$  materials were used. Defects introduced by heating during the LITI process cause leakage currents that are responsible for the low performance in low- $T_g$  materials. LITI patterns of high- $T_g$  materials, however, perform virtually identically to control devices in terms of efficiency, especially at realistic operational (high) luminance levels. Further improvements in pattern transfer fidelity may be made by controlling the cohesive strength in the transfer material film. The extent of cohesion must be large enough to maintain continuity of the printed features but also not so large as to prohibit the separation from the unexposed regions of transfer material on the donor. Small molecules, for example, are more readily patterned by LITI than polymeric light emitters owing to the higher fracture toughness of the latter. Lower molecular weight polymers are thus easier to pattern, as well as phase-

separated polymer blends,<sup>289</sup> both of which show better edge roughness in patterned features than pure higher molecular weight light-emitting polymers. In practice, the selection of polymer transfer material for LITI must balance the ease of fabrication against reduction in operating lifetime and higher operation voltages that come with polymer blends and low molecular weight polymers.<sup>286</sup>

### 4.3. Physical Masks

Electronic materials in fluidic form, either as solutions or vapors, can be patterned through openings in physical masks or nozzles to produce various components (i.e., active layers or passive elements) of electronic devices. Many demonstrations of these capabilities exist, for fabricating organic transistors, light-emitting devices, and other systems. This section provides several examples based on screen printing and shadow masking.

#### 4.3.1. Screen Printing

Screen printing is a simple and low-cost process which relies on a screen that consists of a mesh with patterned areas that block the flow of printed inks. The process begins by tensioning this screen on a frame to pull it slightly away from the substrate to form a small contact gap. An implement that resembles a squeegee then pushes a layer of solution-based ink deposited on the upper surface of the screen through openings in the mesh and, at the same time, forces the screen into physical contact with the substrate. Removing the screen leaves a pattern of ink in the geometry of the openings in the mesh. The viscosity of the ink, its wetting of the substrate, and other parameters govern the operation of this method. Typically the features associated with the mesh itself, which often consists of polyester (thickness = 30–385  $\mu\text{m}$ ) or stainless steel wires (thickness = 40–215  $\mu\text{m}$ ) with meshings of 30–200 threads/cm, do not appear in the printed patterns, but these dimensions can limit the resolution.

Attractive features of screen printing for organic optoelectronics include its simplicity of use, existing applications and commercial manufacturing systems for electronics (printed circuit boards (PCBs), primarily), versatility and compatibility with a range of organic electronic materials, and cost-effectiveness. Commercial devices, such as PCBs and solar cells, can be screen printed over large areas (often larger than 50  $\times$  50 cm<sup>2</sup>) in a few seconds. PCBs (30 cm  $\times$  30 cm size) are printed in 5 s with 100  $\mu\text{m}$  pitch sizes using commercial screen printers (Dualcon screen printer of EKRA GmbH). The relatively modest resolution in the patterns ( $\sim$ 75  $\mu\text{m}$ <sup>290</sup>) represents a disadvantage, especially for forming critical dimensions in transistors, for example.

Most demonstrations in organic optoelectronics involve screen printing to form various components of thin-film transistors, diodes, capacitors, and light-emitting devices. In an early example, screen printing defined source, drain, and gate electrodes of a graphite–polymer mixture ink (Electrodag 423 from Acheson Colloids Co.) for a flexible all-polymer transistor with a channel length of 200  $\mu\text{m}$  and a width of 2 mm on a polyester substrate that served also as a gate dielectric (1.5  $\mu\text{m}$  thickness).<sup>291</sup> This device, which used a 40 nm thick layer of  $\alpha,\omega$ -di(hexyl)sexithiophene semiconductor, exhibited a mobility of 0.06 cm<sup>2</sup>/V·s in the linear regime. In a more recent example, screen-printed source/drain electrodes of a conductive silver ink formed an organic TFT with a thin film of pentacene as the semicon-

ducting layer.<sup>292</sup> The materials flexibility of screen printing was demonstrated through the fabrication of organic TFTs, in which a polyimide gate dielectric, a regioregular poly(3-alkylthiophene) semiconducting layer, and a conducting silver–polymer mixture for electrodes were all printed.<sup>293</sup> Although this example, as well as the others reported in the literature, involves coarse resolution of  $\sim$ 75  $\mu\text{m}$ , recent improvements suggest that features as small as  $\sim$ 20  $\mu\text{m}$  can be achieved. This result and further increases in resolution are important for defining the channel lengths in transistors, for example.<sup>294</sup>

In addition to transistors, screen printing can be used to form plastic capacitors and resistors with conductive inks such as those used in the transistor examples and insulators such as polyimide pastes and other organic packaging materials.<sup>295</sup> OLEDs are also possible. For example, OLEDs using screen-printed hole-transport layers (HTLs) consisting of blends of *N,N'*-diphenyl-*N,N'*-bis(3-methylphenyl)-[1,1'-biphenyl]-4,4'-diamine (TPD) and a polycarbonate and/or light-emitting layers of MEH-PPV show low light-emitting voltage (<5 V) and 0.91% peak external quantum efficiency.<sup>296</sup> Through careful control of the solution viscosity, screen mesh count, and processing variables, very thin and smooth HTL layers (thicknesses of <15 nm with rms surface roughness of <1.5 nm) that support high current densities are possible.<sup>297</sup> Related display systems can also be formed by screen printing. Researchers at Samsung demonstrated an impressive example: a 9 in. multicolor field emission display (FED) with screen-printed pixels of SWNTs using a SWNT paste (mixture of SWNTs, silver powders, and organic binders such as ethyl cellulose).<sup>298,299</sup> The organic binders can be removed by heating at 350 °C for 20 min, after the printing step.

#### 4.3.2. Shadow Masks (Stencil Masks)

Patterning by depositing vaporized materials through shadow masks is conceptually similar to screen printing. Like screen printing, shadow-mask patterning has extensive applications in existing and emerging electronic systems. In fact, several companies have fully commercialized or demonstrated organic devices, such as full-color OLED displays (15 in. active matrix OLED by Kodak-Sanyo, 13 in. active matrix OLED by Sony, Pictiva OLED display by Osram, etc) using this approach.<sup>300,301</sup> In this process, metals or low molecular weight organic molecules emerge in a directed flux from a source in a physical vapor deposition system and travel through openings in masks placed near the surface of the substrate.<sup>302</sup> The deposition typically occurs under high vacuum (10<sup>-8</sup>–10<sup>-6</sup> Torr) such that the mean free path of the evaporated species exceeds the distance between the source and substrate. When this condition is satisfied, the evaporated material travels in a directional manner through the gaps in the mask and onto the substrate.<sup>303</sup> The technique is purely additive at the substrate level, which enables sequential deposition of multiple layers of different materials. Commercially available shadow masks are constructed of thin metal foils with openings fabricated using micromachining, chemical etching, or laser cutting. The resolution of such masks is typically  $\sim$ 25–30  $\mu\text{m}$ .<sup>290</sup> Although finer features are possible, practical limits are set by (i) sizes of openings that can be generated in masks that retain sufficient rigidity (i.e., thickness) to be mechanical stable, (ii) mask/substrate separation distances that can be reproducibly achieved without unwanted physical contact, and (iii) levels

of directionality in the material flux. Multilevel registration comparable to the achievable resolution is possible by use of physical mounting brackets and alignment systems. For certain applications, improved registration can be achieved by precisely shifting the position of a single shadow mask relative to the substrate throughout the deposition process using a mask translating fixture.<sup>304</sup> Multiple organic light-emitting layers and electrodes can be patterned sequentially by successive shadow masks with a mask positioning accuracy of  $\pm 8 \mu\text{m}$  over a  $<1 \text{ cm}^2$  substrate. Figure 30a illustrates a full-color stacked OLED fabricated in this manner. Other demonstrators include artificial skin prototypes fabricated on  $8 \times 8 \text{ cm}^2$  flexible substrates, which use pressure/thermal sensors and organic transistor active matrixes readouts. Shadow-masking techniques pattern the electrodes and organic semiconductors such as pentacene, CuPc, and PTCDI (3,4,9,10-perylene-tetracarboxylic-di-imide)<sup>305,306</sup> in these systems. The transistors, which use pentacene for the semiconductor, show saturation mobilities of  $\sim 1 \text{ cm}^2/\text{V}\cdot\text{s}$  and  $I_{\text{on}}/I_{\text{off}}$  ratios of  $10^5$ – $10^6$ . The thermal sensors use organic diodes composed of a CuPc (p-type) and PTCDI (n-type) semiconducting layer stack.

In spite of these impressive applications, shadow-mask approaches have shortcomings that include moderate resolution, inefficient materials utilization, high vacuum environment requirement, and patterned areas limited by the size of chamber and of the mask. In addition, continuous traces (such as circles) cannot be patterned in a single step. The size of the minimum patternable feature can be reduced using an angled evaporation setup, but this method requires precise positioning of the source relative to the substrate and is not suitable for large-area patterning. Various approaches avoid at least some of these disadvantages. Recent work shows, for example, that polymer masks provide some advantages over conventional metal masks: (i) polymer masks are easy to make and can have high resolution (minimum aperture size  $\sim 5 \mu\text{m}$ ); (ii) the masks can be transparent, and they can be nondestructively contacted with the substrate, thereby simplifying the mask-positioning step and increasing the edge resolution; and (iii) their mechanical flexibility allows patterning on curved or uneven substrates. For example, large-area flexible polymer masks made of  $25 \mu\text{m}$  thickness sheets of polyimide (Kapton)<sup>307–309</sup> can be formed with features as small as  $10 \mu\text{m}$ , through an ablation process with an excimer laser (248 nm wavelength). A set of such masks was used to define patterns of pentacene, alumina and metal, in a set of four to six aligned layers, for radiofrequency identification (RFID) circuitry, as shown in Figure 30b, operating at frequencies between 125 kHz and 6.5 MHz. Other work described elastomeric polymer masks formed by spin-coating and curing PDMS against patterns of photoresist.<sup>310</sup> The lateral dimensions of the photoresist features in this case define the sizes of apertures in the masks; openings with sizes as small as  $5 \mu\text{m}$  were achieved. Furthermore, the low modulus of the PDMS allows soft, conformal contact with a range of substrates. This contact enables patterning of materials deposited from solution, as well as from the vapor phase. Figure 30c shows a photoluminescent image of patterns of Alq<sub>3</sub> formed on the curved surface of a glass rod using a PDMS mask. Arrays of three-color photoluminescent patterns can be formed using two elastomeric masks, as shown in Figure 30d. Here the red, blue, and green dots consist of Nile Red and 2-(4-biphenyl)-5-(4-*tert*-butylphenyl)-1,3,4-oxadiazole(PBD):Coumarin 47, PBD:Coumarin 47,

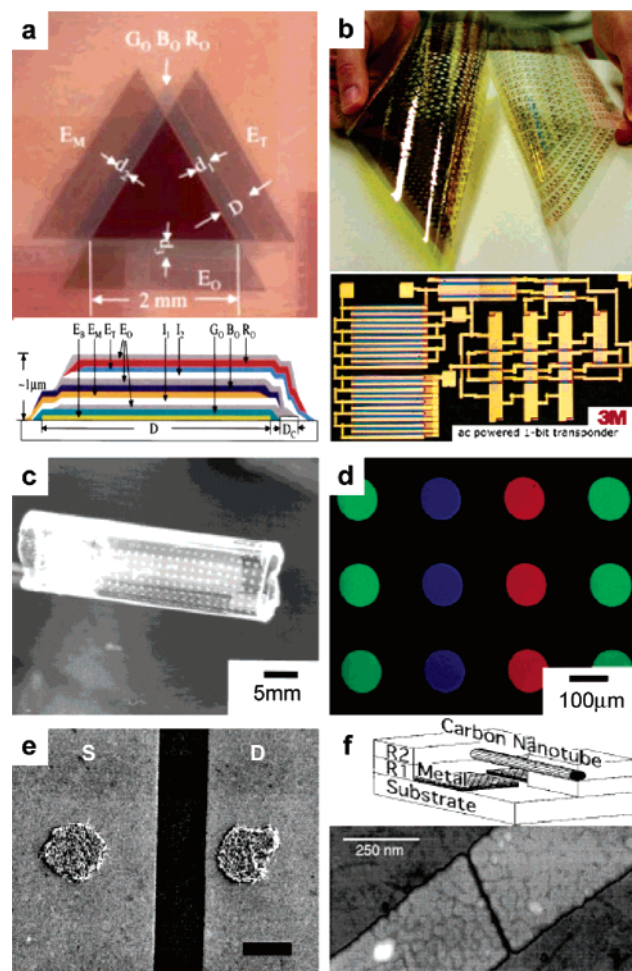


**Figure 30.** (a) Optical micrograph of a triangular OLED pixel patterned sequentially with small translational movements of a single shadow mask (top image) and cross section of the OLED (bottom). R<sub>0</sub>, red-emitting layer [(2-methoxy-6-[2-(2,3,6,7-tetrahydro-1H,5H-benzoquinolin-9-yl)ethenyl]-4H-pyran-4-ylidene)propane-dinitrile] doped Alq<sub>3</sub>; G<sub>0</sub>, green-emitting layer (Alq<sub>3</sub>); B<sub>0</sub>, blue-emitting layer [bis(8-hydroxy)quinaldine aluminum phenoxide]; I<sub>1</sub>, I<sub>2</sub>, isolation layer; E<sub>B</sub>, bottom electrode (ITO); E<sub>M</sub>, anode (ITO); E<sub>O</sub>, cathode (ITO); E<sub>T</sub>, cap electrode (ITO). (Reprinted with permission from ref 304. Copyright 1999 American Vacuum Society.) (b) Large polymeric shadow mask (left in top image) with printed 6 in.  $\times$  6 in. RFID circuit array consisting of 25 rows and 25 columns of circuit cells (right in top), and optical micrograph of shadow mask-patterned pentacene-based one-bit RF transponder circuit with a seven-stage ring oscillator, a NOR gate, and two output inverters (bottom). The gate lengths are  $20 \mu\text{m}$ . (Reprinted with permission from refs 307 and 308. Copyright 2004 American Chemical Society.) (c) Optical micrograph showing photoluminescence (PL) from Alq<sub>3</sub> patterned on a glass rod (outer diameter  $\sim 6 \text{ mm}$ ) using an elastomeric PDMS membrane. (Reprinted with permission from ref 310. Copyright 1999 Wiley-VCH Verlag.) (d) Optical micrograph of PL from circular features formed by use of two PDMS membranes. (Reprinted with permission from ref 310. Copyright 1999 Wiley-VCH Verlag.) (e) Scanning electron micrograph of a carbon nanotube FET (A scale bar indicates  $5 \mu\text{m}$ ), with source (S) and drain (D) electrodes patterned by a metal shadow mask that consists of fine tungsten wires (diameter =  $5 \mu\text{m}$ ) and nickel sheets ( $50 \mu\text{m} \times 2 \text{ mm}$  slits with a spacing of  $50 \mu\text{m}$ ). The two circles are catalyst islands consisting of alumina-supported Fe/Mo. (Reprinted with permission from ref 312. Copyright 2003 American Institute of Physics.) (f) Schematic illustration of the fabrication of nanometer sized gaps in a metal wire formed with a carbon nanotube-based shadow mask (top), and AFM image of a sub-30 nm gap in a 350 nm wide gold wire fabricated using a SWNT bundle. (Reprinted with permission from ref 317. Copyright 2000 American Institute of Physics.)

and Alq<sub>3</sub>, respectively. Reliable manipulation of these masks, which have extremely low flexural rigidity, represents a significant challenge that can be addressed, to some degree, by using mechanical struts and other support structures.

There are also approaches to reduce the aperture sizes of shadow masks. For example, a metal shadow mask that consists of fine tungsten wires (5  $\mu\text{m}$  in diameter) and 5  $\times$  2 mm slits of nickel sheets (25  $\mu\text{m}$  in thickness)<sup>311,312</sup> can reliably form 5  $\mu\text{m}$  gaps in evaporated gold contacts to define the channel length in carbon nanotube TFTs, as shown in Figure 30e.<sup>312</sup> Also, nanoscale stencil shadow masks, based on a Si or SiN etching process, can produce feature sizes below 10 nm.<sup>313–316</sup> Figure 30f presents a shadow-masking method that uses multiwalled carbon nanotubes or SWNTs bundles located between two layers of electron beam resist (R1 and R2) to generate sub-30 nm gaps in evaporated gold wires.<sup>317</sup> These and other demonstrations clearly illustrate the ability to form extremely small features by shadow masking. However, the scale-up of such approaches for realistic manufacturing might pose significant challenges.

#### 4.4. Scanned Nozzles

Printing of active and passive materials using scanned small-diameter nozzles represents an attractive method for organic electronics and optoelectronics, partly because of the high level of sophistication of similar systems used in graphic arts. Because of the additive nature of the process, materials utilization can be high. The materials can be deposited in either the vapor or liquid phase using, respectively, vapor jet printing or inkjet methods. Whereas organic vapor jet printing techniques have been introduced only very recently, inkjet printing techniques are well-established and already have worldwide applications. In 2004, a 40 in. full-color OLED display prototype was fabricated using inkjet printing of light-emitting polymers.<sup>318</sup> The following sections summarize recent developments in organic vapor jet and inkjet printing techniques applied to the fabrication of organic optoelectronic devices.

##### 4.4.1. Organic Vapor Jet Printing

Scanned, small-aperture nozzles can provide an alternative to shadow masking for defining patterns of evaporated organic materials. Figure 31a illustrates the method, which is known as organic vapor jet printing (OVJP).<sup>319–321</sup> Source cells that contain the organic material to be patterned connect upstream to carrier gas inlets and downstream to mixing chambers. A hot inert carrier gas (e.g., helium or nitrogen) vaporizes the organic source (such as Alq<sub>3</sub> or pentacene) and carries it to the nozzle, where it emerges in the form of a vapor jet. This mixed vapor jet impinges onto a cold substrate in close proximity (10–100  $\mu\text{m}$ ) to the nozzle. The light carrier gas molecules quickly disperse, while the relatively heavy organic source molecules condense on the substrate. The printing resolution is a function of the nozzle size, nozzle–substrate distance, and type and pressure of carrier gas. Figure 31b shows a pattern of Alq<sub>3</sub> printed using a 20  $\mu\text{m}$  diameter nozzle and a nozzle–substrate distance of 20  $\pm$  10  $\mu\text{m}$ . In this demonstration, the printing resolution is as high as 500–1000 dpi, with deposition rates of  $\sim$ 130 nm/s. Pentacene can be also printed in this manner, as illustrated by the patterned layer on SiO<sub>2</sub> pretreated with OTS shown in Figure 31c. TFTs formed on this layer using gold source/drain electrodes defined by shadow-mask deposition show  $I_{\text{on}}/I_{\text{off}}$  ratios and saturation regime mobilities of  $7 \times 10^5$  and

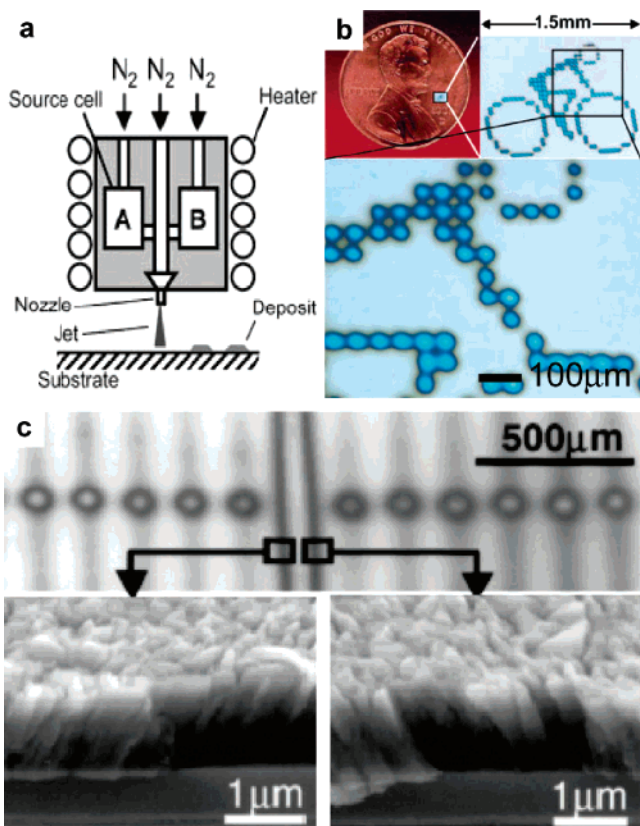


**Figure 31.** (a) Schematic of the organic vapor jet printing (OVJP) apparatus, shown with two source cells and a modular collimating nozzle. (Reprinted with permission from refs 319. Copyright 2004 Wiley-VCH Verlag. Reprinted with permission from ref 320. Copyright 2004 American Institute of Physics.) (b) Image of a cyclist figure printed by OVJP on silicon using Alq<sub>3</sub>. The pattern resolution in this image varies between 500 and 1000 dpi.<sup>319,320</sup> (Reprinted with permission from ref 319. Copyright 2004 Wiley-VCH Verlag. Reprinted with permission from ref 320. Copyright 2004 American Institute of Physics.) (c) Micrographs of a pentacene pattern (top) and pentacene crystallites printed on SiO<sub>2</sub> previously treated with octadecyltrichlorosilane (OTS) using a 50  $\mu\text{m}$  diameter nozzle at the nozzle–substrate distance of  $35 \pm 15 \mu\text{m}$  and deposition rate  $> 30 \text{ nm/s}$  (bottom).<sup>319</sup> (Reprinted with permission from ref 320. Copyright 2004 American Institute of Physics.)

0.2–0.25  $\text{cm}^2/\text{V}\cdot\text{s}$ , respectively. These values compare favorably to those obtained using more established deposition procedures for the pentacene. The morphology of films deposited by OVJP represents an interesting topic of current study. Because OVJP is a mask-free process, it avoids many of the problems of shadow-masking techniques, including damage of predeposited layers by physical contact of the rigid metal mask with the substrate, costs associated with mask fabrication, fixturing, and cleaning, and inefficient materials utilization. On the other hand, OVJP, like other scanned nozzle approaches, is serial in its operation, making multiple nozzles and high scanning speeds necessary for high-throughput manufacturing.

##### 4.4.2. Inkjet Printing

Nozzles can also be used, of course, to print liquids. Beginning shortly after the commercial introduction of inkjet technology in digital-based graphic art printing, there has been interest in developing inkjet printing for manufacturing of physical parts. For example, solders, etch resists, and adhesives are inkjet printed for manufacturing of microelectronics.<sup>322–324</sup> Also, inkjet printing enables rapid prototype

production of complex three-dimensional shapes directly from computer software.<sup>325–327</sup> More recent work explores inkjet printing for organic optoelectronics, motivated mainly by attractive features that it has in common with OVJP, such as (i) purely additive operation, (ii) efficient materials usage, (iii) patterning flexibility, such as registration “on the fly”, and (iv) scalability to large substrate sizes and continuous processing (e.g., reel to reel). The following discussion introduces three different approaches to inkjet printing (thermal, piezoelectric, or electrohydrodynamic), with some device demonstrations.

**4.4.2.1. Thermal/Piezoelectric Inkjet Printing.** Conventional inkjet printers operate in either one of two modes: continuous jetting, in which a continuous stream of drops emerge from the nozzle, or drop-on-demand, in which drops are ejected as they are needed. This latter mode is most widespread due to its high placement accuracy, controllability, and efficient materials usage. Drop-on-demand uses pulses, generated either thermally or piezoelectrically, to eject solution droplets from a reservoir through a nozzle. Figure 32a shows a thermal inkjet printhead.<sup>328</sup> In this device,

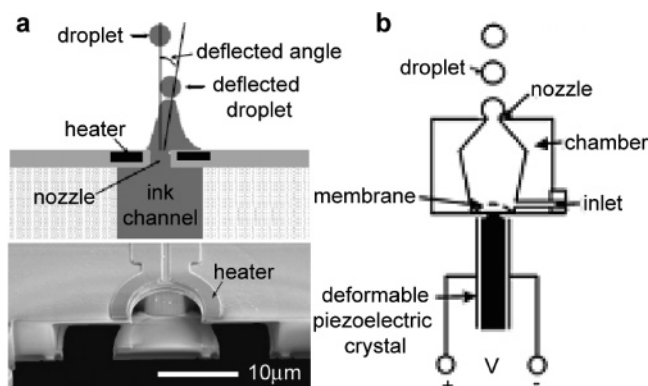


**Figure 32.** (a) Schematic illustration of a thermal inkjet printhead (bubble jet). Electrical heaters located near an orifice heat the ink above its boiling point. The vapor bubble produced in this way ejects ink from the nozzle. Bottom inset shows SEM image of the thermal inkjet printhead. (Reprinted with permission from ref 328. Copyright 2003 IEEE.) (b) Diagram of piezoelectric inkjet printhead. A piezoelectric crystal expands in response to an electrical driving signal, deforms a membrane, and causes a pressure impulse within the ink chamber that ejects a droplet from the orifice. In both thermal and piezoelectric systems, the chamber refills through the inlet by capillary action at the nozzle. (Reprinted with permission from ref 335. Copyright 2005 IEEE.)

electrical pulses applied to heaters that reside near the nozzles generate joule heating to vaporize the ink locally (heating temperature  $\sim 300$  °C for aqueous inks). The bubble nucleus forms near the heater and then expands rapidly (nucleate boiling process). The resulting pressure impulse ejects ink droplets through the nozzle before the bubble collapses. The process of bubble formation and collapse takes place within 10  $\mu$ s, typically.<sup>329–331</sup> As a result, the heating often does not degrade noticeably the properties of inks, even those that are temperature sensitive. Thermal inkjet printing of various organic electronic materials, such as PEDOT, PANI, P3HT, conducting nanoparticle solutions, UV-curable adhesives, etc., has been demonstrated for fabrication of electronic circuits.<sup>332</sup> Even biomaterials such as DNA and oligonucleotides for microarray biochips can be printed in this way.<sup>333,334</sup> Piezoelectric inkjet printheads provide drop-on-demand operation through the use of piezoelectric effects in materials such as lead zirconium titanate (PZT), as shown

in Figure 32b.<sup>335</sup> Here, electrical pulses applied to the piezoelectric element create pressure impulses that rapidly change the volume of the ink chamber to eject droplets. In addition to avoiding the heating associated with thermal printheads, the piezoelectric actuation offers considerable control over the shape of the pressure pulse (e.g., rise and fall time). This control enables optimized, monodisperse single-droplet production often using drive schemes that are simpler than those needed for thermal actuation.<sup>336</sup>

The physical properties of the ink are important for high-resolution inkjet printed patterns. First, to generate droplets with micrometer-scale diameters (picoliter-regime volume), sufficiently high kinetic energies (for example,  $\sim 20$   $\mu$ J for HP 51626A)<sup>330,331</sup> and velocities (normally 1–10 m/s) are necessary to exceed the interfacial energy that holds them to the liquid meniscus in the nozzle. Printing high-viscosity materials is difficult, due to viscous dissipation of energy supplied by the heater or piezoelectric element. Viscosities below 20 cP are typically needed.<sup>33,34</sup> Second, high evaporation rates in the inks can increase the viscosity, locally at the nozzles, leading, in extreme cases, to clogging. The physics of evaporation and drying also affects the thickness uniformity of the printed patterns. The large surface-to-volume ratio of the micrometer-scale droplets leads to high evaporation rates. Evaporation from the edges of the droplet is faster than that from the center, thereby driving flow from the interior to the edge. This flow transports solutes to the edge, thereby causing uneven thicknesses in the dried film.

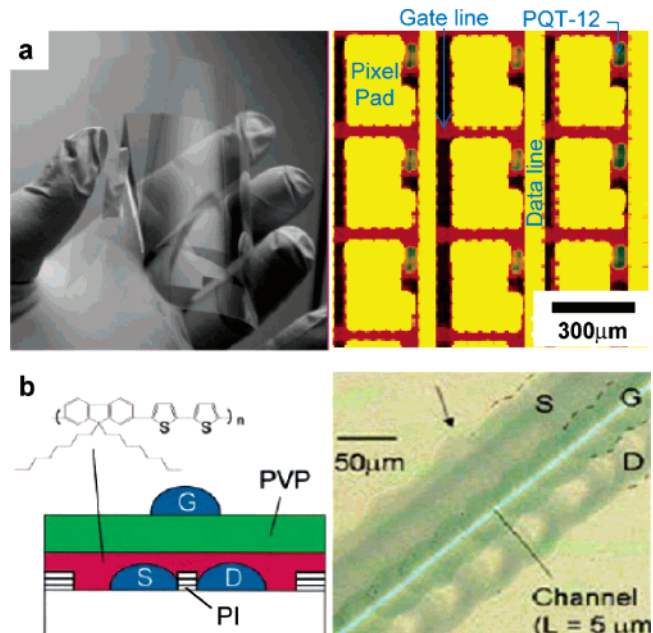


**Figure 33.** (a) Optical micrograph of metal lines patterned on a flexible PEN (polyethylene naphthalate) substrate using inkjet printing of Kemamide wax, which serves as an etch resist (left image) (reprinted with permission from ref 341; copyright 2005 IEEE) and optical micrograph of active matrix –TFT backplane using the inkjetted PQT-12 polymer semiconductor (right). (Reprinted with permission from ref 342. Copyright 2004 American Institute of Physics.) The right image shows part of 128  $\times$  128 TFT array in 300  $\mu$ m pixels. (b) Schematic diagram of a top-gate inkjet printed TFT that uses an F8T2 semiconducting layer and PEDOT-PSS electrodes (left image) and optical micrograph of the device (right). Photolithographically defined wetting patterns on the substrate define the critical dimension (channel length). [Reprinted with permission from Science (http://www.aaas.org), ref 35. Copyright 2000 American Association for the Advancement of Science.]

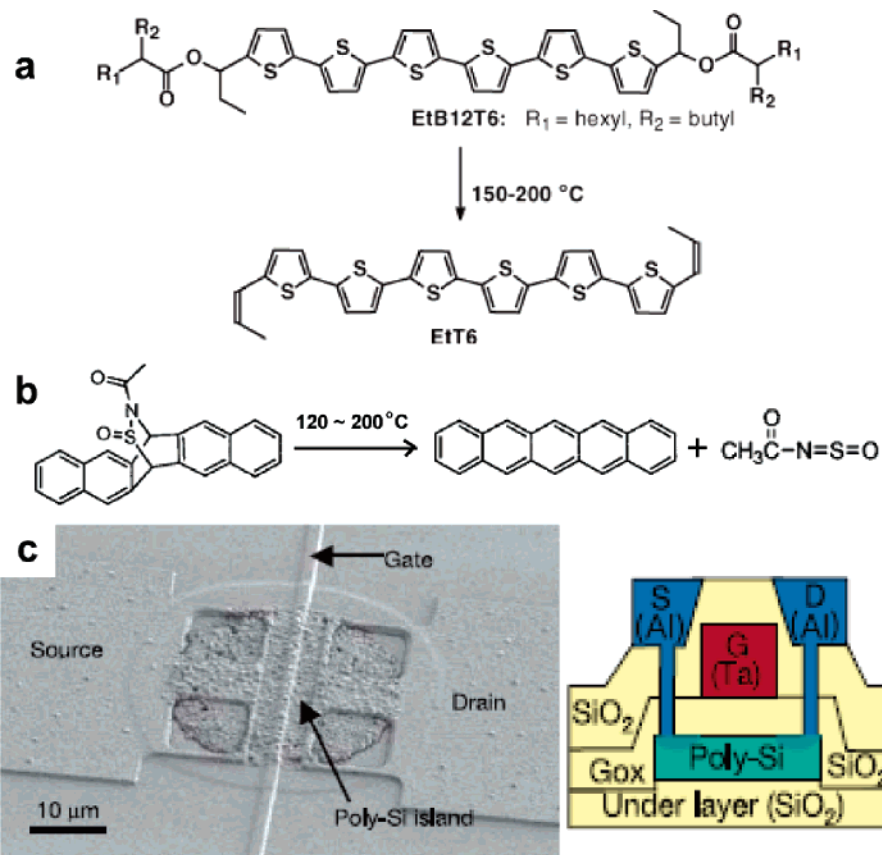


**Figure 34.** (a) Conversion reaction of oligothiophenes from printable form (EtB12T6) into the insoluble molecular structure (EtT6). The bulky end chains render the precursor soluble. (Reprinted with permission from refs 351 and 352. Copyrights 2006 and 2005, respectively, IEEE.) (b) Chemical reaction on thermal conversion of pentacene from the soluble form, where the *N*-sulfinyl group is bonded using Diels–Alder reaction (left) into the insoluble pentacene molecule (right).<sup>353,355,356</sup> (Reprinted with permission from ref 353. Copyright 2002 American Chemical Society.) (c) SEM image of a TFT that uses a semiconducting poly-Si layer generated from an inkjet printed precursor (left) and cross-sectional schematic of this TFT (right). Gate oxide (Gox) is  $\text{SiO}_2$ . [Reprinted with permission from *Nature* (<http://www.nature.com>), ref 360. Copyright 2006 Nature Publishing Group.]

The thickness uniformity can be enhanced by using fast-evaporating solvents.<sup>337</sup> Third, surface tension and surface chemistry play important roles because they determine the wetting behavior of the ink in the nozzle and on the surface. When the outer surface of the nozzle is wet with ink, ejected droplets can be deflected and sprayed in ways that are difficult to control.<sup>34</sup> Also, the wetting characteristics of the printed droplet on the substrate can influence the thickness and size of the printed material. A method to avoid the variation of printed droplet sizes associated with such wetting behaviors involves phase-changing inks. For example, an ink of Kemamide wax in the liquid phase (melting temperature = 60–100 °C) can be ejected from a nozzle, after which it freezes rapidly onto a cold substrate before spreading or dewetting. In this case, the printing resolution depends more on the cooling rate and less on the wetting properties, and a minimum size of ~20  $\mu\text{m}$  was achieved.<sup>338–340</sup> Active matrix-TFT backplanes in a display (e.g., electrophoretic display) can be fabricated, by using the inkjetted wax as an etch resist for patterning of metal electrodes (Cr and Au).<sup>341</sup> Here, poly-[5,5'-bis(3-dodecyl-2-thienyl)-2,2'-bithiophene] (PQT-12), which serves as the semiconductor, is printed using a piezoelectric inkjet, as shown in Figure 33a. Those OTFTs show average mobilities of 0.06  $\text{cm}^2/\text{V}\cdot\text{s}$  and  $I_{\text{on}}/I_{\text{off}}$  ratios of 10<sup>6</sup>.<sup>342</sup>

The wetting behavior, together with the volume and positioning accuracy of the ink droplets, influences the resolution. Typical inkjet printheads used with organic

electronic materials eject droplets with volumes of 2–10 pL and with droplet placement errors of  $\pm 10 \mu\text{m}$  at a 1 mm stand-off distance (without specially treated substrates).<sup>33,34,343</sup> Spherical droplets with volumes of 2 pL have diameters of 16  $\mu\text{m}$ . The diameters of dots formed by printing such droplets are typically 2 times larger than the droplet diameter, for aqueous inks on metal or glass surfaces. Recent results from an experimental inkjet system show the ability to print dots with 3  $\mu\text{m}$  diameters and lines with 3  $\mu\text{m}$  widths, without any prepatterned of the substrate, by use of undisclosed approaches. Inks of conducting silver nanoparticle paste (Harima Chemical Inc.; particle size ~ 5 nm, sintering temperature ~ 200 °C) and the conducting polymer, MEH-PPV, were demonstrated using this system.<sup>344,345</sup>

The resolution can be improved through the use of patterned areas of wettability or surface topography on the substrate, formed by photolithographic or other means. This strategy enables inkjet printing of all-polymer TFTs with channel lengths in the micrometer range,<sup>35</sup> as shown in Figure 33b. The fabrication in this case begins with photolithography to define hydrophobic polyimide structures on a hydrophilic glass substrate. Piezoelectric inkjet printing of an aqueous hydrophilic ink of PEDOT-PSS conducting polymer defines source and drain electrodes. The patterned-surface wettability ensures that the PEDOT-PSS remains only on the hydrophilic regions of substrate.<sup>346</sup> Spin-coating uniform layers of the semiconducting polymer (poly(9,9-diethylfluorene-*co*-bithiophene) (F8T2)) and the insulating polymer (PVP) form the

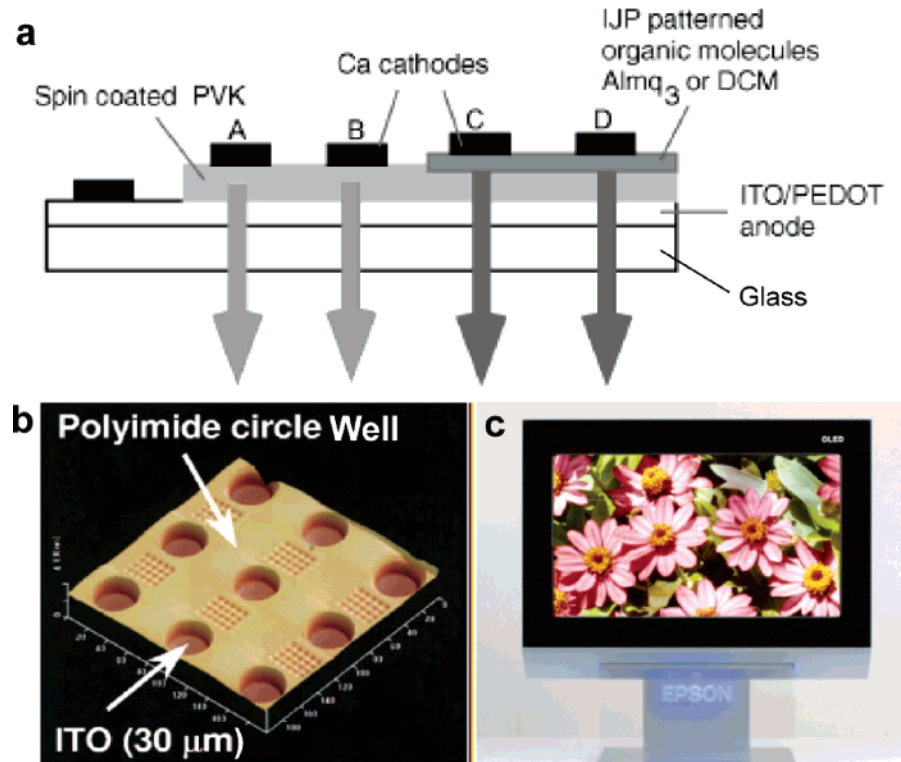


**Figure 35.** (a) Device structure of multicolor organic light-emitting diodes formed by inkjet printing. Devices A and B are blue-emitting LEDs with PVK as the active material. Devices C and D are red-emitting devices with DCM as the active material and green-emission devices with Almq<sub>3</sub> as the active material, respectively. (Reprinted with permission from ref 364. Copyright 1999 Wiley-VCH Verlag.) (b) Atomic force micrograph of polyimide wells for subpixel printing. These wells are patterned by photolithography. The holes in the circle wells are 30  $\mu\text{m}$  in diameter and 3  $\mu\text{m}$  in depth. (Reprinted with permission from ref 337. Copyright 2004 Seiko Epson Corp.) (c) 40 in. full-color OLED display built using inkjet printing to deposit the OLED materials. (Reprinted with permission from ref 318. Copyright 2004 Seiko Epson Corp.)

semiconductor and gate dielectric, respectively. Inkjet printing a line of PEDOT-PSS on top of these layers, positioned to overlap the region between the source and drain electrodes, defines a top gate. The width of the hydrophobic dewetting pattern (5  $\mu\text{m}$ ) defines the channel length. An extension of this approach uses sub-micrometer wide hydrophobic mesa structures defined by electron beam lithography. In this case the printed PEDOT-PSS ink splits into two halves with a narrow gap in between, to form channel lengths as small as 500 nm.<sup>347</sup> Although these approaches enable high-resolution patterns and narrow channel lengths, they require a separate lithographic step to define the wetting patterns.

Inkjet printing can also be applied to certain organic semiconductors and gate insulators.<sup>348–350</sup> Printing of the semiconductor, in particular, can be more challenging than that of other device layers due to its critical sensitivity to morphology, wetting, and other subtle effects that can be difficult to control. In addition, most soluble organic semiconductors that can be inkjetted exhibit low mobilities ( $10^{-3}$ – $10^{-1}$   $\text{cm}^2/\text{V}\cdot\text{s}$ ) because the solubilizing functional groups often disrupt  $\pi$ -orbital overlap between adjacent molecules and frustrate the level of crystallinity needed for efficient transport. Methods that avoid this problem by use of solution processable precursors that are thermally converted after printing appear to be promising. Figure 34a shows this conversion reaction for the case of oligothiophene. Low-cost small-molecule OTFTs with mobilities of  $\sim 0.1$   $\text{cm}^2/\text{V}\cdot\text{s}$  and 135 kHz RFIDs can be fabricated using this approach.<sup>351,352</sup> Soluble forms of pentacene derivatives with an *N*-sulfinyl group<sup>353</sup> or an alkoxy-substituted silylethynyl group<sup>354</sup> can also be synthesized. The former can be inkjet

printed and then converted into pentacene by heating at 120–200 °C, as illustrated in Figure 34b.<sup>355,356</sup> This inkjet-printed pentacene transistor shows a mobility of 0.17  $\text{cm}^2/\text{V}\cdot\text{s}$  and an  $I_{\text{on}}/I_{\text{off}}$  ratio of 10<sup>4</sup>.

Inkjet printing can also work well with a range of inorganic inks that are useful for flexible electronics. For example, suspensions of various metal nanoparticles such as Ag, Cu, and Au can be printed to produce continuous electrode lines and interconnects after a postprinting sintering process.<sup>357–359</sup> This sintering can be performed at relatively low temperatures (130–300 °C) that are compatible with many plastic substrates, due to melting point depression effects in metal nanoparticles. Inorganic semiconductors such as silicon can be also inkjet printed by using a route similar to the soluble organic precursor method described in the previous section. In particular, a Si-based liquid precursor (cyclopentasilane, Si<sub>5</sub>H<sub>10</sub>) can be printed and then converted to large-grain poly-Si by pulsed laser annealing, as illustrated in Figure 34c.<sup>360</sup> TFTs formed in this manner exhibit mobilities of  $\sim 6.5$   $\text{cm}^2/\text{V}\cdot\text{s}$ , which exceed those of solution-processed organic TFTs and amorphous Si TFTs, yet, encouragingly, are still much smaller than values that should be achievable with this type of approach.

Although substantial efforts in inkjet printing focus on transistors, the most well-developed systems are OLEDs for displays and other applications. For the fabrication of multicolor OLED displays, inkjet printing can simultaneously pattern subpixels using multiple nozzles and inks without any damage on the predeposited layer.<sup>361–364</sup> For example, OLEDs can be fabricated by inkjet printing of polyvinylcarbazole (PVK) polymer solutions doped with the dyes of

Coumarin 47 (blue photoluminescence), Coumarin 6 (green), and Nile red (orange-red) onto a polyester sheet coated with ITO. The printed subpixel sizes range from 150 to 200  $\mu\text{m}$  in diameter and from 40 to 70 nm in thickness, with turn-on voltages of 6–8 V.<sup>365</sup> OLEDs can be also patterned by inkjet printing of HTLs such as PEDOT, instead of the emitting layers, on ITO before blanket deposition of light-emitting layers by spin-coating. Because the charge injection efficiency of the HTLs is superior to the efficiency of ITO, only the HTL-covered areas emit light.<sup>366</sup> Multicolor light-emitting pixels can be fabricated using diffusion of the ink-jetted dyes.<sup>364</sup> In this case, green-emitting Almq<sub>3</sub> (tris(4-methyl-8-quinolinolato)Al<sub>III</sub>) and red-emitting 4-(dicyanomethylene)-2-methyl-6-(4-dimethylaminostyryl)-4H-pyran (DCM) dye molecules are inkjetted on a pre-spin-coated blue-emission PVK hole-transport layer (thickness: ~150 nm), as illustrated in Figure 35a. These two dyes diffuse into the PVK buffer layer. In regions where the Almq<sub>3</sub> or DCM diffuses into PVK, the pixels show green or red emission, respectively. Otherwise, the device emits blue light. These devices turn on at around 8 V, with the external quantum efficiencies of ~0.05%.

Many of the OLED systems use polymer wells to define subpixel sizes on the substrate surface. For example, Figure 35b shows polyimide wells (diameter = 30  $\mu\text{m}$ , depth = 3  $\mu\text{m}$ ) patterned on ITO by photolithography.<sup>337</sup> Inks flow directly into these wells and spread at their bottoms to form R, G, and B subpixels. Recently, a 40 in. full-color OLED display was achieved using this inkjet method, as shown in Figure 35c.<sup>318</sup>

**4.4.2.2. Electrohydrodynamic Inkjet Printing.** In thermal and piezoelectric inkjet technology, the size of the nozzle often plays a critical role in determining the resolution. Reducing this size can lead to clogging, especially with inks consisting of suspensions of nanoparticles or micro-/nanowires in high concentration. Another limitation of conventional inkjet printing is that the structures (wetting patterns, wells, etc.) needed to control flow and droplet movement on the substrate require conventional lithographic processing. Therefore, ink-based printing methods capable of generating small jets from big nozzles and of controlling in a non-lithographic manner the motion of droplets on the substrate might provide important new patterning capabilities and operating modes. A new strategy, aimed at achieving these and other objectives, uses electrohydrodynamic effects to perform the printing. Figure 36a shows a schematic illustration of this technique. A conducting metal film coats the nozzle in this system, and the substrate rests on a grounded electrode. When a voltage is applied to an ink solution, by use of the metal-coated nozzle assembly, surface charges accumulate in the liquid meniscus near the end of the nozzle. Whereas surface tension tends to hold the meniscus in a spherical shape, repulsive forces between the induced charges deform the sphere into cone. At sufficiently large electric fields, a jet with a diameter smaller than the nozzle size emerges from the apex of this cone (Figure 36b). In this situation, the jet diameter and jetting behavior (for example, pulsating, stable cone jet, or multijet mode) can be different, depending on the electric field and ink properties.<sup>367</sup> By controlling the applied voltage and moving the substrate relative to the nozzle, this jet can be used to write patterns of ink onto the substrate. Whereas this electrohydrodynamic inkjet printing method was first explored for graphic art printing applications in which pigment inks are printed on

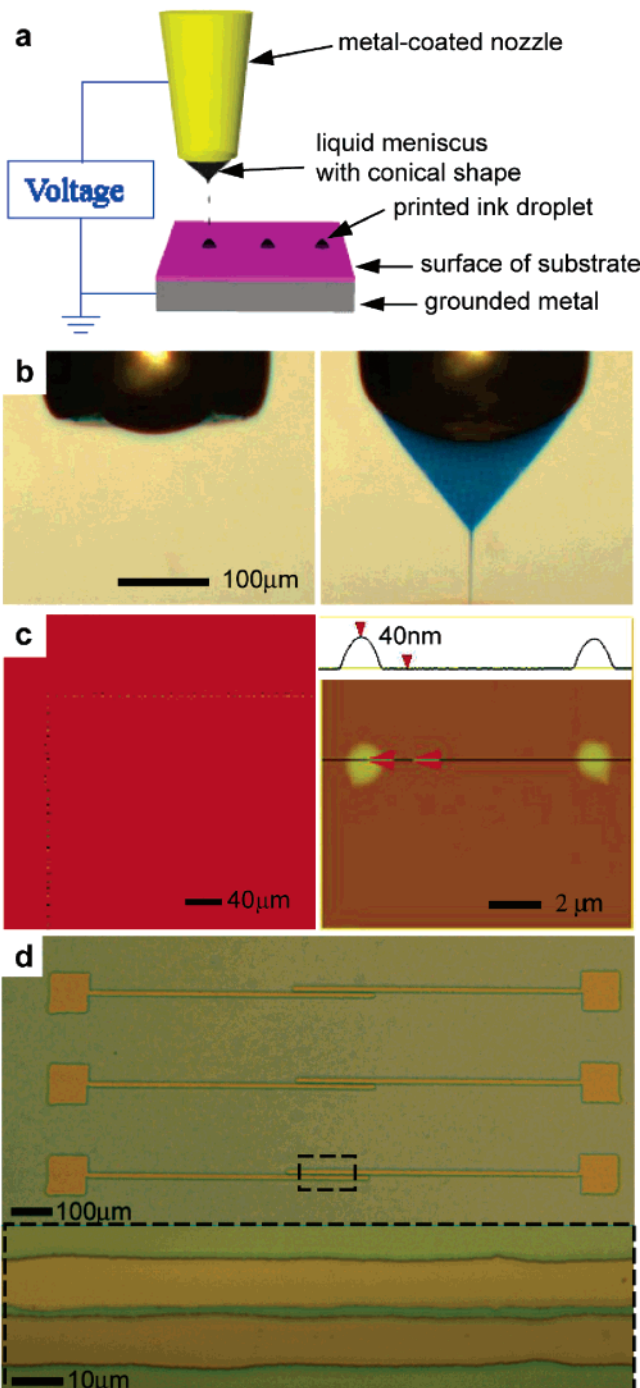


**Figure 36.** (a) Schematic illustration of electrohydrodynamic jet (e-jet) printing. (b) Optical micrograph showing the spherical shape of the liquid meniscus near the nozzle, at no voltage condition (left) and with voltages large enough to create a jet (right). (c) Optical micrograph showing e-jet printed patterns of PEDOT-PSS droplets with diameters of 2  $\mu\text{m}$  (left) and AFM image of the droplet (right). (d) Patterned gold source/drain electrode array after printing a polymer etch resist onto a flat nontreated gold surface. The bottom inset shows the minimum channel length of 2  $\mu\text{m}$ .

papers with relatively low printing resolutions (dot diameter  $\geq$  20  $\mu\text{m}$ ),<sup>368–371</sup> it has been recently demonstrated for high-resolution printing of various functional inks for electronic device fabrications. Figure 36c shows images of the PEDOT-PSS ink printed in this manner (dot diameters  $\sim$  2  $\mu\text{m}$ ). Dot sizes of <10  $\mu\text{m}$  are possible with a wide range of inks (for example, high concentration (>10 wt %) gold/silver/Si nanoparticle solutions, UV-curable polyurethane precursor,

SWNTs), and complex images can be formed. Also, polymer etch resists can be printed onto a flat nontreated gold surface, and electrode lines for electronic devices can be patterned after etching and stripping steps. For example, Figure 36d shows the array of source and drain patterned in this way. A channel length of  $\sim 2 \mu\text{m}$  is achieved without any substrate pretreatment, as shown in Figure 36d.

If the inks have sufficient viscosity or evaporation rates, the jet forms fibers rather than droplets, and the printing technique is known as electrospinning.<sup>372,373</sup> Organic semiconducting nanofibers of binary blends of MEH-PPV with regioregular P3HT can be electrospun to fiber diameters of 30–50 nm and then incorporated into OTFTs.<sup>372</sup> Transistors based on networks of such fibers showed mobilities in the range of  $10^{-4}$ – $5 \times 10^{-6} \text{ cm}^2/\text{V}\cdot\text{s}$ , depending on blend composition. The mobility values use the physical width of the transistor channel. Because the fibers occupy only 10% of the channel area, these mobilities are 1 order of magnitude lower than the mobilities of the individual fibers.

## 5. Conclusion

The economics associated with conventional electronics/optoelectronics and the resulting importance of the lithographic techniques used for those systems both strongly suggest that manufacturing approaches for organic devices will play critical roles in determining the success of the technology and the range of its applications. The patterning techniques presented in this review are diverse in their operational characteristics, their patterning capabilities, and the materials that they can manipulate. Many represent adaptations of mature technologies, such as inkjet, thermal laser transfer, or embossing techniques, that have already been scaled up for manufacturing in other areas. Others are newer and remain in a research exploratory phase. The use of shadow masking for the fabrication of OLED displays represents a good example of the successful transition to manufacturing. More exciting, in terms of novel patterning processes, is the recent emergence of large-area, prototype OLED displays that use active layers formed by inkjet and thermal laser transfer printing. As a benchmark of progress in this area, it is interesting to note that the first liquid crystal prototypes were demonstrated in 1968 with commercial production following in 1987. Polymer-based OLEDs were first reported in 1996 and the first inkjet printed display prototypes, based on these emissive polymers, were demonstrated in 2004. Although much of the work during this development period has focused on the materials and their behavior in active devices, substantial efforts were needed to invent the printing methods needed to pattern the electroluminescent polymers in cost-effective ways. The associated pilot line manufacturing systems, which now exist at large and small companies, suggest that further developed versions of these methods may have some promise for commercial scale production. If these efforts achieve their goal in the next few years, then one could conclude that the speed of development was comparable to that of liquid crystal technologies.

Displays, as well as organic solar cells, do not have, however, the demanding resolution and registration requirements (ignoring certain elements such as output couplers and concentrators and, of course, the circuit components of these devices) of organic transistors and circuits. For electronics, the patterning techniques must simultaneously achieve micrometer resolution and registration, at least for the source/

drain level, together with low-cost, large-area operation on plastic substrates. These challenging requirements might be achieved with microcontact printing or imprint lithography or by the combined use of such approaches with inkjet delivery of the active materials. In a particular example, high-resolution relief structures or wettability patterns formed with the former techniques could control the movement and position of droplets printed with the latter. In this strategy, the high-resolution methods, which have limited ability to pattern active materials, define critical features (e.g., transistor channel lengths) where resolution is of paramount importance, whereas other methods with lower resolution capabilities but the capacity to pattern active materials form the other elements. An overall approach that mixes and matches different techniques in this manner is attractive because it exploits the various strengths of the different techniques. To date, however, no clearly compelling manufacturing strategy has emerged for organic electronics, in spite of several impressive demonstrations of circuits that involve all or many of the key elements patterned using printing type processes. Benchmarked against inorganic transistor technology, the evolution of organic electronics has been slow: only  $\sim 20$  years separated the invention of the first inorganic transistor from mass production of medium-scale integrated (MSI) circuits containing hundreds of transistors; but today,  $\sim 20$  years after the demonstration of the first organic transistor, systems with hundreds of organic transistors have been demonstrated, but the path to mass production is still unclear. The challenges involve mainly (i) developing manufacturing-ready and cost-effective patterning techniques for large-area, low-cost systems while achieving, simultaneously, the necessary resolution and registration on plastic (which is known to be dimensionally unstable, at the micrometer level, in large-substrate form) and (ii) implementing organic semiconductors, the known versions of which have relatively modest performance and uncertain reliability. These two challenges are strongly linked. For example, a high-performance, reliable materials set would reduce the demands on patterning resolution and enable large-area printed circuits that could compete effectively on the basis of cost and, in some cases, performance with adapted versions of existing electronics technologies. Partly for this reason, a growing amount of research focuses on understanding the upper limits in mobilities of small molecule and polymer semiconductors and, perhaps more important, on developing new classes of “printable” semiconductor materials, such as those based on thin films of carbon nanotubes and inorganic wires, ribbons, sheets, and particles. The former efforts are beginning to identify certain organic systems with interesting performance characteristics (e.g., mobilities in the range of  $10$ – $20 \text{ cm}^2/\text{V}\cdot\text{s}$ ) and the underlying physics that governs charge transport.<sup>266–275,374–376</sup> The latter work is also yielding significant progress, based on strategies that involve “bottom up” growth of wires,<sup>377,378</sup> particles<sup>379,380</sup> or tubes,<sup>233,235–240,243,245–248,381</sup> followed by integration and/or assembly on plastic substrates, as well as “top down” micromachining of similar structures from wafers followed by printing.<sup>249–254,256,258–260</sup> Such methods can produce bendable transistors on plastic substrates, with mobilities of several hundred  $\text{cm}^2/\text{V}\cdot\text{s}$  and higher and with operating frequencies in the GHz regime using GaAs<sup>253</sup> wires and hundreds of MHz using Si ribbons,<sup>260</sup> even with modest critical dimensions (micrometers). Films of carbon nanotubes, in random networks or

aligned arrays,<sup>236–240,245</sup> can offer comparable or even better performance,<sup>236,237,248</sup> with other interesting attributes such as extreme levels of bendability<sup>233,239</sup> and optical transparency.<sup>234,239</sup> At the same time, efforts to integrate large-grained polysilicon on plastic by use of specialized laser annealing procedures applied to solution-deposited silicon precursors are yielding impressive results.<sup>360,382,383</sup> Circuits that use these and other high-performance materials can be achieved with greatly reduced requirements on patterning resolution and registration. In many cases, these materials also offer paths to highly robust and reproducible devices, which exploit the decades of research on wafer-based devices that use similar materials sets. The compatibility of the printing techniques reviewed here with these and other materials, as well as the more heavily explored organics, represents a key strength that will enhance their likelihood of evolving into meaningful approaches to manufacturing. In this sense, the development of unconventional patterning techniques for electronics and optoelectronics is becoming a field of its own, as the work broadens from early efforts configured to answer the question, “Now that we have organic electronic materials, can we develop optimized unconventional patterning methods to form circuits with them?”, to include a related, but much different question, “Now that we have unconventional patterning techniques, can we develop optimized electronic materials to form circuits with them?”

## 6. Acknowledgment

Y.S. acknowledges the support of the U.S. Department of Energy, Office of Science, Office of Basic Energy Sciences, under Contract DE-AC02-06CH11357. M.A.M. acknowledges a graduate fellowship from the Fannie and John Hertz Foundation.

## 7. References

- Garnier, F.; Horowitz, G.; Peng, X. H.; Fichou, D. *Adv. Mater.* **1990**, *2*, 592.
- Peng, X. Z.; Horowitz, G.; Fichou, D.; Garnier, F. *Appl. Phys. Lett.* **1990**, *57*, 2013.
- Tsumura, A.; Koezuka, H.; Ando, T. *Appl. Phys. Lett.* **1986**, *49*, 1210.
- Vincett, P. S.; Barlow, W. A.; Hann, R. A.; Roberts, G. G. *Thin Solid Films* **1982**, *94*, 171.
- Burroughes, J. H.; Bradley, D. D. C.; Brown, A. R.; Marks, R. N.; Mackay, K.; Friend, R. H.; Burns, P. L.; Holmes, A. B. *Nature* **1990**, *347*, 539.
- Riordan, M.; Hoddeson, L. *Crystal Fire: The Invention of the Transistor and the Birth of the Information Age*; W. W. Norton: New York, 1997.
- den Boer, W. *Active Matrix Liquid Crystal Displays: Fundamentals and Applications*; Newnes: Oxford, U.K., 2005.
- Rogers, J. A.; Paul, K. E.; Jackman, R. J.; Whitesides, G. M. *Appl. Phys. Lett.* **1997**, *70*, 2658.
- Schmid, H.; Biebuyck, H.; Michel, B.; Martin, O. J. F. *Appl. Phys. Lett.* **1998**, *72*, 2379.
- Rogers, J. A.; Meier, M.; Dodabalapur, A.; Laskowski, E. J.; Cappuzzo, M. A. *Appl. Phys. Lett.* **1999**, *74*, 3257.
- Schueler, O. J. A.; Whitesides, G. M.; Rogers, J. A.; Meier, M.; Dodabalapur, A. *Appl. Opt.* **1999**, *38*, 5799.
- Meier, M.; Dodabalapur, A.; Rogers, J. A.; Slusher, R. E.; Mekis, A.; Timko, A.; Murray, C. A.; Ruel, R.; Nalamasu, O. *J. Appl. Phys.* **1999**, *86*, 3502.
- Rogers, J. A.; Bao, Z. N.; Dhar, L. *Appl. Phys. Lett.* **1998**, *73*, 294.
- Gates, B. D.; Whitesides, G. M. *J. Am. Chem. Soc.* **2003**, *125*, 14986.
- Bailey, T. C.; Johnson, S. C.; Sreenivasan, S. V.; Ekerdt, J. G.; Willson, C. G.; Resnick, D. J. *J. Photopolym. Sci. Technol.* **2002**, *15*, 481.
- Cheng, X.; Hong, Y. T.; Kanicki, J.; Guo, L. *J. Vac. Sci. Technol. B* **2002**, *20*, 2877.
- Colburn, M.; Grot, A.; Choi, B. J.; Amistoso, M.; Bailey, T.; Sreenivasan, S. V.; Ekerdt, J. G.; Willson, C. G. *J. Vac. Sci. Technol. B* **2001**, *19*, 2162.
- Kao, P. C.; Chu, S. Y.; Chen, T. Y.; Zhan, C. Y.; Hong, F. C.; Chang, C. Y.; Hsu, L. C.; Liao, W. C.; Hon, M. H. *IEEE Trans. Electron Devices* **2005**, *52*, 1722.
- Stewart, M. D.; Johnson, S. C.; Sreenivasan, S. V.; Resnick, D. J.; Willson, C. G. *J. Microlithogr., Microfabr., Microsyst.* **2005**, *4*.
- Khang, D. Y.; Kang, H.; Kim, T.; Lee, H. H. *Nano Lett.* **2004**, *4*, 633.
- Zhang, F. L.; Nyberg, T.; Inganäs, O. *Nano Lett.* **2002**, *2*, 1373.
- Pisignano, D.; Sarconi, E.; Mazzeo, M.; Gigli, G.; Cingolani, R. *Adv. Mater.* **2002**, *14*, 1565.
- Rogers, J. A.; Bao, Z. N.; Raju, V. R. *Appl. Phys. Lett.* **1998**, *72*, 2716.
- Jeon, N. L.; Choi, I. S.; Xu, B.; Whitesides, G. M. *Adv. Mater.* **1999**, *11*, 946.
- Wilbur, J. L.; Kumar, A.; Kim, E.; Whitesides, G. M. *Adv. Mater.* **1994**, *6*, 600.
- Burgin, T.; Choong, V. E.; Maracas, G. *Langmuir* **2000**, *16*, 5371.
- Michel, B.; Bernard, A.; Bietsch, A.; Delamarche, E.; Geissler, M.; Juncker, D.; Kind, H.; Renault, J. P.; Rothuizen, H.; Schmid, H.; Schmidt-Winkel, P.; Stutz, R.; Wolf, H. *IBM J. Res. Dev.* **2001**, *45*, 870.
- Menard, E.; Bilhaut, L.; Zaumseil, J.; Rogers, J. A. *Langmuir* **2004**, *20*, 6871.
- Decre, M. M. J.; Schneider, R.; Burdinski, D.; Schellekens, J.; Saalmink, M.; Dona, R. Presented at the Materials Research Society Fall Meeting, 2003; p M4.9.1.
- Blanchet, G. B.; Fincher, C. R.; Gao, F. *Appl. Phys. Lett.* **2003**, *82*, 1290.
- Blanchet, G. B.; Loo, Y. L.; Rogers, J. A.; Gao, F.; Fincher, C. R. *Appl. Phys. Lett.* **2003**, *82*, 463.
- Lefenfeld, M.; Blanchet, G.; Rogers, J. A. *Adv. Mater.* **2003**, *15*, 1188.
- Creagh, L. T.; McDonald, M. *MRS Bul.* **2003**, *28*, 807.
- de Gans, B. J.; Duineveld, P. C.; Schubert, U. S. *Adv. Mater.* **2004**, *16*, 203.
- Sirringhaus, H.; Kawase, T.; Friend, R. H.; Shimoda, T.; Inbasekaran, M.; Wu, W.; Woo, E. P. *Science* **2000**, *290*, 2123.
- Ogawa, T.; Yashiro, T.; Arai, E. *Oyo Buturi* **1978**, *47*, 402.
- Pathak, H. T.; Sareen, L.; Khurana, K.; Chhabra, K. C. *IETE Tech. Rev.* **1986**, *3*, 73.
- Rothschild, M.; Bloomstein, T. M.; Efremow, N.; Fedynyshyn, T. H.; Fritze, M.; Pottebaum, I.; Switkes, M. *MRS Bull.* **2005**, *30*, 942.
- Wallraff, G. M.; Hinsberg, W. D. *Chem. Rev.* **1999**, *99*, 1801.
- Schellenberg, F. M. *Proc. SPIE* **2004**, *5377*, 1.
- Zhou, L. S.; Wang, A.; Wu, S. C.; Sun, J.; Park, S.; Jackson, T. N. *Appl. Phys. Lett.* **2006**, *88*, 083502.
- Afzali, A.; Dimitrakopoulos, C. D.; Graham, T. O. *Adv. Mater.* **2003**, *15*, 2066.
- Weidkamp, K. P.; Afzali, A.; Tromp, R. M.; Hamers, R. J. *J. Am. Chem. Soc.* **2004**, *126*, 12740.
- Klauk, H. *Organic Electronics, Materials, Manufacturing and Applications*; Wiley: New York, 2006.
- Grosso, G. *Organic Electronic Materials*; Springer: Berlin, Germany, 2001.
- Angelopoulos, M.; Shaw, J. M.; Kaplan, R. D.; Perreault, S. *J. Vac. Sci. Technol. B* **1989**, *7*, 1519.
- Angelopoulos, M.; Shaw, J. M.; Lee, K. L.; Huang, W. S.; Lecorre, M. A.; Tissier, M. *J. Vac. Sci. Technol. B* **1991**, *9*, 3428.
- Angelopoulos, M.; Patel, N.; Shaw, J. M.; Labianca, N. C.; Rishton, S. A. *J. Vac. Sci. Technol. B* **1993**, *11*, 2794.
- Drury, C. J.; Mutsaers, C. M. J.; Hart, C. M.; Matters, M.; de Leeuw, D. M. *Appl. Phys. Lett.* **1998**, *73*, 108.
- de Leeuw, D. M.; Blom, P. W. M.; Hart, C. M.; Mutsaers, C. M. J.; Drury, C. J.; Matters, M.; Termeer, H. *IEDM Tech. Dig.* **1997**, *13*, 331.
- Stejkal, J.; Kratochvil, P.; Jenkins, A. D. *Collect. Czech. Chem. Commun.* **1995**, *60*, 1747.
- Lee, C. W.; Seo, Y. H.; Lee, S. H. *Macromolecules* **2004**, *37*, 4070.
- Yu, J. F.; Abley, M.; Yang, C.; Holdcroft, S. *Chem. Commun.* **1998**, *1503*.
- Bacher, E.; Jungermann, S.; Rojahn, M.; Wiederhirn, V.; Nuyken, O. *Macromol. Rapid Commun.* **2004**, *25*, 1191.
- Domercq, B.; Hreha, R. D.; Zhang, Y. D.; Haldi, A.; Barlow, S.; Marder, S. R.; Kippelen, B. *J. Polym. Sci., Part B: Polym. Phys.* **2003**, *41*, 2726.
- Abdou, M. S. A.; Holdcroft, S. *Can. J. Chem.* **1995**, *73*, 1893.
- Wong, T. K. S.; Gao, S.; Hu, X.; Liu, H.; Chan, Y. C.; Lam, Y. L. *Mater. Sci. Eng., B* **1998**, *55*, 71.
- Abdou, M. S. A.; Diazguijada, G. A.; Arroyo, M. I.; Holdcroft, S. *Chem. Mater.* **1991**, *3*, 1003.
- Muller, C. D.; Falcon, A.; Reckefuss, N.; Rojahn, M.; Wiederhirn, V.; Rudati, P.; Frohne, H.; Nuyken, O.; Becker, H.; Meerholz, K. *Nature* **2003**, *421*, 829.

- (60) Crivello, J. V.; Falk, R.; Zonca, M. R. *J. Polym. Sci. Part A: Polym. Chem.* **2004**, *42*, 1630.
- (61) Pogantsch, A.; Rentenberger, S.; Langer, G.; Keplinger, J.; Kern, W.; Zojer, E. *Adv. Funct. Mater.* **2005**, *15*, 403.
- (62) Krebs, F. C.; Spanggaard, H. *Synth. Met.* **2005**, *148*, 53.
- (63) Kocher, C.; Montali, A.; Smith, P.; Weder, C. *Adv. Funct. Mater.* **2001**, *11*, 31.
- (64) Xia, Y. N.; Rogers, J. A.; Paul, K. E.; Whitesides, G. M. *Chem. Rev.* **1999**, *99*, 1823.
- (65) Xia, Y. N.; Whitesides, G. M. *Angew. Chem. Int. Ed.* **1998**, *37*, 551.
- (66) Aizenberg, J.; Rogers, J. A.; Paul, K. E.; Whitesides, G. M. *Appl. Phys. Lett.* **1997**, *71*, 3773.
- (67) Rogers, J. A.; Paul, K. E.; Jackman, R. J.; Whitesides, G. M. *J. Vac. Sci. Technol., B* **1998**, *B 16*, 59.
- (68) Rogers, J. A.; Dodabalapur, A.; Bao, Z. N.; Katz, H. E. *Appl. Phys. Lett.* **1999**, *75*, 1010.
- (69) Jeon, S.; Park, J.-U.; Cirelli, R.; Yang, S.; Heitzman, C. E.; Braun, P. V.; Kenis, P. J. A.; Rogers, J. A. *Proc. Natl. Acad. Sci. U.S.A.* **2004**, *101*, 12428.
- (70) Maria, J.; Jeon, S.; Rogers, J. A. *J. Photochem. Photobiol., A* **2004**, *166*, 149.
- (71) Lee, T. W.; Jeon, S.; Maria, J.; Zaumseil, J.; Hsu, J. W. P.; Rogers, J. A. *Adv. Funct. Mater.* **2005**, *15*, 1435.
- (72) Jeon, S.; Malyarchuk, V.; Rogers, J. A.; Wiederrecht, G. P. *Optics Express* **2006**, *14*, 2300.
- (73) Maria, J.; Malyarchuk, V.; White, J.; Rogers, J. A. *J. Vac. Sci. Technol., B* **2006**, *24*, 828.
- (74) Huang, Y. G. Y.; Zhou, W. X.; Hsia, K. J.; Menard, E.; Park, J. U.; Rogers, J. A.; Alleyne, A. G. *Langmuir* **2005**, *21*, 8058.
- (75) Zhou, W.; Huang, Y.; Menard, E.; Aluru, N. R.; Rogers, J. A.; Alleyne, A. G. *Appl. Phys. Lett.* **2005**, *87*, 251925.
- (76) Hsia, K. J.; Huang, Y.; Menard, E.; Park, J. U.; Zhou, W.; Rogers, J.; Fulton, J. M. *Appl. Phys. Lett.* **2005**, *86*, 154106.
- (77) Zaumseil, J.; Someya, T.; Bao, Z. N.; Loo, Y. L.; Cirelli, R.; Rogers, J. A. *Appl. Phys. Lett.* **2003**, *82*, 793.
- (78) Lee, T. W.; Zaumseil, J.; Bao, Z. N.; Hsu, J. W. P.; Rogers, J. A. *Proc. Natl. Acad. Sci. U.S.A.* **2004**, *101*, 429.
- (79) Lee, T. W.; Maria, J.; Zaumseil, J.; Hsu, J. W. P. and Rogers, J. A. *Advanced Functional Materials* **2005**, *15*, 1435–1439.
- (80) Yagi, I.; Tsukagoshi, K.; Aoyagi, Y. *Appl. Phys. Lett.* **2004**, *84*, 813.
- (81) Schrodner, M.; Stohn, R. I.; Schultheis, K.; Sensfuss, S.; Roth, H. K. *Org. Electronics* **2005**, *6*, 161.
- (82) Abdou, M. S. A.; Zi, W. X.; Leung, A. M.; Holdcroft, S. *Synth. Met.* **1992**, *52*, 159.
- (83) Itoh, E.; Torres, I.; Hayden, C.; Taylor, D. M. *Synth. Met.* **2006**, *156*, 129.
- (84) Chou, S. Y.; Krauss, P. R.; Renstrom, P. J. *Science* **1996**, *272*, 85.
- (85) Guo, L. J. *J. Phys. D: Appl. Phys.* **2004**, *37*, R123.
- (86) Chou, S. Y. *MRS Bull.* **2001**, *26*, 512.
- (87) Gates, B. D.; Xu, Q. B.; Stewart, M.; Ryan, D.; Willson, C. G.; Whitesides, G. M. *Chem. Rev.* **2005**, *105*, 1171.
- (88) Rijn, J. M. *J. Microlithogr., Microfabr., Microsyst.* **2006**, *5*, 011012.
- (89) van Wolferen, H. A. G. M.; Hoekstra, H. J. W. M.; de Ridder, R. M.; Worhoff, K.; Lambeck, P. V. *Jpn. J. Appl. Phys. Lett.* **2005**, *44*, 6568.
- (90) Liu, Z. W.; Wei, Q. H.; Zhang, X. *Nano Lett.* **2005**, *5*, 957.
- (91) Cerrina, F. *J. Phys. D: Appl. Phys.* **2000**, *33*, R103.
- (92) Pisignano, D.; D'Amone, S.; Gigli, G.; Cingolani, R. *J. Vac. Sci. Technol., B* **2004**, *22*, 1759.
- (93) Pfeiffer, K.; Fink, M.; Ahrens, G.; Gruetzner, G.; Reuther, F.; Seekamp, J.; Zankovich, S.; Torres, C. M. S.; Maximov, I.; Beck, M.; Graczyk, M.; Montelius, L.; Schulz, H.; Scheer, H. C.; Steingrueber, F. *Microelectron. Eng.* **2002**, *61*–*62*, 393.
- (94) Rolland, J. P.; Hagberg, E. C.; Denison, G. M.; Carter, K. R.; De Simone, J. M. *Angew. Chem. Int. Ed.* **2004**, *43*, 5796.
- (95) Hua, F.; Gaur, A.; Sun, Y. G.; Word, M.; Jin, N.; Adesida, I.; Shim, M.; Shim, A.; Rogers, J. A. *IEEE Trans. Nanotechnol.* **2006**, *5*, 301.
- (96) Austin, M. D.; Ge, H. X.; Wu, W.; Li, M. T.; Yu, Z. N.; Wasserman, D.; Lyon, S. A.; Chou, S. Y. *Appl. Phys. Lett.* **2004**, *84*, 5299.
- (97) Austin, M. D.; Zhang, W.; Ge, H. X.; Wasserman, D.; Lyon, S. A.; Chou, S. Y. *Nanotechnology* **2005**, *16*, 1058.
- (98) Hua, F.; Sun, Y. G.; Gaur, A.; Meitl, M. A.; Bilhaut, L.; Rotkina, L.; Wang, J. F.; Geil, P.; Shim, M.; Rogers, J. A.; Shim, A. *Nano Lett.* **2004**, *4*, 2467.
- (99) Truong, T. T.; Lin, R.; Jeon, S.; Lee, H. H.; Maria, J.; Gaur, A.; Hua, F.; Meinel, I.; Rogers, J. A. *Langmuir* **2007**, *23*, 2898.
- (100) Torres, C. M. S. *Alternative Lithography: Unleashing the Potentials of Nanotechnology*; Kluwer Academic/Plenum: New York, 2003.
- (101) Zhao, X. M.; Smith, S. P.; Wadman, S. J.; Whitesides, G. M.; Prentiss, M. *Appl. Phys. Lett.* **1997**, *71*, 1017.
- (102) Li, Y. G.; Chen, D.; Yang, C. S. *Optics Laser Technol.* **2001**, *33*, 623.
- (103) Ahn, S. W.; Lee, K. D.; Kim, D. H.; Lee, S. S. *IEEE Photonics Technol. Lett.* **2005**, *17*, 2122.
- (104) Kim, D. H.; Chin, W. J.; Lee, S. S.; Ahn, S. W.; Lee, K. D. *Appl. Phys. Lett.* **2006**, *88*, 071120.
- (105) Wang, J. J.; Chen, L.; Kwan, S.; Liu, F.; Deng, X. G. *J. Vac. Sci. Technol., B* **2005**, *23*, 3006.
- (106) Malyarchuk, V.; Hua, F.; Mack, N. H.; Velasquez, V. T.; White, J. O.; Nuzzo, R. G.; Rogers, J. A. *Optics Express* **2005**, *13*, 5669.
- (107) Que, W. X.; Hu, X.; Zhang, Q. Y. *Chem. Phys. Lett.* **2003**, *369*, 354.
- (108) Kim, W. S.; Lee, J. H.; Shin, S. Y.; Bae, B. S.; Kim, Y. C. *IEEE Photonics Technol. Lett.* **2004**, *16*, 1888.
- (109) Bae, B. S. *J. Sol-Gel Sci. Technol.* **2004**, *31*, 309.
- (110) Graupner, W.; Leising, G.; Lanzani, G.; Nisoli, M.; DeSilvestri, S.; Scherf, U. *Phys. Rev. Lett.* **1996**, *76*, 847.
- (111) Ichikawa, M.; Tanaka, Y.; Suganuma, N.; Koyama, T.; Taniguchi, Y. *Jpn. J. Appl. Phys. Part I* **2003**, *42*, 5590.
- (112) Gaal, M.; Gadermaier, C.; Plank, H.; Moderegger, E.; Pogantsch, A.; Leising, G.; List, E. J. W. *Adv. Mater.* **2003**, *15*, 1165.
- (113) Lawrence, J. R.; Turnbull, G. A.; Samuel, I. D. W. *Appl. Phys. Lett.* **2003**, *82*, 4023.
- (114) Pisignano, D.; Persano, L.; Visconti, P.; Cingolani, R.; Gigli, G.; Barbarella, G.; Favaretto, L. *Appl. Phys. Lett.* **2003**, *83*, 2545.
- (115) Pisignano, D.; Raganato, M. F.; Persano, L.; Gigli, G.; Visconti, P.; Barbarella, G.; Favaretto, L.; Zambianchi, M.; Cingolani, R. *Nanotechnology* **2004**, *15*, 953.
- (116) Pisignano, D.; Persano, L.; Mele, E.; Visconti, P.; Cingolani, R.; Gigli, G.; Barbarella, G.; Favaretto, L. *Opt. Lett.* **2005**, *30*, 260.
- (117) Pisignano, D.; Persano, L.; Mele, E.; Visconti, P.; Anni, M.; Gigli, G.; Cingolani, R.; Favaretto, L.; Barbarella, G. *Synth. Met.* **2005**, *153*, 237.
- (118) Leung, W. Y.; Kang, H.; Constant, K.; Cann, D.; Kim, C. H.; Biswas, R.; Sigalas, M. M.; Ho, K. M. *J. Appl. Phys.* **2003**, *93*, 5866.
- (119) Mele, E.; Di Benedetto, F.; Persano, L.; Cingolani, R.; Pisignano, D. *Nano Lett.* **2005**, *5*, 1915.
- (120) Huang, Y. Y.; Paloczi, G. T.; Yariv, A.; Zhang, C.; Dalton, L. R. *J. Phys. Chem. B* **2004**, *108*, 8606.
- (121) Lee, M.; Katz, H. E.; Erben, C.; Gill, D. M.; Gopalan, P.; Heber, J. D.; McGee, D. J. *Science* **2002**, *298*, 1401.
- (122) Guo, L. J.; Cheng, X.; Chao, C. Y. *J. Mod. Opt.* **2002**, *49*, 663.
- (123) Ma, H.; Jen, A. K. Y.; Dalton, L. R. *Adv. Mater.* **2002**, *14*, 1339.
- (124) Ma, H.; Liu, S.; Luo, J. D.; Suresh, S.; Liu, L.; Kang, S. H.; Haller, M.; Sassa, T.; Dalton, L. R.; Jen, A. K. Y. *Adv. Funct. Mater.* **2002**, *12*, 565.
- (125) Firestone, K. A.; Reid, P.; Lawson, R.; Jang, S. H.; Dalton, L. R. *Inorg. Chim. Acta* **2004**, *357*, 3957.
- (126) Chang, C. C.; Chen, C. P.; Chou, C. C.; Kuo, W. J.; Jeng, R. J. *J. Macromol. Sci.—Polym. Rev.* **2005**, *C45*, 125.
- (127) Yesodha, S. K.; Pillai, C. K. S.; Tsutsumi, N. *Prog. Polym. Sci.* **2004**, *29*, 45.
- (128) Ziebarth, J. M.; Saafir, A. K.; Fan, S.; McGehee, M. D. *Adv. Funct. Mater.* **2004**, *14*, 451.
- (129) Dickey, M. D.; Willson, C. G. *AIChE J.* **2006**, *52*, 777.
- (130) “Fundamental Research Needs in Organic Electronic Materials,” Executive Summary of U.S. DOE Basic Energy Sciences/Energy Efficiency and Renewable Energy OLED Workshop, May 23–25, 2003.
- (131) <http://www.netl.doe.gov/ssl/>.
- (132) Beinhoff, M.; Appapillai, A. T.; Underwood, L. D.; Frommer, J. E.; Carter, K. R. *Langmuir* **2006**, *22*, 2411.
- (133) Wang, J.; Sun, X. Y.; Chen, L.; Chou, S. Y. *Appl. Phys. Lett.* **1999**, *75*, 2767.
- (134) Mele, E.; Pisignano, D.; Mazzeo, M.; Persano, L.; Gigli, G.; Cingolani, R. *J. Vac. Sci. Technol., B* **2004**, *22*, 981.
- (135) Pisignano, D.; Persano, L.; Cingolani, R.; Gigli, G.; Babudri, F.; Farinola, G. M.; Naso, F. *Appl. Phys. Lett.* **2004**, *84*, 1365.
- (136) Cavallini, M.; Murgia, M.; Biscarini, F. *Mater. Sci. Eng. C: Biomimetic Supramol. Syst.* **2002**, *19*, 275.
- (137) Austin, M. D.; Chou, S. Y. *Appl. Phys. Lett.* **2002**, *81*, 4431.
- (138) Gottschalch, F.; Hoffmann, T.; Torres, C. M. S.; Schulz, H.; Scheer, H. C. *Solid-State Electron.* **1999**, *43*, 1079.
- (139) Cheng, X.; Li, D. W.; Guo, L. J. *Nanotechnology* **2006**, *17*, 927.
- (140) Stutzmann, N.; Friend, R. H.; Sirringhaus, H. *Science* **2003**, *299*, 1881.
- (141) Zhang, W.; Chou, S. Y. *Appl. Phys. Lett.* **2003**, *83*, 1632.
- (142) Jeon, N. L.; Choi, I. S.; Xu, B.; Whitesides, G. M. *Adv. Mater.* **1999**, *11*, 946.
- (143) Maltezos, G.; Nortrup, R.; Jeon, S.; Zaumseil, J.; Rogers, J. A. *Appl. Phys. Lett.* **2003**, *83*, 2067.
- (144) Kenis, P. J. A.; Ismagilov, R. F.; Whitesides, G. M. *Science* **1999**, *285*, 83.
- (145) Atencia, J.; Beebe, D. J. *Nature* **2005**, *437*, 648.

- (146) Park, J. U.; Meitl, M. A.; Hur, S. H.; Usrey, M. L.; Strano, M. S.; Kenis, P. J. A.; Rogers, J. A. *Angew. Chem. Int. Ed.* **2006**, *45*, 581.
- (147) Fu, Q.; Liu, J. *J. Phys. Chem. B* **2005**, *109*, 13406.
- (148) Kumar, A.; Whitesides, G. M. *Appl. Phys. Lett.* **1993**, *63*, 2002.
- (149) Geissler, M.; Schmid, H.; Michel, B.; Delamarche, E. *Microelectron. Eng.* **2003**, *67*–*68*, 326.
- (150) Kumar, A.; Biebuyck, H. A.; Whitesides, G. M. *Langmuir* **1994**, *10*, 1498.
- (151) Tate, J.; Rogers, J. A.; Jones, C. D. W.; Vyas, B.; Murphy, D. W.; Li, W. J.; Bao, Z. A.; Slusher, R. E.; Dodabalapur, A.; Katz, H. E. *Langmuir* **2000**, *16*, 6054.
- (152) Geissler, M.; Wolf, H.; Stutz, R.; Delamarche, E.; Grummt, U. W.; Michel, B.; Bietsch, A. *Langmuir* **2003**, *19*, 6301.
- (153) Goetting, L. B.; Deng, T.; Whitesides, G. M. *Langmuir* **1999**, *15*, 1182.
- (154) Kagan, C. R.; Breen, T. L.; Kosbar, L. L. *Appl. Phys. Lett.* **2001**, *79*, 3536.
- (155) Truong, T. T.; Lin, R.; Jeon, S.; Lee, H. H.; Maria, J.; Gaur, A.; Hua, F.; Meinel, I. and Rogers, J. A. *Langmuir* **2007**, *23*, 2898.
- (156) Balmer, T. E.; Schmid, H.; Stutz, R.; Delamarche, E.; Michel, B.; Spencer, N. D.; Wolf, H. *Langmuir* **2005**, *21*, 622.
- (157) Liboullle, L.; Bietsch, A.; Schmid, H.; Michel, B.; Delamarche, E. *Langmuir* **1999**, *15*, 300.
- (158) Biebuyck, H. A.; Whitesides, G. M. *Langmuir* **1994**, *10*, 4581.
- (159) Biebuyck, H. A.; Whitesides, G. M. *Langmuir* **1994**, *10*, 2790.
- (160) Delamarche, E.; Geissler, M.; Bernard, A.; Wolf, H.; Michel, B.; Hilborn, J.; Donzel, C. *Adv. Mater.* **2001**, *13*, 1164.
- (161) Xia, Y. N.; Zhao, X. M.; Whitesides, G. M. *Microelectron. Eng.* **1996**, *32*, 255.
- (162) Geissler, M.; Schmid, H.; Bietsch, A.; Michel, B.; Delamarche, E. *Langmuir* **2002**, *18*, 2374.
- (163) Xia, Y.; Kim, E.; Whitesides, G. M. *J. Electrochem. Soc.* **1996**, *143*, 1070.
- (164) Xia, Y. N.; Kim, E.; Mrksich, M.; Whitesides, G. M. *Chem. Mater.* **1996**, *8*, 601.
- (165) Wolfe, D. B.; Love, J. C.; Paul, K. E.; Chabinyc, M. L.; Whitesides, G. M. *Appl. Phys. Lett.* **2002**, *80*, 2222.
- (166) Love, J. C.; Wolfe, D. B.; Chabinyc, M. L.; Paul, K. E.; Whitesides, G. M. *J. Am. Chem. Soc.* **2002**, *124*, 1576.
- (167) Carvalho, A.; Geissler, M.; Schmid, H.; Michel, B.; Delamarche, E. *Langmuir* **2002**, *18*, 2406.
- (168) Zhao, X. M.; Wilbur, J. L.; Whitesides, G. M. *Langmuir* **1996**, *12*, 3257.
- (169) Burdinski, D.; Brans, H. J. A.; Decre, M. M. *J. Am. Chem. Soc.* **2005**, *127*, 10786.
- (170) Delamarche, E.; Geissler, M.; Magnuson, R. H.; Schmid, H.; Michel, B. *Langmuir* **2003**, *19*, 5892.
- (171) Delamarche, E.; Schmid, H.; Bietsch, A.; Larsen, N. B.; Rothuizen, H.; Michel, B.; Biebuyck, H. *J. Phys. Chem. B* **1998**, *102*, 3324.
- (172) Leufgen, M.; Lebib, A.; Muck, T.; Bass, U.; Wagner, V.; Borzenko, T.; Schmidt, G.; Geurts, J.; Molenkamp, L. W. *Appl. Phys. Lett.* **2004**, *84*, 1582.
- (173) Rogers, J. A.; Bao, Z.; Baldwin, K.; Dodabalapur, A.; Crone, B.; Raju, V. R.; Kuck, V.; Katz, H.; Amundson, K.; Ewing, J.; Drzaic, P. *Proc. Natl. Acad. Sci. U.S.A.* **2001**, *98*, 4835.
- (174) Rogers, J. A.; Bao, Z. N.; Dodabalapur, A.; Makhija, A. *IEEE Electron Device Lett.* **2000**, *21*, 100.
- (175) Rogers, J. A.; Bao, Z. N.; Makhija, A.; Braun, P. *Adv. Mater.* **1999**, *11*, 741.
- (176) Blanchet, G.; Rogers, J. J. *Imaging Sci. Technol.* **2003**, *47*, 296.
- (177) Mach, P.; Rodriguez, S. J.; Nortrup, R.; Wiltzius, P.; Rogers, J. A. *Appl. Phys. Lett.* **2001**, *78*, 3592.
- (178) Michel, B.; Bernard, A.; Bietsch, A.; Delamarche, E.; Geissler, M.; Juncker, D.; Kind, H.; Renault, J. P.; Rothuizen, H.; Schmid, H.; Schmidt-Winkel, P.; Stutz, R.; Wolf, H. *IBM J. Res. Dev.* **2001**, *45*, 697.
- (179) Rogers, J. A.; Paul, K. E.; Whitesides, G. M. *J. Vac. Sci. Technol., B* **1998**, *16*, 88.
- (180) Schellekens, J.; Burdinski, D.; Saalmink, M.; Beenhakkers, M.; Gelinck, G.; Decre, M. M. J. Presented at the Materials Research Society Fall Meeting, 2003; p M2.9.1.
- (181) Lee, K. S.; Blanchet, G. B.; Gao, F.; Loo, Y. L. *Appl. Phys. Lett.* **2005**, *86*, 074102.
- (182) Briseno, A. L.; Roberts, M.; Ling, M. M.; Moon, H.; Nemanick, E. J.; Bao, Z. N. *J. Am. Chem. Soc.* **2006**, *128*, 3880.
- (183) Glasmasdar, K.; Gold, J.; Andersson, A. S.; Sutherland, D. S.; Kasemo, B. *Langmuir* **2003**, *19*, 5475.
- (184) Briseno, A. L.; Aizenberg, J.; Han, Y. J.; Penkala, R. A.; Moon, H.; Lovinger, A. J.; Kloc, C.; Bao, Z. A. *J. Am. Chem. Soc.* **2005**, *127*, 12164.
- (185) Choi, H. Y.; Kim, S. H.; Jang, J. *Adv. Mater.* **2004**, *16*, 732.
- (186) Huang, Z.; Wang, P. C.; Feng, J.; MacDiarmid, A. G.; Xia, Y.; Whitesides, G. M. *Synth. Met.* **1997**, *85*, 1375.
- (187) Zschieschang, U.; Klauk, H.; Halik, M.; Schmid, G.; Dehm, C. *Adv. Mater.* **2003**, *15*, 1147.
- (188) Huang, Z. Y.; Wang, P. C.; MacDiarmid, A. G.; Xia, Y. N.; Whitesides, G. *Langmuir* **1997**, *13*, 6480.
- (189) Hidber, P. C.; Helbig, W.; Kim, E.; Whitesides, G. M. *Langmuir* **1996**, *12*, 1375.
- (190) Kind, H.; Geissler, M.; Schmid, H.; Michel, B.; Kern, K.; Delamarche, E. *Langmuir* **2000**, *16*, 6367.
- (191) Ng, W. K.; Wu, L.; Moran, P. M. *Appl. Phys. Lett.* **2002**, *81*, 3097.
- (192) Görman, C. B.; Biebuyck, H. A.; Whitesides, G. M. *Chem. Mater.* **1995**, *7*, 526.
- (193) Parashkov, R.; Becker, E.; Riedl, T.; Johannes, H. H.; Kowalsky, W. *Adv. Mater.* **2005**, *17*, 1523.
- (194) Zhou, F.; Chen, M.; Liu, W. M.; Liu, J. X.; Liu, Z. L.; Mu, Z. G. *Adv. Mater.* **2003**, *15*, 1367.
- (195) Koide, Y.; Wang, Q. W.; Cui, J.; Benson, D. D.; Marks, T. J. *J. Am. Chem. Soc.* **2000**, *122*, 11266.
- (196) Cosseddu, P.; Bonfiglio, A. *Appl. Phys. Lett.* **2006**, *88*, 023506.
- (197) Hur, S. H.; Khang, D. Y.; Kocabas, C.; Rogers, J. A. *Appl. Phys. Lett.* **2004**, *85*, 5730.
- (198) Hur, S. H.; Kocabas, C.; Gaur, A.; Park, O. O.; Shim, M.; Rogers, J. A. *J. Appl. Phys.* **2005**, *98*, 114302.
- (199) Kim, C.; Shtein, M.; Forrest, S. R. *Appl. Phys. Lett.* **2002**, *80*, 4051.
- (200) Li, D. W.; Guo, L. *J. Appl. Phys. Lett.* **2006**, *88*, 063513.
- (201) Loo, Y. L.; Willett, R. L.; Baldwin, K. W.; Rogers, J. A. *Appl. Phys. Lett.* **2002**, *81*, 562.
- (202) Wang, Z.; Xing, R. B.; Zhang, J.; Yuan, J. F.; Yu, X. H.; Han, Y. C. *Appl. Phys. Lett.* **2004**, *85*, 831.
- (203) Wang, Z.; Yuan, J. F.; Zhang, J.; Xing, R. B.; Yan, D. H.; Han, Y. C. *Adv. Mater.* **2003**, *15*, 1009.
- (204) Kim, C.; Burrows, P. E.; Forrest, S. R. *Science* **2000**, *288*, 831.
- (205) Rhee, J.; Lee, H. H. *Appl. Phys. Lett.* **2002**, *81*, 4165.
- (206) Granlund, T.; Nyberg, T.; Roman, L. S.; Svensson, M.; Inganäs, O. *Adv. Mater.* **2000**, *12*, 269.
- (207) Loo, Y. L.; Hsu, J. W. P.; Willett, R. L.; Baldwin, K. W.; West, K. W.; Rogers, J. A. *J. Vac. Sci. Technol., B* **2002**, *20*, 2853.
- (208) Loo, Y. L.; Willett, R. L.; Baldwin, K. W.; Rogers, J. A. *J. Am. Chem. Soc.* **2002**, *124*, 7654.
- (209) Choi, J. H.; Kim, K. H.; Choi, S. J.; Lee, H. H. *Nanotechnology* **2006**, *17*, 2246.
- (210) Hsu, J. W. P.; Loo, Y. L.; Lang, D. V.; Rogers, J. A. *J. Vac. Sci. Technol., B* **2003**, *21*, 1928.
- (211) Loo, Y. L.; Lang, D. V.; Rogers, J. A.; Hsu, J. W. P. *Nano Lett.* **2003**, *3*, 913.
- (212) Kim, C.; Forrest, S. R. *Adv. Mater.* **2003**, *15*, 541.
- (213) Cao, Y. F.; Kim, C.; Forrest, S. R.; Soboyejo, W. *J. Appl. Phys.* **2005**, *98*, 033713.
- (214) Schmid, H.; Wolf, H.; Allenspach, R.; Riel, H.; Karg, S.; Michel, B.; Delamarche, E. *Adv. Funct. Mater.* **2003**, *13*, 145.
- (215) Hines, D. R.; Mezhenny, S.; Breban, M.; Williams, E. D.; Ballarotto, V. W.; Esen, G.; Southard, A.; Fuhrer, M. S. *Appl. Phys. Lett.* **2005**, *86*, 163101.
- (216) Felmet, K.; Loo, Y. L.; Sun, Y. M. *Appl. Phys. Lett.* **2004**, *85*, 3316.
- (217) Kaneko, E. *Displays* **1993**, *14*, 125.
- (218) Suh, D.; Rhee, J.; Lee, H. H. *Nanotechnology* **2004**, *15*, 1103.
- (219) Wu, Y. L.; Li, Y. N.; Ong, B. S. *J. Am. Chem. Soc.* **2006**, *128*, 4202.
- (220) Chang, N. A.; Richardson, J. J.; Clem, P. G.; Hsu, J. W. P. *Small* **2006**, *2*, 75.
- (221) Kim, C.; Cao, Y.; Soboyejo, W. O.; Forrest, S. R. *J. Appl. Phys.* **2005**, *97*, 113512.
- (222) Park, S. K.; Kim, Y. H.; Han, J. I.; Moon, D. G.; Kim, W. K. *IEEE Trans. Electron Devices* **2002**, *49*, 2008.
- (223) Park, J.; Shim, S. O.; Lee, H. H. *Appl. Phys. Lett.* **2005**, *86*, 074102.
- (224) Ofuji, M.; Lovinger, A. J.; Kloc, C.; Siegrist, T.; Maliakal, A. J.; Katz, H. E. *Chem. Mater.* **2005**, *17*, 5748.
- (225) Kim, Y. H.; Park, S. K.; Moon, D. G.; Kim, W. K.; Han, J. I. *Displays* **2004**, *25*, 167.
- (226) Luan, S. F.; Cheng, Z. Y.; Xing, R. B.; Wang, Z.; Yu, X. H.; Han, Y. C. *J. Appl. Phys.* **2005**, *97*, 086102.
- (227) Luan, S. F.; Xing, R. B.; Wang, Z.; Yu, X. H.; Han, Y. C. *J. Vac. Sci. Technol., B* **2005**, *23*, 236.
- (228) Swanson, S. A.; Wallraff, G. M.; Chen, J. P.; Zhang, W. J.; Bozano, L. D.; Carter, K. R.; Salem, J. R.; Villa, R.; Scott, J. C. *Chem. Mater.* **2003**, *15*, 2305.
- (229) Choi, J. H.; Kim, D.; Yoo, P. J.; Lee, H. H. *Adv. Mater.* **2005**, *17*, 166.
- (230) Wang, Z.; Zhang, J.; Xing, R.; Yuan, J. F.; Yan, D. H.; Han, Y. C. *J. Am. Chem. Soc.* **2003**, *125*, 15278.
- (231) Kim, J. K.; Park, J. W.; Yang, H.; Choi, M.; Choi, J. H.; Suh, K. Y. *Nanotechnology* **2006**, *17*, 940.
- (232) Salleo, A.; Wong, W. S.; Chabinyc, M. L.; Paul, K. E.; Street, R. A. *Adv. Funct. Mater.* **2005**, *15*, 1105.

- (233) Hur, S. H.; Park, O. O.; Rogers, J. A. *Appl. Phys. Lett.* **2005**, *86*, 243502.
- (234) Cao, Q.; Zhu, Z. T.; Lemaitre, M. G.; Xia, M. G.; Shim, M.; Rogers, J. A. *Appl. Phys. Lett.* **2006**, *88*, 113511.
- (235) Snow, E. S.; Campbell, P. M.; Ancona, M. G.; Novak, J. P. *Appl. Phys. Lett.* **2005**, *86*, 033105.
- (236) Kocabas, C.; Pimparkar, N.; Yesilyurt, O.; Kang, S. J.; Alam, M. A.; Rogers, J. A. *Nano Lett.*, in press.
- (237) Kocabas, C.; Hur, S. H.; Gaur, A.; Meitl, M. A.; Shim, M.; Rogers, J. A. *Small* **2005**, *1*, 1110.
- (238) Meitl, M. A.; Zhou, Y. X.; Gaur, A.; Jeon, S.; Usrey, M. L.; Strano, M. S.; Rogers, J. A. *Nano Lett.* **2004**, *4*, 1643.
- (239) Cao, Q.; Hur, S. H.; Zhu, Z. T.; Sun, Y.; Wang, C. J.; Meitl, M. A.; Shim, M.; Rogers, J. A. *Adv. Mater.* **2006**, *18*, 304.
- (240) Hur, S. H.; Yoon, M. H.; Gaur, A.; Shim, M.; Faccetti, A.; Marks, T. J.; Rogers, J. A. *J. Am. Chem. Soc.* **2005**, *127*, 13808.
- (241) Allen, A. C.; Sundén, E.; Cannon, A.; Graham, S.; King, W. *Appl. Phys. Lett.* **2006**, *88*, 083112.
- (242) Zhou, Y. X.; Hu, L. B.; Gruner, G. *Appl. Phys. Lett.* **2006**, *88*, 123109.
- (243) Wang, C. J.; Cao, Q.; Ozel, T.; Gaur, A.; Rogers, J. A.; Shim, M. J. *Am. Chem. Soc.* **2005**, *127*, 11460.
- (244) Balasubramanian, K.; Friedrich, M.; Jiang, C. Y.; Fan, Y. W.; Mews, A.; Burghard, M.; Kern, K. *Adv. Mater.* **2003**, *15*, 1515.
- (245) Zhou, Y. X.; Gaur, A.; Hur, S. H.; Kocabas, C.; Meitl, M. A.; Shim, M.; Rogers, J. A. *Nano Lett.* **2004**, *4*, 2031.
- (246) Snow, E. S.; Novak, J. P.; Campbell, P. M.; Park, D. *Appl. Phys. Lett.* **2003**, *82*, 2145.
- (247) Kocabas, C.; Shim, M.; Rogers, J. A. *J. Am. Chem. Soc.* **2006**, *128*, 4540.
- (248) Kang, S. J.; Kocabas, C.; Ozel, T.; Shim, M.; Pimparkar, N.; Alam, M. A.; Rotkin, S. V.; Rogers, J. A. *Nature Nanotechnology*, in press.
- (249) Menard, E.; Lee, K. J.; Khang, D. Y.; Nuzzo, R. G.; Rogers, J. A. *Appl. Phys. Lett.* **2004**, *84*, 5398.
- (250) Menard, E.; Nuzzo, R. G.; Rogers, J. A. *Appl. Phys. Lett.* **2005**, *86*, 093507.
- (251) Zhu, Z. T.; Menard, E.; Hurley, K.; Nuzzo, R. G.; Rogers, J. A. *Appl. Phys. Lett.* **2005**, *86*, 133507.
- (252) Sun, Y. G.; Khang, D. Y.; Hua, F.; Hurley, K.; Nuzzo, R. G.; Rogers, J. A. *Adv. Funct. Mater.* **2005**, *15*, 30.
- (253) Sun, Y. G.; Menard, E.; Rogers, J. A.; Kim, H. S.; Kim, S.; Chen, G.; Adesida, I.; Dettmer, R.; Cortez, R.; Tewksbury, A. *Appl. Phys. Lett.* **2006**, *88*, 183509.
- (254) Sun, Y. G.; Rogers, J. A. *Nano Lett.* **2004**, *4*, 1953.
- (255) Khang, D. Y.; Jiang, H. Q.; Huang, Y.; Rogers, J. A. *Science* **2006**, *311*, 208.
- (256) Meitl, M. A.; Zhu, Z. T.; Kumar, V.; Lee, K. J.; Feng, X.; Huang, Y. Y.; Adesida, I.; Nuzzo, R. G.; Rogers, J. A. *Nat. Mater.* **2006**, *5*, 33.
- (257) Mack, S.; Meitl, M. A.; Baca, A. J.; Zhu, Z. T.; Rogers, J. A. *Appl. Phys. Lett.* **2006**, *88*, 213101.
- (258) Lee, K. J.; Motala, M. J.; Meitl, M. A.; Childs, W. R.; Menard, E.; Shim, A. K.; Rogers, J. A.; Nuzzo, R. G. *Adv. Mater.* **2005**, *17*, 2332.
- (259) Lee, K. J.; Lee, J.; Hwang, H. D.; Reitmeyer, Z. J.; Davis, R. F.; Rogers, J. A.; Nuzzo, R. G. *Small* **2005**, *1*, 1164.
- (260) Ahn, J.-H.; Kim, H.-S.; Lee, K. J.; Menard, E.; Nuzzo, R. G.; Rogers, J. A. *IEEE Electron Device Lett.* **2006**, *27*, 460.
- (261) Sun, Y. G.; Kim, H. S.; Menard, E.; Kim, S.; Adesida, I.; Rogers, J. A. *Small* **2006**, *2*, 1330.
- (262) Ahn, J. H.; Kim, H. S.; Lee, K. J.; Jeon, S.; Kang, S. J.; Sun, Y. G.; Nuzzo, R. G.; Rogers, J. A. *Science* **2006**, *314*, 1754.
- (263) Baca, A. J. Unpublished results.
- (264) Sun, Y.; Choi, W. M.; Jiang, H.; Huang, Y. Y.; Rogers, J. A. *Nat. Nanotechnol.* **2006**, *1*, 201.
- (265) Lee, K. J.; Motala, M. J.; Meitl, M. A.; Childs, W. R.; Menard, E.; Shim, A. K.; Rogers, J. A.; Nuzzo, R. G. *Adv. Mater.* **2005**, *17*, 2332.
- (266) de Boer, R. W. I.; Gershenson, M. E.; Morpurgo, A. F.; Podzorov, V. *Phys. Status Solidi A: Appl. Res.* **2004**, *201*, 1302.
- (267) Podzorov, V.; Menard, E.; Rogers, J. A.; Gershenson, M. E. *Phys. Rev. Lett.* **2005**, *95*, 226601.
- (268) Menard, E.; Podzorov, V.; Hur, S. H.; Gaur, A.; Gershenson, M. E.; Rogers, J. A. *Adv. Mater.* **2004**, *16*, 2097.
- (269) Newman, C. R.; Chesterfield, R. J.; Merlo, J. A.; Frisbie, C. D. *Appl. Phys. Lett.* **2004**, *85*, 422.
- (270) Goldmann, C.; Haas, S.; Krellner, C.; Pernstich, K. P.; Gundlach, D. J.; Batlogg, B. *J. Appl. Phys.* **2004**, *96*, 2080.
- (271) Takeya, J.; Goldmann, C.; Haas, S.; Pernstich, K. P.; Ketterer, B.; Batlogg, B. *J. Appl. Phys.* **2003**, *94*, 5800.
- (272) Takahashi, T.; Takenobu, T.; Takeya, J.; Iwasa, Y. *Appl. Phys. Lett.* **2006**, *88*, 033505.
- (273) Podzorov, V.; Menard, E.; Pereversev, S.; Yakshinsky, B.; Madey, T.; Rogers, J. A.; Gershenson, M. E. *Appl. Phys. Lett.* **2005**, *87*, 093505.
- (274) Sundar, V. C.; Zaumseil, J.; Podzorov, V.; Menard, E.; Willett, R. L.; Someya, T.; Gershenson, M. E.; Rogers, J. A. *Science* **2004**, *303*, 1644.
- (275) Zeis, R.; Besnard, C.; Siegrist, T.; Schlockermann, C.; Chi, X. L.; Kloc, C. *Chem. Mater.* **2006**, *18*, 244.
- (276) Loo, Y. L.; Someya, T.; Baldwin, K. W.; Bao, Z. N.; Ho, P.; Dodabalapur, A.; Katz, H. E.; Rogers, J. A. *Proc. Natl. Acad. Sci. U.S.A.* **2002**, *99*, 10252.
- (277) Guo, T. F.; Pyo, S.; Chang, S. C.; Yang, Y. *Adv. Funct. Mater.* **2001**, *11*, 339.
- (278) Lee, T. W.; Zaumseil, J.; Kim, S. H.; Hsu, J. W. P. *Adv. Mater.* **2004**, *16*, 2040.
- (279) Zaumseil, J.; Baldwin, K. W.; Rogers, J. A. *J. Appl. Phys.* **2003**, *93*, 6117.
- (280) Chabinyc, M. L.; Salleo, A.; Wu, Y. L.; Liu, P.; Ong, B. S.; Heeney, M.; McCulloch, L. *J. Am. Chem. Soc.* **2004**, *126*, 13928.
- (281) Ling, M. M.; Bao, Z. N.; Li, D. W. *Appl. Phys. Lett.* **2006**, *88*, 033502.
- (282) Gleskova, H.; Wagner, S. *Mater. Lett.* **2002**, *52*, 150.
- (283) Parikh, K.; Cattanach, K.; Rao, R.; Suh, D. S.; Wu, A. M.; Manohar, S. K. *Sensors Actuators B: Chem.* **2006**, *113*, 55.
- (284) Saran, N.; Parikh, K.; Suh, D. S.; Munoz, E.; Kolla, H.; Manohar, S. K. *J. Am. Chem. Soc.* **2004**, *126*, 4462.
- (285) Lamansky, S.; Hoffend, T. R.; Ha, L.; Jones, V.; Wolk, M. B.; Tolbert, W. A. *Proc. SPIE* **2005**, 5937.
- (286) Wolk, M. B.; Baetzold, J.; Bellmann, E.; Hoffend, T. R.; Lamansky, S.; Li, Y.; Roberts, R. R.; Savvateev, V.; Staral, J. S.; Tolbert, W. A. *Proc. SPIE* **2004**, *5519*, 12.
- (287) Blanchet, G. B.; Fincher, C. R.; Lefenfeld, M.; Rogers, J. A. *Appl. Phys. Lett.* **2004**, *84*, 296.
- (288) Hulea, I. N.; Fratini, S.; Xie, H.; Mulder, C. L.; Iossad, N. N.; Rastelli, G.; Ciuchi, S. and Morpurgo, A. F. *Nature Materials* **2006**, *5*, 982.
- (289) Lee, J. Y.; Lee, S. T. *Adv. Mater.* **2004**, *16*, 51.
- (290) Ling, M. M.; Bao, Z. N. *Chem. Mater.* **2004**, *16*, 4824.
- (291) Garnier, F.; Hajlaoui, R.; Yassar, A.; Srivastava, P. *Science* **1994**, *265*, 1684.
- (292) Gray, C.; Wang, J.; Duthaler, G.; Ritenour, A.; Drzaic, P. S. *Proc. SPIE* **2001**, *4466*, 89.
- (293) Bao, Z. N.; Feng, Y.; Dodabalapur, A.; Raju, V. R.; Lovinger, A. J. *Chem. Mater.* **1997**, *9*, 1299.
- (294) Someya, T.; Kitamura, M.; Arakawa, Y.; Sano, Y. Presented at the Fall Materials Research Society (MRS) Meeting, Boston, MA, Dec 1–5, 2003.
- (295) Min, G. *Synth. Met.* **2003**, *135*, 141.
- (296) Pardo, D. A.; Jabbari, G. E.; Peyghambarian, N. *Adv. Mater.* **2000**, *12*, 1249.
- (297) Jabbari, G. E.; Radspinner, R.; Peyghambarian, N. *IEEE J. Sel. Top. Quantum Electron.* **2001**, *7*, 769.
- (298) Kim, J. M.; Choi, W. B.; Lee, N. S.; Jung, J. E. *Diamond Relat. Mater.* **2000**, *9*, 1184.
- (299) Lee, N. S.; Chung, D. S.; Han, I. T.; Kang, J. H.; Choi, Y. S.; Kim, H. Y.; Park, S. H.; Jin, Y. W.; Yi, W. K.; Yun, M. J.; Jung, J. E.; Lee, C. J.; You, J. H.; Jo, S. H.; Lee, C. G.; Kim, J. M. *Diamond Relat. Mater.* **2001**, *10*, 265.
- (300) Bartic, C.; Jansen, H.; Campitelli, A.; Borghs, S. *Org. Electronics* **2002**, *3*, 65.
- (301) Forrest, S. R. *Nature* **2004**, *428*, 911.
- (302) Waser, R. *Nanoelectronics and Information Technology*; Wiley-VCH Verlag: Weinheim, Germany, 2003.
- (303) Sze, S. *Semiconductor Devices, Physics and Technology*; Wiley: New York, 1985.
- (304) Tian, P. F.; Bulovic, V.; Burrows, P. E.; Gu, G.; Forrest, S. R.; Zhou, T. X. *J. Vac. Sci. Technol., A: Vac. Surf. Films* **1999**, *17*, 2975.
- (305) Someya, T.; Sekitani, T.; Iba, S.; Kato, Y.; Kawaguchi, H.; Sakurai, T. *Proc. Natl. Acad. Sci. U.S.A.* **2004**, *101*, 9966.
- (306) Someya, T.; Kato, Y.; Sekitani, T.; Iba, S.; Noguchi, Y.; Murase, Y.; Kawaguchi, H.; Sakurai, T. *Proc. Natl. Acad. Sci. U.S.A.* **2005**, *102*, 12321.
- (307) Muyres, D. V.; Baude, P. F.; Theiss, S.; Haase, M.; Kelley, T. W.; Fleming, P. *J. Vac. Sci. Technol., A* **2004**, *22*, 1892.
- (308) Kelley, T. W.; Baude, P. F.; Gerlach, C.; Ender, D. E.; Muyres, D.; Haase, M. A.; Vogel, D. E.; Theiss, S. D. *Chem. Mater.* **2004**, *16*, 4413.
- (309) Baude, P. F.; Ender, D. A.; Haase, M. A.; Kelley, T. W.; Muyres, D. V.; Theiss, S. D. *Appl. Phys. Lett.* **2003**, *82*, 3964.
- (310) Duffy, D. C.; Jackman, R. J.; Vaeth, K. M.; Jensen, K. F.; Whitesides, G. M. *Adv. Mater.* **1999**, *11*, 546.
- (311) Someya, T.; Katz, H. E.; Gelperin, A.; Lovinger, A. J.; Dodabalapur, A. *Appl. Phys. Lett.* **2002**, *81*, 3079.
- (312) Someya, T.; Kim, P.; Nuckolls, C. *Appl. Phys. Lett.* **2003**, *82*, 2338.
- (313) Zhou, Y. X.; Johnson, A. T. *Nano Lett.* **2003**, *3*, 1371.
- (314) Ono, K.; Shimada, H.; Kobayashi, S. I.; Ootuka, Y. *Jpn. J. Appl. Phys. Part 1* **1996**, *35*, 2369.

- (315) Deshmukh, M. M.; Ralph, D. C.; Thomas, M.; Silcox, J. *Appl. Phys. Lett.* **1999**, *75*, 1631.
- (316) Stamm, C.; Marty, F.; Vaterlaus, A.; Weich, V.; Egger, S.; Maier, U.; Ramsperger, U.; Fuhrmann, H.; Pescia, D. *Science* **1998**, *282*, 449.
- (317) Lefebvre, J.; Radosavljevic, M.; Johnson, A. T. *Appl. Phys. Lett.* **2000**, *76*, 3828.
- (318) Epson Technology newsroom from Epson on May 2004 ([http://www.epson.co.jp/e/newsroom/tech\\_news/tl0408single.pdf](http://www.epson.co.jp/e/newsroom/tech_news/tl0408single.pdf)).
- (319) Shtein, M.; Peumans, P.; Benziger, J. B.; Forrest, S. R. *Adv. Mater.* **2004**, *16*, 1615.
- (320) Shtein, M.; Peumans, P.; Benziger, J. B.; Forrest, S. R. *J. Appl. Phys.* **2004**, *96*, 4500.
- (321) Preisler, E. J.; Guha, S.; Perkins, B. R.; Kazazis, D.; Zaslavsky, A. *Appl. Phys. Lett.* **2005**, *86*, 223504.
- (322) Hayes, D. J.; Cox, W. R.; Grove, M. E. *J. Electron. Manuf.* **1998**, *8*, 209.
- (323) Son, H. Y.; Nah, J. W.; Paik, K. W. *IEEE Trans. Electron. Packag. Manuf.* **2005**, *28*, 274.
- (324) Hayes, D. J.; Cox, W. R.; Grove, M. E. *Display Works '99* **1999**, *1*.
- (325) Moon, J.; Grau, J. E.; Knezevic, V.; Cima, M. J.; Sachs, E. M. *J. Am. Ceram. Soc.* **2002**, *85*, 755.
- (326) Blazdell, P. F.; Evans, J. R. G.; Edirisinghe, M. J.; Shaw, P.; Binstead, M. J. *J. Mater. Sci. Lett.* **1995**, *14*, 1562.
- (327) Blazdell, P. F.; Evans, J. R. G. *J. Mater. Synth. Process.* **1999**, *7*, 349.
- (328) Anagnostopoulos, C. N.; Chwalek, J. M.; Delametter, C. N.; Hawkins, G. A.; Jeanmaire, D. L.; Lebents, J. A.; Lopez, A.; Trauernicht, D. P. Presented at the 12th International Conference on Solid State Sensors, Actuators and Microsystems, Boston, MA, 2003; p 368.
- (329) Le, H. P. *J. Imaging Sci. Technol.* **1998**, *42*, 49.
- (330) Tseng, F. G.; Kim, C. J.; Ho, C. M. *J. Microelectromech. Syst.* **2002**, *11*, 427.
- (331) Tseng, F. G.; Kim, C. J.; Ho, C. M. *J. Microelectromech. Syst.* **2002**, *11*, 437.
- (332) Lindner, T. J. In *Printed Electronics Europe 2005*; available at <http://www.idtechex.com/products/en/presentation.asp?presentation-id=209>, 2005.
- (333) Cooley, P.; Hinson, D.; Trost, H. J.; Antohe, B.; Wallace, D. *Methods in Molecular Biology*; Humana Press: Totowa, NJ, 2001.
- (334) Okamoto, T.; Suzuki, T.; Yamamoto, N. *Nat. Biotechnol.* **2000**, *18*, 438.
- (335) Parashkov, R.; Becker, E.; Riedl, T.; Johannes, H. H.; Kowalsky, W. *Proc. IEEE* **2005**, *93*, 1321.
- (336) Lee, E. R. *Microdrop Generation*; CRC Press: New York, 2003.
- (337) Shimoda, T.; Morii, K.; Seki, S.; Kiguchi, H. *MRS Bull.* **2003**, *28*, 821.
- (338) Wong, W. S.; Ready, S.; Matusiak, R.; White, S. D.; Lu, J. P.; Ho, J.; Street, R. A. *Appl. Phys. Lett.* **2002**, *80*, 610.
- (339) Wong, W. S.; Ready, S. E.; Lu, J. P.; Street, R. A. *IEEE Electron. Device Lett.* **2003**, *24*, 577.
- (340) Wong, W. S.; Street, R. A.; White, S. D.; Matusiak, R.; Apte, R. B. U.S. Patent 6742884, 2004.
- (341) Chabinyc, M. L.; Wong, W. S.; Arias, A. C.; Ready, S.; Lujan, R. A.; Daniel, J. H.; Krusor, B.; Apte, R. B.; Salleo, A.; Street, R. A. *Proc. IEEE* **2005**, *93*, 1491.
- (342) Arias, A. C.; Ready, S. E.; Lujan, R.; Wong, W. S.; Paul, K. E.; Salleo, A.; Chabinyc, M. L.; Apte, R.; Street, R. A.; Wu, Y.; Liu, P.; Ong, B. *Appl. Phys. Lett.* **2004**, *85*, 3304.
- (343) Cheng, K.; Yang, M. H.; Chiu, W. W. W.; Huang, C. Y.; Chang, J.; Ying, T. F.; Yang, Y. *Macromol. Rapid Commun.* **2005**, *26*, 247.
- (344) Murata, K.; Matsumoto, J.; Tezuka, A.; Matsuba, Y.; Yokoyama, H. *Microsyst. Technol.—Micro-Nanosyst. Inf. Storage Process. Syst.* **2005**, *12*, 2.
- (345) Murata, K. *Proceedings for the International Conference on MEMS, NANO and Smart Systems (ICMENS '03)*, Alberta, Canada, 2003; p 346.
- (346) Khatavkar, V. V.; Anderson, P. D.; Duineveld, P. C.; Meijer, H. H. E. *Macromol. Rapid Commun.* **2005**, *26*, 298.
- (347) Wang, J. Z.; Zheng, Z. H.; Li, H. W.; Huck, W. T. S.; Sirringhaus, H. *Nat. Mater.* **2004**, *3*, 171.
- (348) Paul, K. E.; Wong, W. S.; Ready, S. E.; Street, R. A. *Appl. Phys. Lett.* **2003**, *83*, 2070.
- (349) Liu, Y.; Varahramyan, K.; Cui, T. H. *Macromol. Rapid Commun.* **2005**, *26*, 1955.
- (350) Burns, S. E.; Cain, P.; Mills, J.; Wang, J. Z.; Sirringhaus, H. *MRS Bull.* **2003**, *28*, 829.
- (351) Chang, P. C.; Molesa, S. E.; Murphy, A. R.; Frechet, J. M. J.; Subramanian, V. *IEEE Trans. Electron. Devices* **2006**, *53*, 594.
- (352) Subramanian, V.; Chang, P. C.; Lee, J. B.; Molesa, S. E.; Volkman, S. K. *IEEE Trans. Components Packag. Technol.* **2005**, *28*, 742.
- (353) Afzali, A.; Dimitrakopoulos, C. D.; Breen, T. L. *J. Am. Chem. Soc.* **2002**, *124*, 8812.
- (354) Payne, M. M.; Delcamp, J. H.; Parkin, S. R.; Anthony, J. E. *Org. Lett.* **2004**, *6*, 1609.
- (355) Molesa, S. E.; Volkman, S. K.; Redinger, D. R.; de la Fuente, V. A.; Subramanian, V. *Technical Digest—International Electron Devices Meeting*; IEDM: San Francisco, CA, 2004; p 1072.
- (356) Volkman, S. K.; Molesa, S. E.; Mattis, B.; Chang, P. C.; Subramanian, V. *Materials Research Society Symposium Proceedings*; Warrendale, PA, 2003; p 391.
- (357) Szczecz, J. B.; Megaridis, C. M.; Gamota, D. R.; Zhang, J. *IEEE Trans. Electron. Packag. Manuf.* **2002**, *25*, 26.
- (358) Dearden, A. L.; Smith, P. J.; Shin, D. Y.; Reis, N.; Derby, B.; O'Brien, P. *Macromol. Rapid Commun.* **2005**, *26*, 315.
- (359) Redinger, D.; Molesa, S.; Yin, S.; Farschi, R.; Subramanian, V. *IEEE Trans. Electron Devices* **2004**, *51*, 1978.
- (360) Shimoda, T.; Matsuki, Y.; Furusawa, M.; Aoki, T.; Yudasaka, I.; Tanaka, H.; Iwasawa, H.; Wang, D. H.; Miyasaka, M.; Takeuchi, Y. *Nature* **2006**, *440*, 783.
- (361) Chang, S. C.; Bharathan, J.; Yang, Y.; Helgeson, R.; Wudl, F.; Ramey, M. B.; Reynolds, J. R. *Appl. Phys. Lett.* **1998**, *73*, 2561.
- (362) Kobayashi, H.; Kanbe, S.; Seki, S.; Kiguchi, H.; Kimura, M.; Yudasaka, I.; Miyashita, S.; Shimoda, T.; Towns, C. R.; Burroughes, J. H.; Friend, R. H. *Synth. Met.* **2000**, *111*, 125.
- (363) Funamoto, T.; Mastueda, Y.; Yokoyama, O.; Tsuda, A.; Takeshida, H.; Miyashita, S. *Proceedings of the 22nd International Display Research Conference*, Boston, MA, 2002; p 1403.
- (364) Chang, S. C.; Liu, J.; Bharathan, J.; Yang, Y.; Onohara, J.; Kido, J. *Adv. Mater.* **1999**, *11*, 734.
- (365) Sturm, J. C.; Pschenitzka, F.; Hebner, T. R.; Lu, M. H.; Wu, C. C.; Wilson, W. Presented at the SPIE Conference on Organic Light-Emitting Materials and Devices, 1998; p 208.
- (366) Bharathan, J.; Yang, Y. *Appl. Phys. Lett.* **1998**, *72*, 2660.
- (367) Li, D.; Xia, Y. N. *Adv. Mater.* **2004**, *16*, 1151.
- (368) Mills, R. S. *Recent Progress in Ink Jet Technologies II*; E. Hanson and R. Eschbach, Eds.; The Society for Imaging Science and Technology: 1999; p 286.
- (369) Nakao, H.; Murakami, T.; Hirahara, S.; Nagato, H.; Nomura, Y. *Proceedings of IS&T's NIP15: International Conference on Digital Printing Technologies*, IS&T: Orlando, FL, 1999; p 319.
- (370) Choi, D. H.; Lee, F. C. *Proceedings of IS&T's Ninth International Congress on Advances in Non-Impact Printing Technologies*, Yokohama, Japan, 1993.
- (371) Kawamoto, H.; Umezu, S.; Koizumi, R. *J. Imaging Sci. Technol.* **2005**, *49*, 19.
- (372) Babel, A.; Li, D.; Xia, Y. N.; Jenekhe, S. A. *Macromolecules* **2005**, *38*, 4705.
- (373) Bocanegra, R.; Galan, D.; Marquez, M.; Loscertales, I. G.; Barrero, A. J. *Aerosol Sci.* **2005**, *36*, 1387.
- (374) de Boer, R. W. I.; Iosad, N. N.; Stassen, A. F.; Klapwijk, T. M.; Morpurgo, A. F. *Appl. Phys. Lett.* **2005**, *86*, 032103.
- (375) Goldmann, C.; Krellner, C.; Pernstich, K. P.; Haas, S.; Gundlach, D. J.; Batlogg, B. J. *Appl. Phys.* **2006**, *99*, 034507.
- (376) Panzer, M. J.; Frisbie, C. D. *Appl. Phys. Lett.* **2006**, *88*, 203504.
- (377) McAlpine, M. C.; Friedman, R. S.; Lieber, C. M. *Proc. IEEE* **2005**, *93*, 1357.
- (378) Duan, X. F.; Niu, C. M.; Sahi, V.; Chen, J.; Parce, J. W.; Empedocles, S.; Goldman, J. L. *Nature* **2003**, *425*, 274.
- (379) Ridley, B. A.; Nivi, B.; Jacobson, J. M. *Science* **1999**, *286*, 746.
- (380) Shevchenko, E. V.; Talapin, D. V.; Kotov, N. A.; O'Brien, S.; Murray, C. B. *Nature* **2006**, *439*, 55.
- (381) Artukovic, E.; Kaempgen, M.; Hecht, D. S.; Roth, S.; Gruner, G. *Nano Lett.* **2005**, *5*, 757.
- (382) Kane, M. G.; Firester, A. H. Presented at the USDC Flexible Microelectronics and Displays Conference, Phoenix, AZ, 2005.
- (383) Limanov, A. B.; van der Wilt, P. C.; Choi, J.; Maley, N.; Lee, J.; Abelson, J. R.; Kane, M. G. Presented at the International Display Manufacturing Conference, Taipei, Taiwan, 2005.